INVESTIGATION ON USE OF E-WASTE FOR CORROSION PROTECTION IN RC STRUCTURES

Thesis Submitted to AcSIR for the Award of

the Degree of

MASTER OF TECHNOLOGY

in

BUILDING ENGINEERING AND DISASTER MITIGATION

AcSIR

By

ANUJAY RAWAT

30EE15A01002

Under the Guidance of

Dr. S. R. Karade

CBRI

केंद्रीय भवन अनुसंधान संस्थान, रूड़की
CENTRAL BUILDING RESEARCH INSTITUTE ROORKEE

CSIR-Central Building Research Institute

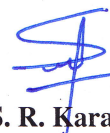## Roorkee-247667, Uttarakhand (India)

May, 2016

CERTIFICATE

This is to certify that the work incorporated in this M. Tech. thesis entitled *"Investigation on Use of E-Waste for Corrosion Protection in RC Structures"* submitted by *Mr. Anujay Rawat* to Academy of Scientific and Innovative Research (AcSIR) in fulfilment of the requirements for the award of the Degree of *Master of Technology,* embodies original research work under my guidance. I further certify that this work has not been submitted to any other university or institution in part or full for the award of any degree or diploma. Research material obtained from other sources has been duly acknowledged in the thesis. Any text, illustration, table etc., used in the thesis from other sources, have been duly cited and acknowledged.

(Anujay Rawat)
M.Tech. Student
AcSIR
CSIR-CBRI
Roorkee

(Dr. S. R. Karade)
Professor
AcSIR
CSIR-CBRI
Roorkee

ACKNOWLEDGEMENT

Date: 15/05/17

Place: Roorkee

Anujay Rawat

ANUJAY RAWAT

ABSTRACT

The generation of e-waste has increased many folds in the recent years owing to the technological development across the globe and India's prominent presence in the IT sector. The recycling of e-waste involves high cost in developed countries and is therefore sent to the developing countries for recycling and disposal. Due to the hazardous nature of e-waste, it endangers human-health and environment. So, there is an immediate need to find a solution for e-waste disposal. Printed Circuit Boards (PCBs) are a major component of every electrical equipment and disposal of PCBs is the most difficult task due to its complex composition of metals and plastics. A heterogeneous mixture of metals can be easily separated from plastics by milling of the PCBs and is conductive in nature. The metals and plastics can be recycled and can be used in different fields according to their properties.

Concrete is the most abundantly used building material and its durability is to be ensured to avoid deterioration, and minimise repairs and casualties. Corrosion of reinforcing bars in concrete is the biggest durability issue faced by the construction industry. To control and prevent corrosion, various electrochemical techniques are employed which requires a cost-effective and efficient anode to supply external current. Being the most important component of the protection system, development of newer anodes is the hot topic for research across the globe.

The present study is aimed to explore the possibility to use e-waste metallic powder as conductive fillers to develop a cementitious anodic overlay. This thesis describes the work carried out to achieve the aim. The cement composite was developed by use of e-waste metallic powder. The use of lower percentages of e-waste ($< 25\%$ by volume of cement composite) does not reduces the resistivity of the cement composite by great extent due to lower amount used and the size of the metal particles. So, to further reduce the resistivity and to study the effect of addition of higher percentages of e-waste, graphite powder was used in combination as a conductive filler.

The optimum combination identified on the basis of most preferential response of compressive strength and resistivity was 20% (by volume) e-waste metallic powder and 30% graphite powder. The compressive strength of the anode developed was 27.4 MPa and the resistance of the applied layer is 2.37 kΩ. Performance evaluation of anode layer was conducted by using various non-destructive electrochemical techniques like polarisation studies, linear polarisation measurements and electrochemical impedance spectroscopy. The developed anodes was found to meet the various performance criteria for anodes used in ICCP.

TABLE OF CONTENTS

CHAPTER 5: CONCLUSIONS AND RECOMMENDATIONS

LIST OF FIGURES

ix

LIST OF TABLES

ABBREVIATIONS

AC	Alternating Current
AGT	Accelerated Galvanostatic Test
CCD	Central Composite Design
CF	Carbon Fibre
CP	Cathodic Protection
CPrev	Cathodic Prevention
CRT	Cathode Ray Tube
DC	Direct Current
DOE	Design of Experiments
EEE	Electrical and Electronic Equipment
EIS	Electrochemical Impedance Spectroscopy
GDP	Gross Domestic Product
ICCP	Impressed Current Cathodic Protection
ICPOES	Inductively Coupled Plasma Atomic Emission Spectroscopy
LCD	Liquid Crystal Display
LED	Light Emitting Diode
LPR	Linear Polarization Resistance
PCB	Printed Circuit Board
RSM	Response Surface Method
SACP	Sacrificial Anode Cathodic Protection
SEM	Scanning Electron Microscope
SP	Super Plasticiser
SSD	Surface Saturated Dry
WEEE	Waste of Electrical and Electronic Equipment
XRF	X-Ray Fluorescence

CHAPTER 1

INTRODUCTION

1.1 Background

The industrialisation and the technological development of the countries have led to increased use of electrical and electronic equipment. This in turn has led to increased production of Electronic and Electrical Equipment (EEE).However, rapid upgradation of technology in the area resulted in the large amount of e-waste generation all around the globe. Due to the high cost involved in recycling of e-waste in developed countries, they tend to export it to developing countries for recycling and disposal. Since, this waste is hazardous in nature, it endangers human-health and environment. The hazards are increased many folds as e-waste is largely recycled in an informal way in developing countries. So, there is an immediate need to find a solution for recycling and suppressing the hazard imposed due to e-waste. The use of e-waste in construction industry can be a solution to e-waste disposal. It can result in massive energy savings and can act as an urban mine for metals. The heterogeneous mixture of metals which can be easily extracted by milling of printed circuit boards can be used in different fields.

Concrete is considered to be the most suitable construction material around the world for various benefits. Corrosion of reinforcement bars is a major durability issue in the reinforced concrete structures. Losses due to corrosion can be by the wastage of material and energy, economical losses and the impact on health and environment (Javaherdashti, 2000). Corrosion leads to direct and indirect economic losses. Direct economic losses alone costs around $2.76 billion/year in US or 3.1 % of US GDP (Virmani and Clemena, 1998), this trend may be true all around the world. In the Indian context so far there has been no corrosion auditing, but it is reported in CORCON – 2010 (International Conference on Corrosion held in Goa) that around Rs. 2 lakh crores is lost in India every year due to corrosion in terms of energy, resources and life. To control corrosion, besides conventional techniques like coatings, patch repairs, membranes etc. various electrochemical techniques like electrochemical chloride extraction, electrochemical realkalisation and cathodic protection are employed. Cathodic protection is the most effective method to reduce and halt corrosion throughout the service life of the structure. This technique is seldom used in developing countries owing to its high initial and application cost. For cathodic protection, an anode is needed to distribute current. Most metallic anodes possess some inherent drawbacks like high cost, difficulty in installation, disbondment and so on. To overcome the drawbacks, new cementitious based anodes are being developed and are

a potential area of research. Carbonaceous fillers like graphite powder, coke breeze and carbon fibers are added to the cementitious mix to make it electrically conductive. Metallic materials like steel wool, fibers and steel shavings are also capable of reducing the electrical resistivity of the cementitious mix (Chung, 2004). Thus, by using the e-waste development of a low cost and highly efficient anodic material can help in reducing the high amount of losses occurring due to corrosion. This study deals in exploring the possibilities for use of metallic fraction of e-waste as a conductive filler to reduce resistivity of cementitious mix and its use as an anodic overlay for cathodic protection of reinforced cement concrete (RCC) structures.

The effect of addition of e-waste metallic powder on various mechanical and electeochemical properties of the cementitious mix is studied. The performance of the developed conductive cement composite is evaluated by means of different electrical and electrochemical tests which will govern the protection of steel reinforcement against corrosion.

1.2 Research Objective

The main aim of this study was to explore the possibility of use of e-waste metallic powder as conductive filler for making cementitious conductive composite, which can be used as secondary anode in the cathodic protection of RC structures. To achieve this aim, following objectives were identified:

- To evaluate the mechanical and electrochemical properties of the developed cementitious composite by addition of conductive fillers.
- To assess the efficiency of the conductive cement composite as a secondary anode in the cathodic protection technique for corrosion mitigation of RC structures.

1.3 Outline of the Thesis

This thesis consists of five chapters including this **Introductory Chapter,** which deals with the introduction of the problem and need to conduct further research in this area.

The second chapter briefly discusses the **Literature** available on the e-waste, its recycling and use in the construction industry. The effect of using e-waste in concrete on various important mechanical properties of concrete. It also focuses on the mechanism of corrosion, various repair techniques employed for corrosion control, and the anodes used in various electrochemical techniques. A brief study over patents in this field was also conducted and patents were analysed to understand the status of research being carried in this area.

The third chapter describes the details of the **Experimental Program.** It also covers the characterisation of the raw materials used, mix proportioning, casting and curing methods for different specimens and details of different tests conducted for evaluation of conductive cement composite properties, monitoring and controlling corrosion using it as a secondary anode.

The fourth chapter contains the **Results and Discussion.** This chapter encompasses the results and findings from the experiments performed. The results are analysed and are discussed in detail in view of the current understanding in this area.

The fifth chapter covers the **Conclusions and Recommendations.** It summarises the work carried out in the present study and conclusions are drawn from the findings. Also, the future scope of the work is recommended which can be carried out for further studies is discussed.

At the end a list of **References** cited in the thesis is provided.

CHAPTER 2
LITERATURE REVIEW

2.1 General

"E-waste or Waste of Electrical and Electronic Equipment (WEEE) is a term used to cover all items of Electrical and Electronic Equipment (EEE) and its constituents that have been discarded by its owner as waste without the intent of reuse" (Adrian, 2014). These include all the components, sub-assemblies and the consumables that an equipment would have required through its life-time and are discarded with it (EU WEEE directive). E-waste incorporates a broad range of equipment from small size equipment to large equipment. The examples of small equipment are refrigerators, air conditioners, microwaves, vacuum cleaners, personal care appliances, washing machines, stereos, television etc.; IT equipment like desktop PCs, laptops, printers, mobile phones, flash drives, routers etc.; and lamps and lighting products including Cathode Ray Tube (CRT) and Liquid Crystal Display (LCD) TVs, flat display panel TVs, compact fluorescent lamps, LED lamps etc.; and consumer products that have reached their end of life, while the large equipment include industrial machines, central heating, dish washers, photovoltaic panels etc. (Puckett and Smith, 2002) . Thus, it can be stated that all the electrical and electronic equipment those have served their purpose and are no longer satisfy their owner/consumer is considered as E-waste or WEEE.

According to United Nations University (UNU), an autonomous body of the United Nations (UN) General Assembly, e-waste can be classified into six categories (Baldé *et. al.,* 2015):

a) Temperature exchange equipment: These include all the cooling and freezing equipment like refrigerators, freezers, air conditioners, heat pumps etc.

b) Screens and monitors: These typically includes all the telecommunication medium for transmitting moving images like televisions, laptops, notes, tablets etc.

c) Lamps: These encompasses all the lighting devices as high intensity discharge lamps, LED lamps, fluorescent lamps, compact fluorescent lamps, straight fluorescent lamps, incandescent lamps etc.

d) Large equipment: These comprises of printing machines, electric stoves, copying equipment, washing machines, photovoltaic panels etc.

e) Small equipment: These includes radio sets, stereos, calculators, microwaves, electric kettles, toasters, battery chargers, vacuum cleaners, video cameras, toys, small medical devices, small electrically powered tools, small monitoring and control devices etc.

f) Small IT and telecommunication equipment: These comprises of GPS, pocket calculators, routers, mobile phones, personal computers, telephones, flash drives, remote control, printers, digital writing pads etc.

The contribution of each type of waste based on their source is shown in Fig. 2.1.
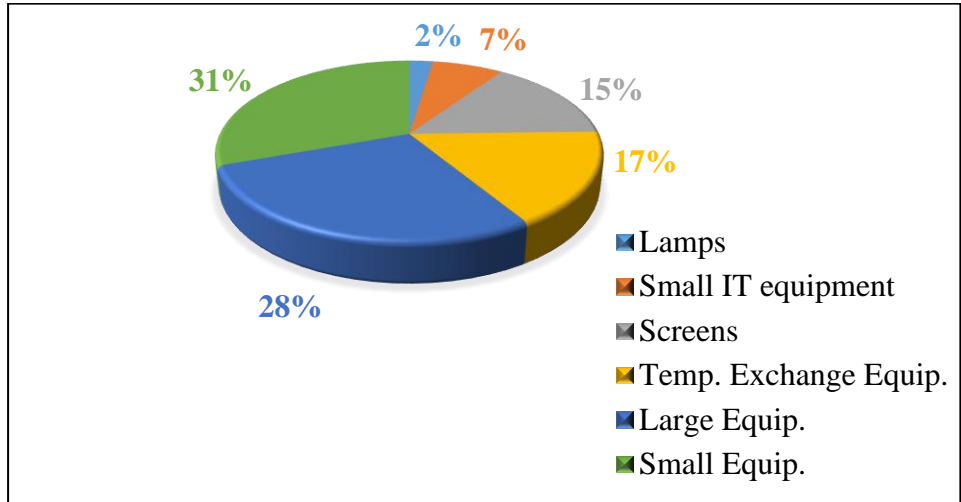
Figure 2.1 Categories of E-waste (Baldé *et al*., 2015)

For each of the six categories the function, size, material composition, weight is different from each other. Each category has its own way of collection, transit, handling and recycling because of differences in their financial worth, volumes of waste generation and socio-environmental impact.

2.2 e-Waste Generation

The electronic industry is the fastest growing manufacturing sector of the world. It is divided into three parts namely consumer electronics, general electronics and electric utilities. The consumer electronics section have the highest growth rate and leading to an average growth rate of 2% to 4% equating to a whopping $10 billion to $14 billion per year or more (Baldé *et al.,* 2015). The use of electrical and electronic equipment has elevated all round the world due to technological development, industrialisation, economic and population growth, and up-gradation in the living standards in recent decades. The increase in the use of electronic devices, higher obsolescence rate and decrease in the life span of the equipment is leading to the growth in the generation of e-waste. The obsolescence rate is increasing due to decreasing life-span of products, changing consumption patterns, routine replacement of equipment due to technological advancement. The life span and estimated probability of discarding is shown in Fig. 2.2.

5
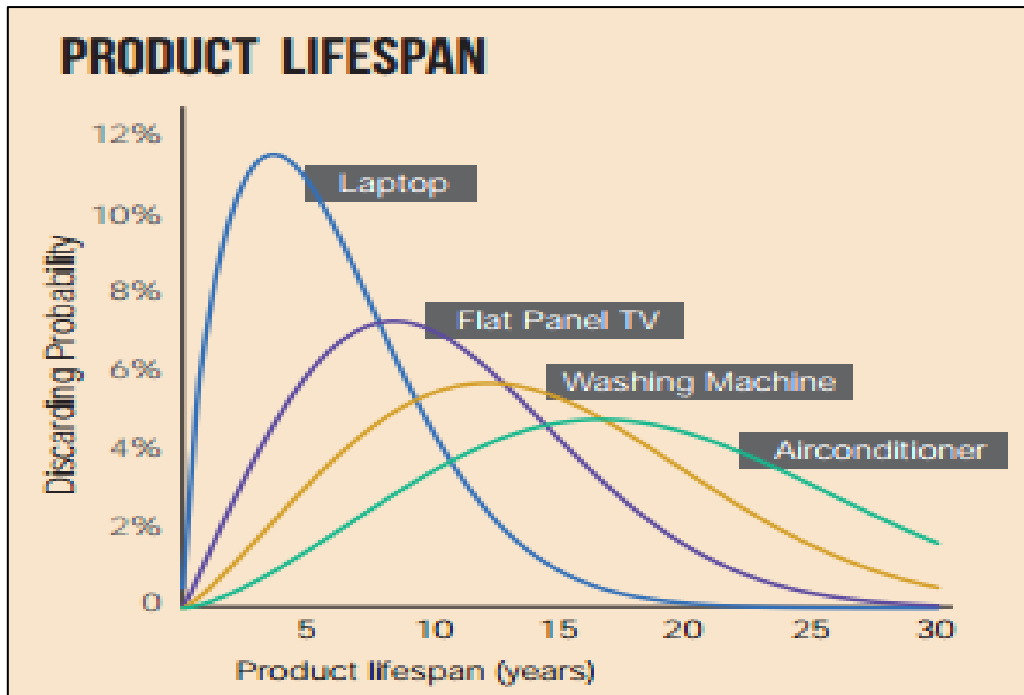
Figure 2.2 Product lifespan and discarding probability (after Baldé *et al*., 2015)

2.2.1   e-Waste Generation – Global Scenario

The generation of e-waste globally is expeditiously increasing and the rate of generation is also expected to rise in the near future. The global production of WEEE was around 41.8 million tonnes in 2014 and only 6.5 million tonnes of it was treated formally by take-back systems. In other words, the e-waste generated can fill enough containers of the train that can encircle the world. The globally generated consisted of 12.8 million tonnes of small equipment, 11.8 million tonnes of large equipment, 7.0 million tonnes of temperature exchange equipment, 6.3 million tonnes of screens and monitors, 3.0 million tonnes of small IT equipment and 1.0 million tonnes of lamps and lighting equipment. This amount is to surge to 49.8 million tonnes by 2018 growing with a pace of 4 to 5% annually (Baldé *et al*.., 2015).

Asia accounts for the highest production of WEEE i.e. 16 million tonnes in 2014 with 3.7 kilograms per capita (kgpc). North America and South America accounts for 11.7 million tonnes generation of e-waste combined with 12.2 kgpc. Europe holds the third place for generation of e-waste with 11.6 Million tonnes produced in 2014 having 15.6 kgpc. With 1.7 kgpc only, Africa produced 1.9 million tonnes of e-waste and 15.6 million tonnes was produced in Oceania with 15.2 kgpc (Baldé *et al*.., 2015).

United States of America produces the highest amount of e-waste annually, at 7.1 million tonnes per year followed by China producing 6 million tonnes per year. Most of the African

6

nations produce lowest e-waste annually, i.e. lower than 0.2 million tonnes per year. However, the EU and the United States recycle only 40% and 12%, respectively of the WEEE generated domestically in the respective countries.

More than 30 million computers are discarded in USA annually and around 100 million phones are discarded and disposed off in European Union annually. Out of the WEEE generated globally, only 15 to 20% is recycled back and rest find its way to landfills and incinerators creating environmental problems and health hazards (Jahan & Begum, 2013). A United Nations study has reported that e-waste from computers will grow by 400% in China and 500% in India, and from mobile phones it would be seven times higher in China and eighteen times higher in India by 2020 over the generation levels reported in 2007 (Rajya Sabha Secretariat, 2011).Thus, the amount of generation and forecasts urges to address the problem of WEEE on a global scale and regulate the management, recycling and disposal processes. According to Achim Steiner, former Executive Director of United Nations Environmental Program (UNEP), India, China, Mexico, Brazil and few other countries would face escalating health and environmental problems due to informal and unauthorised e-waste handling and recycling. The growth of e-waste generated through the years is shown in Fig. 2.3.
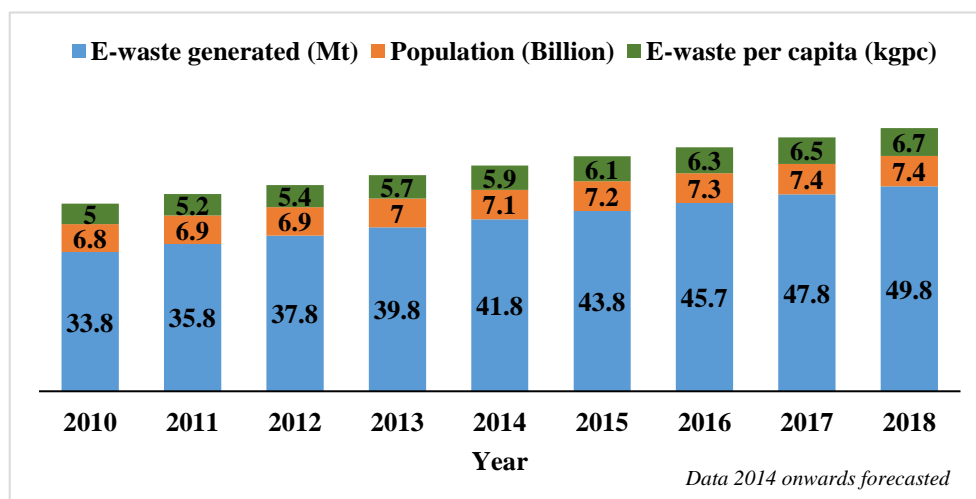
Figure 2.3 E-waste generation per year (Baldé *et al.,* 2015)

Despite all the rules and regulations which are enacted after the Basel Convention to control the trans-boundary flow of e-waste, most of the e-waste generated in the developed countries is sent formally or informally to the developing countries in the shadow of charity and waste. The e-waste is sent to developing countries as recycling in developed countries is costly and difficult because of numerous enacted laws and increased advocacy of environmental conservation and sustainability by NGOs and various other government agencies. Thus, the

developed countries are getting liberated of e-waste and burdening the developing countries with this hazard. The waste also pitches a commercial opportunity in developing economies and also satisfying need for cheap and affordable second hand electronic equipment for those having low purchasing capacities.
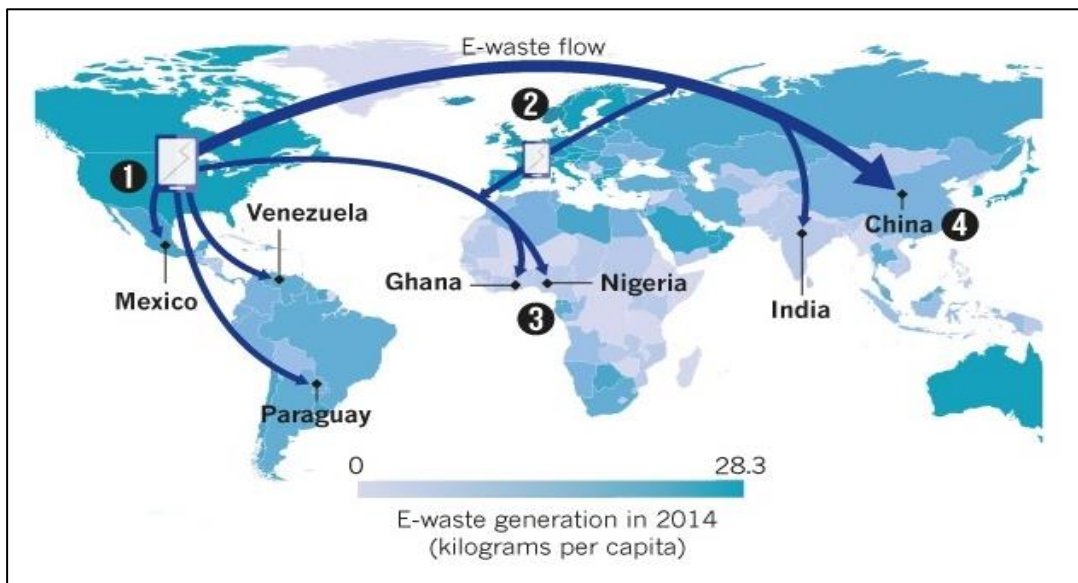
Figure 2.4 Illegal flow of WEEE (Wang *et al.,* 2016)

The Fig. 2.4 shows unfair flow of e-waste from developed countries to the developing ones. China receives as much as 90 % of global recycling market of WEEE and processed 70 % of it in 2012 and rest is sent to India and few other countries. Unauthorised and informal recycling adds to the hazards of the e-waste in these countries (Wang *et al.,* 2016).

2.2.2   e-Waste Generation – Scenario in India

India is one of the fastest growing economy of the world and the Indian information technology industry has a very prominent place in the world because of the software sector. The development of the Indian software sector was owing to the new opportunities opening up due to use of electronics innovatively and efficiently. Therefore, to keep up with the changing world, Indian electronics industry hit the trail in 1965, controlled by the Indian government. It was oriented towards defence and space initially but was soon followed with the consumer electronics. The government policies gave importance to electronics for efficient industrialisation and development of the nation. Since then, electronics sector found a prominent place in strategies for development of the nation leading to an electronics revolution all over the country. The years between 1984 and 1990 was considered to be the golden period because it witnessed speedy growth in the electronics industry (Rajya Sabha Secretariat, 2011).

With liberalisation and privatisation and industrialisation, the electronics industry continued to grow and contributed notably to the Indian economy. In recent years, the electronics industry has grown promptly and has surpassed $150 billion in 2010 (Rajya Sabha Secretariat, 2011). Also, India has become the greatest market for consumer electronics because of its high population which has also helped in growth of electronics industry.

In recent few years, introduction of liberal policies like Make in India, increase in FDI etc. and shift in the governance systems to e-governance, use of IT enabled services, improvement in quality of education has led to a greater inflow of the foreign companies to set up manufacturing plants, research and development centres etc. All of it has led to higher consumption of the electronics and electrical equipment. Higher consumption and obsolescence rates due to change in lifestyle, urbanization, technological development and increased purchasing power has led to massive growth in the amount of e-waste generated in the country. The business sector account for 78% of total computers sold in India. It is estimated that computers to be discarded will be around 1.38 million per year by 2007. The per capita generation is relatively lower in India i.e. lower than 1 kgpc, but owing to its gigantic population the total amount of e-waste generated is very high and increasing. There were 4.64 million desktops, 431 notes, and 89 thousand servers installed by the end of 2006 (Jahan & Begum, 2013). The Indian PC industry is estimated to grow at a rate of 25% per year. The e-waste generated in India was 3,80,000 tonnes for the year 2007 and was expected to surpass 800,000 tonnes by 2012. According to United Nations report (2015), 1.7 million tonnes of e-waste was generated in the year 2014 in India and is growing at a rate of 15% compounded annually. In the year 2009, 5.9 million tonnes of hazardous waste was generated in India and additional 6.4 million tonnes was imported. About, 1 to 2 million tonnes of the e-waste is generated within the country itself, while another 70,000 tonnes to 100,000 tonnes is imported annually. Out of the total e-waste generated in the country, almost 60% is accounted by only 65 cities. The status of top 10 e-waste generating states is listed in Table 2.3.

Table 2.1 Top 10 e-waste generating states (Research Unit, Rajya Sabha, 2011)

Sr. No.	State	Amount of e-waste generated (Tonnes)
1.	Maharashtra	20270.60
2.	Tamil Nadu	13486.24
3.	Andhra Pradesh	12780.30
4.	Uttar Pradesh	10381.10
5.	West Bengal	10059.40
6.	Delhi	9729.20
7.	Karnataka	9118.74
8.	Gujarat	8994.30
9.	Madhya Pradesh	7800.60
10.	Punjab	6958.50

Of the total e-waste generated in India, only 10% is recycled formally, rest is refurbished and stockpiled in landfills or incinerated, creating environmental problems and human-health hazard. As per records of Ministry of Environment and Forests (MOEF) published in Amar Ujala (2016), the authorised dismantlers and recyclers are dispersed throughout the country as shown in Fig. 2.5.
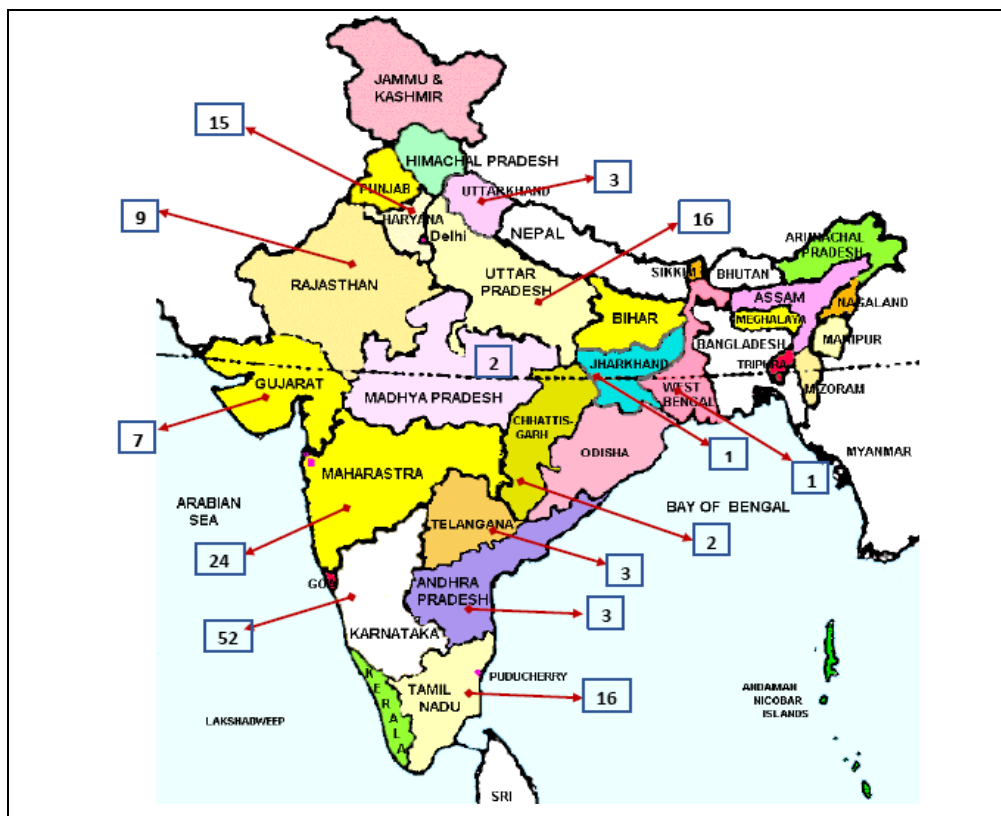
Figure 2.5 WEEE Recyclers in India (Amar Ujala, 2016)

There are 151 centres for e-waste recycling in India which can handle a maximum of 4,46,900 tonnes of e-waste that accounts for only 26% of e-waste generated in India. Out of the total e-waste, around 90% is valuable and can be recycled effectively (Rawat and Karade, 2017).

2.3 e-Waste Composition

Considering the wide range and complexity of the electronic equipment, it seems difficult and challenging to generalise composition of entire e-waste stream. However, most studies (Sodhi and Reimer, 2001; Cui and Forssberg, 2003; Widmer *et al*., 2005) have divided e-waste into six categories (on the basis of materials present): ferrous materials, non-ferrous materials, plastics, glass, wood, and other materials. The material-wise composition of e-waste is listed in Table 2.1.

Table 2.2 Composition of e-waste (Cui and Forssberg, 2003)

Materials	Content (% by mass)
Ferrous Metals	38
Non-ferrous Metals	28
Plastics	19
Glass	4
Wood	1
Others	10

The Association of Plastics Manufactures in Europe (APME) has also characterised e-waste as listed in Fig. 2.6.
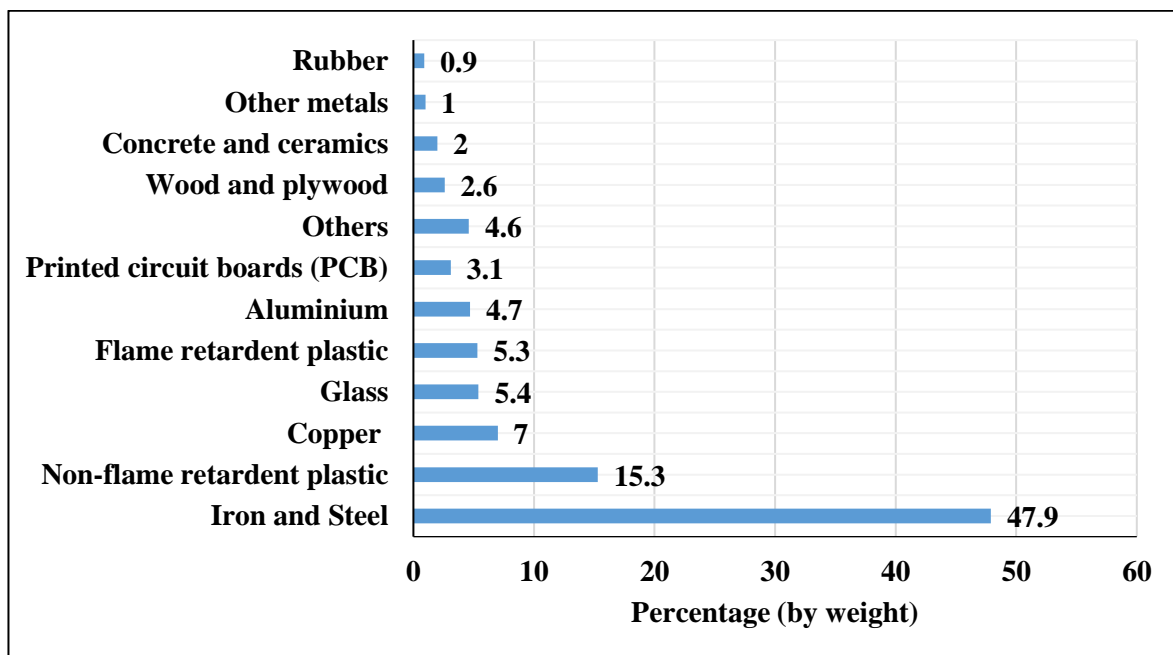
Figure 2.6 Distribution of components in e-waste (Widmer et al., 2005)

11

It can be said that iron and steel are the most abundant materials in the e-waste which acquires around 50 % of e-waste by weight. After iron and steel, plastics are approximately 21 % by weight and non-ferrous metals account for 13% of e-waste by weight (including 7% of copper). PCBs that accounts for 3.1% by weight of e-waste contains 30% ceramics, 30% plastics and 40% metals (Cui and Frossberg, 2003), while the composition published by Sodhi and Reimer (2001) is shown in Fig. 2.3. It can be said that PCBs contain 31% platics, 32% refractory oxides, 21% copper, 8% iron, 2% lead, 2% nickel, 2%aluminium and 2% other metals (Sodhi and Reimer, 2001). It is shown in Fig. 2.7.

Plastics used in EEE (electrical and electronics equipment) are generally Polyvinyl Chloride (PVC), Polyethylene (PE), Acrylonitrile butadienestyrene (ABS), Polystyrene (PS), Polypropylene (PP), Nylon and Polyamide (PA), Polyesters (PET and PBT), Polycarbonates (PC) and Elastomer (neoprene, SBR, silicone etc.) (Cui and Frossberg, 2003).

E-waste constitutes of about 63% metals out of which 50% is iron and steel and 13% is non-ferrous metals which includes copper, aluminium and precious metals like gold, silver, platinum, palladium and few others (Rajya Sabha Secretariat, 2011). The metals present in e-waste can be grouped into five major categories as follows:

a) Precious metals (PMs) – Gold (Au) and Silver (Ag)

b) Platinum group metals (PGMs) – Palladium (Pd), Platinum (Pt), Rhodium (Rh), Iridium (Ir), and Ruthenium (Ru)

c) Base Metals (BMs) – Copper (Cu), Aluminium (Al), Nickel (Ni), Tin (Sn), Zinc (Zn) and Iron (Fe)

d) Metals of concern (Hazardous in nature) (MCs) – Mercury (Hg), Beryllium (Be), Indium (In), Lead (Pb), Cadmium (Cd), Arsenic (As) and Antimony (Sb)

e) Scarce elements (SEs) – Tellurium (Te), Gallium (Ga), Selenium (Se) and Tantalum (Ta).

WEEE is classified as hazardous waste. WEEE contains over a thousand of different materials many of which are toxic in nature and creates environmental problems like air pollution and contamination of natural water resources when burnt in incinerators and disposed off in landfills. E-waste becomes hazardous due to presence of mercury, lead, selenium, hexavalent chromium, arsenic, cadmium and flame retardants in excess of the prescribed limits (Rajya Sabha Secretariat, 2011; Joseph, 2007).
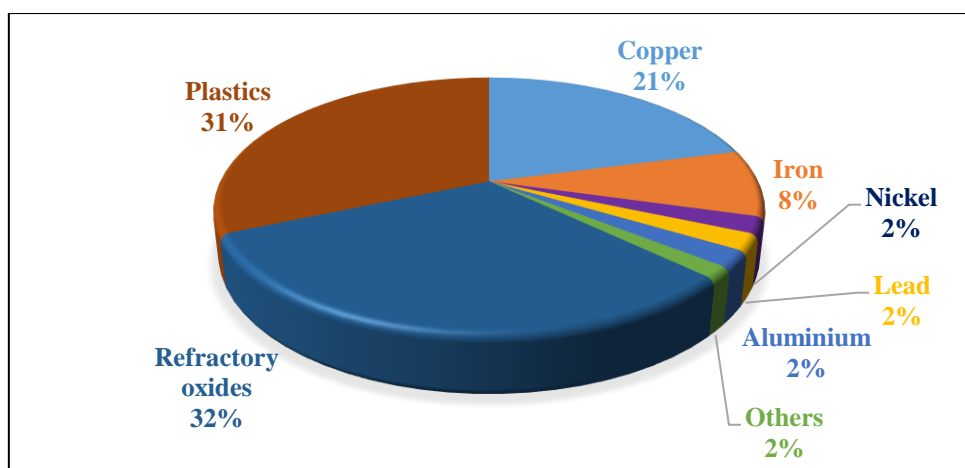
Figure 2.7 Components of E-waste (PCB) (Sodhi and Reimer, 2001)

The hazardous substances occurs mainly from condensers, transformers, PCBs, cooling unit, CRTs, batteries, lamps, LCDs, printer cartridges, PCBs, asbestos waste etc. The components and materials which possess an environmental and health hazard are presented in Table 2.2.

Table 2.3 Major hazardous substances in WEEE and their occurrences (Jahan & Begum, 2013; Cui and Forssberg, 2003)

Materials and Components	Description
Batteries	Heavy metals as lead, cadmium and mercury are present.
Cathode Ray Tubes (CRTs)	Lead in cone glass and fluorescent coating
Asbestos Waste	Asbestos sheet used in electrical boards
PCBs	Cadmium and lead are present in certain components.
Capacitors	Can contain polychlorinated biphenyls (PCB).
Appliances containing CFCs	CFCs are present in foam and refrigerating circuits.
HFCs	HFCs are present in refrigerating circuits
Gas discharge lamps	Mercury shall be removed
Printer Cartridges	Should be treated separately
Medical equipment, switches, mobile phones, sensors, thermostat, relays	Contains mercury
Zinc sulphide	Used in CRT screens
Toxic organic substances	Used in condensers and CRTs
Chromium (VI)	Present in data tapes, floppy disks

The metals make 60% of the e-waste, plastics accounts for 30% and pollutants comprises only about 2.7% (Widmer *et al.,* 2005).Thus, maximum care should be taken during handling and recycling so as to minimise the risk to environment and human-health involved in disposal of e-waste or WEEE.

2.4 e-Waste Hazards

E-waste is classified as hazardous by Basel Action Convention, European directives (2002/96/EC and 2012/19/EU), MOEF, and "The hazardous wastes management and handling rules, 2003 given by CPCB". Anything is classified as hazardous when any of the component due to its physical, chemical, explosive, toxicity, corrosive nature and reactivity is likely to cause harm to environment and human or animal health alone by itself or in liaison with other substances (Patil and Sharma, 2013).

All the electronic and electrical equipment are composed of components that are hazardous in nature due to use of toxic elements like lead, mercury, biphenyls, brominated flame retardants, cadmium, selenium etc. Major hazards by the elements and occurrences are listed in Table 2.4.

The problems arises when WEEE is treated informally or by use of cheap and primitive measures for recycling. There are plentiful ways in which e-waste possesses threat to the ecosystem. If the acids or sludge obtained from acid treatment of e-waste are discharged into soil causes acidification, and loss of fecundity and also water resources can be contaminated by the discharge into water streams. Incineration can lead to emission of toxic fumes and gases in the air which is harmful to both human health and environment. One of the processes that poses high threat to environment is open burning of PCBs and wires, to reclaim metals, degrades air quality to a great extent. When plastics and other components are land filled, mercury, lead, cadmium and few other toxic elements may leach to soil, air and to ground water resources, polluting them and posing a health hazard if that water is consumed. About 70% of the toxic heavy metals present in landfills are due to disposal of WEEE in landfills. Therefore, proper recycling is of great importance for e-waste.

Table 2.4 Hazards of WEEE (Jahan & Begum, 2013; Rajya Sabha Secretariat, 2011)

Elements/compounds	Occurrences	Hazards
PVC (Poly Vinyl Chlorides)	Cable insulation	Releases dioxins and furans which can cause reproductive problems, cancer and damage to immune system.
Chloroflouro carbon (CFC)	Insulation and cooling component	Combustion of halogenated substances releases toxic gases.
Polychlorinated biphenyls (PCBs)	Capacitors, transformers	Carcinogenic, effects immune system, reproductive system, endocrine system etc.
PBDE*, TBBA*, PBB*	Fire retardants and Plastics	Poisonous when burnt and can cause long term injuries
Arsenic	Semiconductors, Microwaves, Light emitting diodes (LEDs), Solar cells	Long term exposure caused severe injuries, acutely poisonous
Barium	Electron tubes, filler for rubber and plastics, CRTs, lubricants	Explosive gases may develop on wetting
Cadmium	Batteries, pigments, solder, alloys, PCBs, printer inks, cathode ray tubes (CRTs)	Poisonous and injurious to health on long term basis
Chromium (VI)	Floppy disks, dyes, solar insulators	Allergic, poisonous and injurious to health on long term basis
Lithium	Batteries of mobile phones, photographic equipment etc.	Explosive gases may develop on wetting
Mercury	LCDs, switches, steam irons, Fluorescent lamps, pocket calculators	Acutely poisonous and injurious to health on long term basis
Nickel	Rechargeable battery, CRTs, alloys, relays, pigments, semiconductors	Allergic
Lead	Batteries, CRTs, printed circuit boards, solar transistors, PVC	Damages circulatory system, nervous system, kidneys, and may cause debility in children
Beryllium	Power supplies, rectifiers	Carcinogenic, causes lung diseases.

*PBDE-Polybrominated diphenyl ethers, *TBBA-Tetrabromo-bisphenol-A, *PBB-Polybrominated biphenyls

2.5 e -Waste in Concrete

Attempts to replace cement and aggregates with finely ground e-waste plastics have been made. This can reduce the cost of construction, reduction in landfill cost, energy saving, and can reduce the environmental hazard and pollution. There are no attempts made to use metallic powder from e-waste in either mortar or concrete.

Plastic from e-waste (printed circuit boards) increases air content, improves water retention, and decrease the bulk density of hardened mortar or concrete (Panneerselvam and Gopalakrishana, 2015).

The plastics mainly used in concrete are:

1. Virgin polypropylene
2. Recycled plastic (melted processed)
3. Recycled plastic (automobile shredded residue)
4. Recycled plastic (shredded)

Plastics can be recycled by mechanical recycling, chemical recycling, thermal recycling or by few other methods like dissolution/reprecipitation (Poulakis and Papaspyrides, 1997), radiation technology (Burillo *et al.,* 2002), melt-processing (Mantia and Gardette, 2002), cryo-comminution (Gente *et al.,* 2004). Mechanical recycling of plastics has less environmental burden than energy recovery and is more attractive option of recycling (Dodbiba *et al.,* 2008).

2.6 Effect of e-waste on concrete and mortar properties

2.6.1 Bulk Density

Al-Manaseer and Dalal (1997) used angular post-consumer plastic aggregate shredded with maximum size of 13 mm and observed that bulk density of concrete decreased with increasing content of plastics. This is mainly due to the lower density of plastic i.e. 485 kg/m^3 dry-rodded (Al-Manaseer and Dalal, 1997, Choi *et al.*, *2005)*. Volume replacement of aggregates by 10%, and 20% plastic aggregates reduced density of concrete by 32%, 12%, 4.8% and 4.34% as found by Wang *et al.* (2012), Kariminia et al. (2014), Kumar and Baskar (2014), and Alagusankareshwari et al. (2016), respectively (Fig. 2.8).
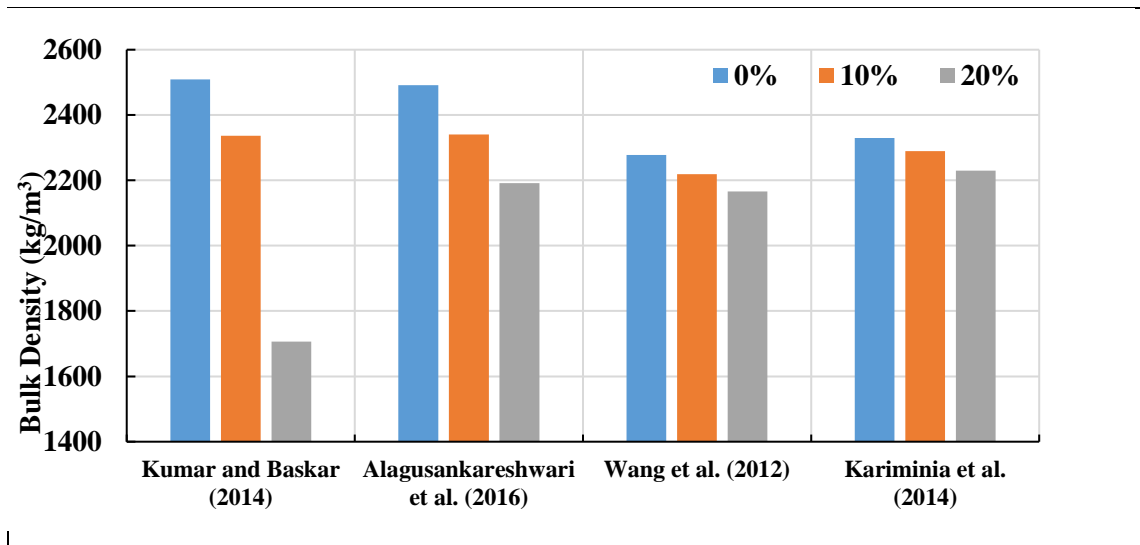
Figure 2.8 Effect on bulk density by addition of plastic aggregates

2.6.2 Workability

Various researchers studied the effect of incorporation of plastics on air content/entrainment in concrete. Wang *et al.* (2012) found that the air content increases with the content of e-waste plastic incorporated in the concrete. The air content has increased from 9% to 28% when the e-waste plastic content rises from 0 to 25%.
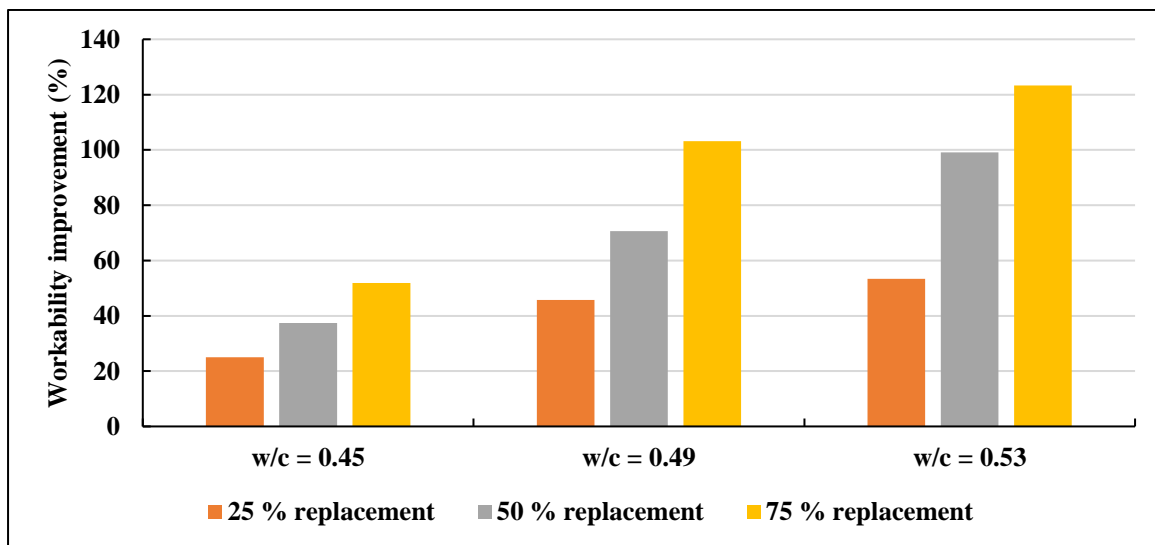
Figure 2.9 Workability improvement with plastic replacement (Choi *et al.*, 2005)

Soroushian *et al.* (2003) added recycled plastics to concrete and observed a decrease of about 2% in the air content and 56% in consistency relative to control specimen. Al-Manaseer and Dalal (1997) determined slump for concrete with 10, 30, and 50 % plastic aggregates and observed the similar results.

Choi *et al.* (2005) used recycled aggregates from PET bottles and found an increase of 123% in workability of concrete at 0.53 water cement ratio, due to spherical shape of recycled aggregates and nearly zero water absorption (Fig. 2.9). The reduction of 25% in **slump value** was observed when ground plastic was used to replace fine aggregates by 20% to prepare concrete (Batayneh *et al.*, 2007). Choi *et al.* (2009) also used recycled PET bottle aggregates in mortar and found that flow value showed a linear increase with increase in replacement ratio (Fig. 2.10). In fact, flow value increased by 16% with 100% aggregate replacement.
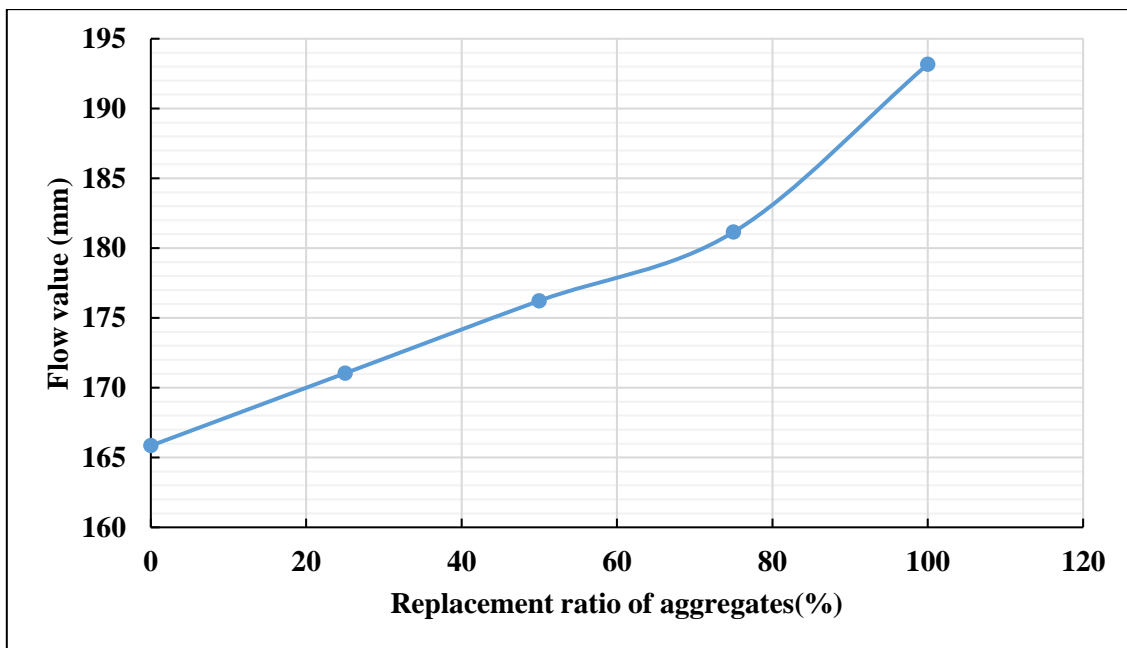
Figure 2.10 Evaluation of flow value (Choi *et al.*, 2009)

2.6.3   Compressive Strength

Al-Manaseer and Dalal (1997) found a decrease of 68% in the compressive strength with 50% replacement of coarse aggregates using plastics (Fig. 2.11). It was due to the fact that plastics themselves has low strength and poor bond with cement composite compared to the natural aggregates. Also, the rate of reduction of strength was found to decrease with increase in plastic content. But, the ductility of concrete has increased with addition of plastic fibres.
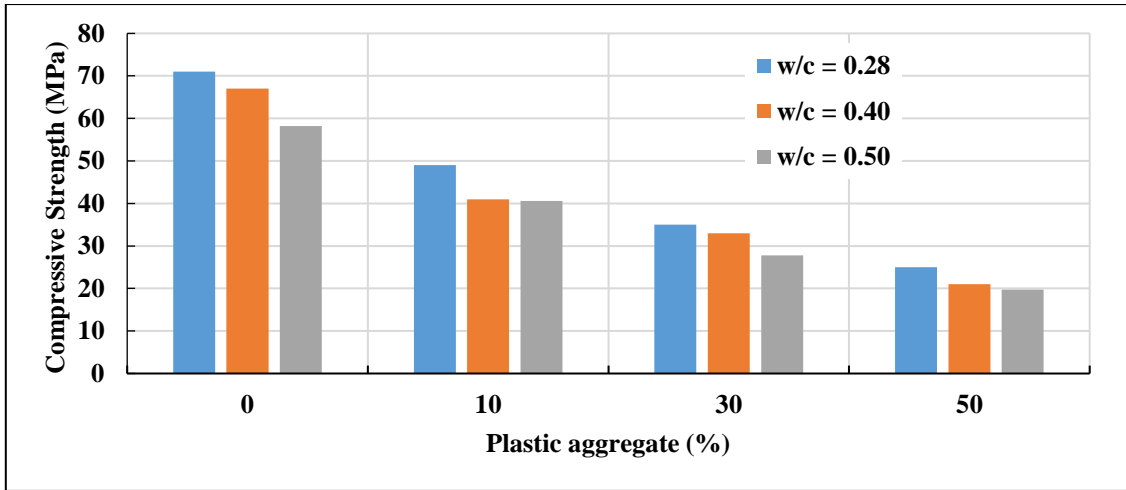
Figure 2.11 Compressive strength vs. plastic aggregates content (Al-Manaseer and Dalal, 1997)

Choi *et al.* (2005) added recycled aggregates from PET bottles plastic in concrete and observed that compressive strength decreased by 33% with replacement level of 75% plastic aggregates but it increased when plastic aggregate content was kept constant and water-cement ratio was decreased. On incorporation of recycled plastic aggregates in mortar with replacement percentages of 0%, 25%, 75 % and 100%, compressive strength reduced by 42% with 100% replacement ratio (Choi *et al.*, 2005). Wang *et al.* (2012) used PCBs non-metallic powder with 0%, 5%, 15%, 20% and 25% by weight of cement as additive in mortar and found that compressive strength decreased by 67% when 25% powder was added (Fig. 2.12). A reduction of 72% and 23% in compressive strength of concrete was observed when ground plastic replaced fine aggregates by 20% and 5%, respectively (Batayneh *et al.* 2007).
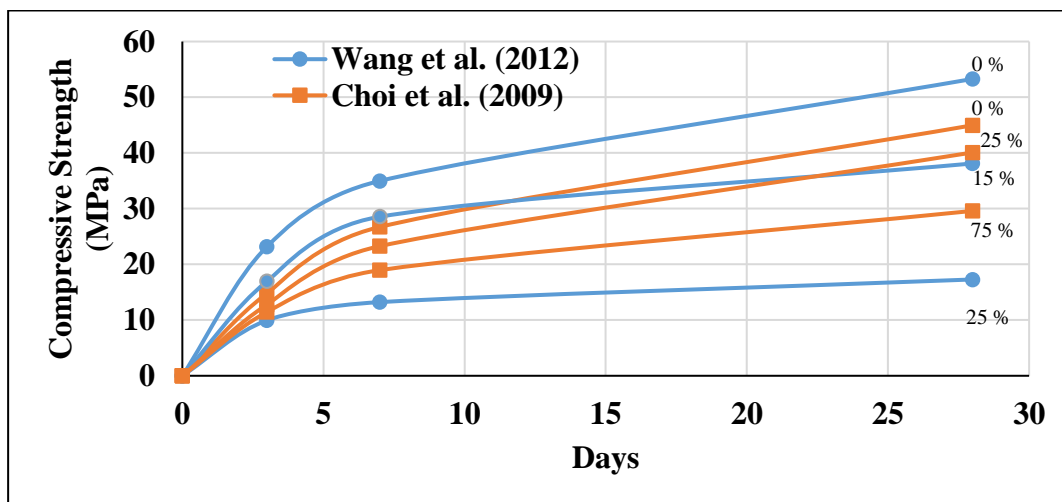
Figure 2.12 Variation of compressive strength of mortar with age and percentage replacement

19

Marzouk *et al.* (2007) concluded that by addition of plastic aggregates (granulated and shredded PET) till 50% with size smaller than 5 mm did not affect compressive strength. He also suggested that use of shredded plastic can bring down the construction cost and help reduce the environmental hazard that these plastics carry. Lakshmi and Nagan (2010) also found similar results when the use e-waste plastic for replacement of coarse aggregate. Compressive strength decreased by 18% at 16% replacement was done. But on only 9% on incorporating 10 % fly ash and 16% e-waste plastic (Fig. 2.13).
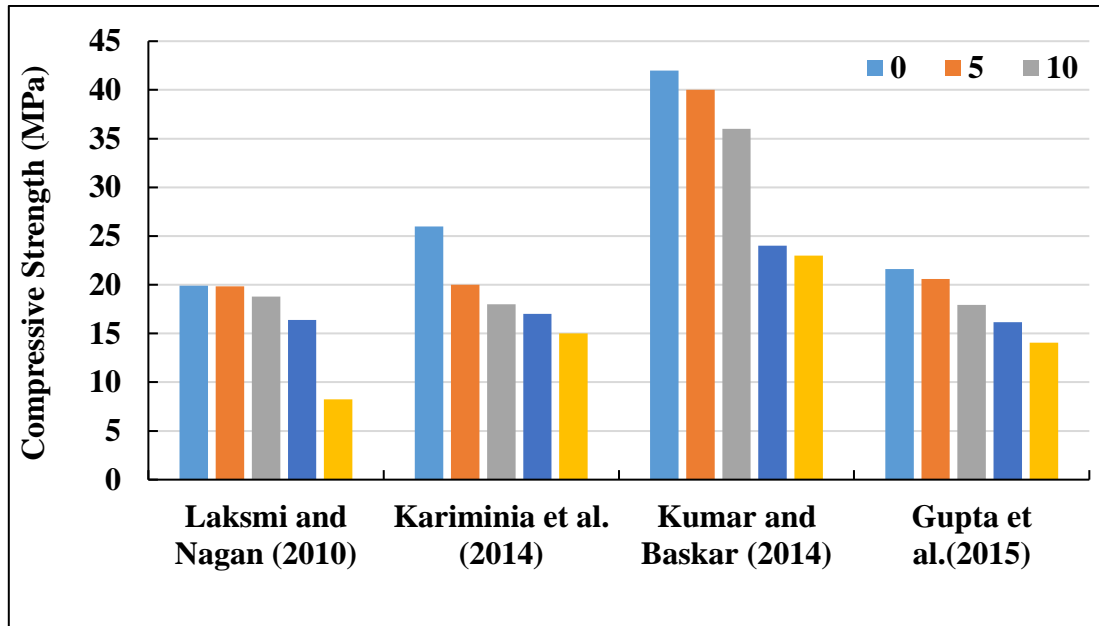
Figure 2.13 Effect of plastic addition (%) on compressive strength

2.6.4 *Split Tensile Strength*

Split tensile strength decreased with increase in the plastic aggregate content as observed by Al-Manaseer and Dalal (1997) and for a constant plastic aggregate %age, the split tensile strength decreased by 53% with 50% replacement of aggregates and the failure was found to be more ductile relative to the control specimen (Fig. 2.14). They also found that split tensile strength decreased by 17% and 53% when plastic aggregate content was 10% and 50%, respectively. Choi *et al.* (2005) studied the effect of PET bottle light weight aggregate and recorded 40.6 % decrease in split tensile strength with 75 % replacement of aggregate at a w/c ratio of 0.49 and if aggregate content was kept constant, the split tensile strength increased with decreasing water-cement ratio. Lakshmi and Nagan (2010) found that there was 29 % decrease with 16 % e-waste plastic replacement and only 2 % decrease when 10 % fly-ash was also incorporated.
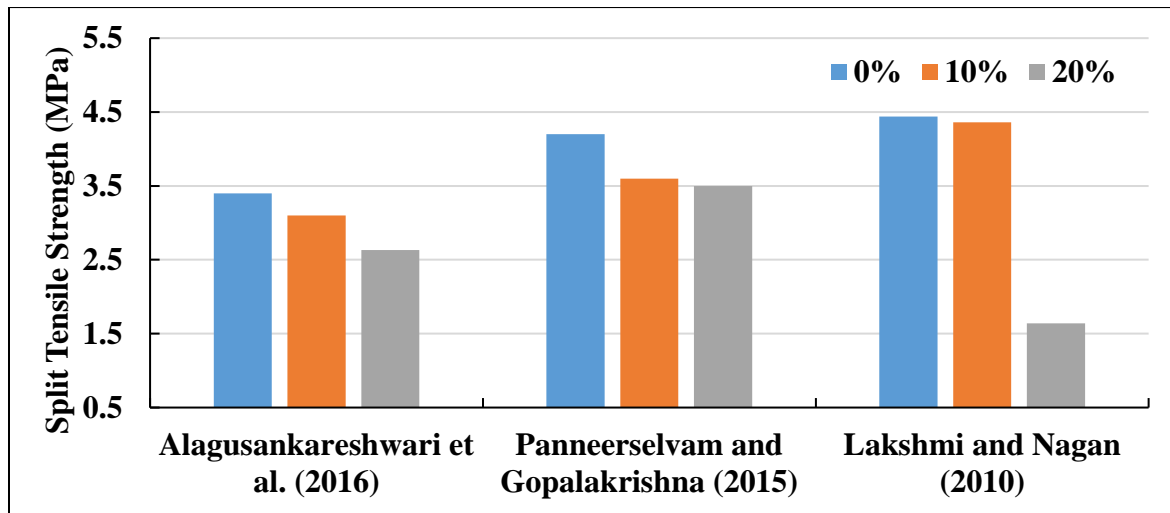
Figure 2.14 Split tensile strength vs. plastic aggregate (%)

Al-Manaseer and Dalal (1997) reported that **modulus of elasticity** decreased with increase in plastic aggregate content. With 50 % plastic aggregates, modulus of elasticity was around 8.6 GPa and was 24.3 GPa with no plastic aggregates. On keeping the %age of aggregate constant the modulus of elasticity decreased with increase in water-cement ratio. Similar, result were published by Choi *et al.* (2005) when he used PET bottle light weight aggregates in concrete.

Al- Manaseer and Dalal (1997) also found that ductility of concrete has increased by replacement of coarse aggregates by plastic. The modulus of elasticity of concrete has reduced as shown in Fig. 2.15.
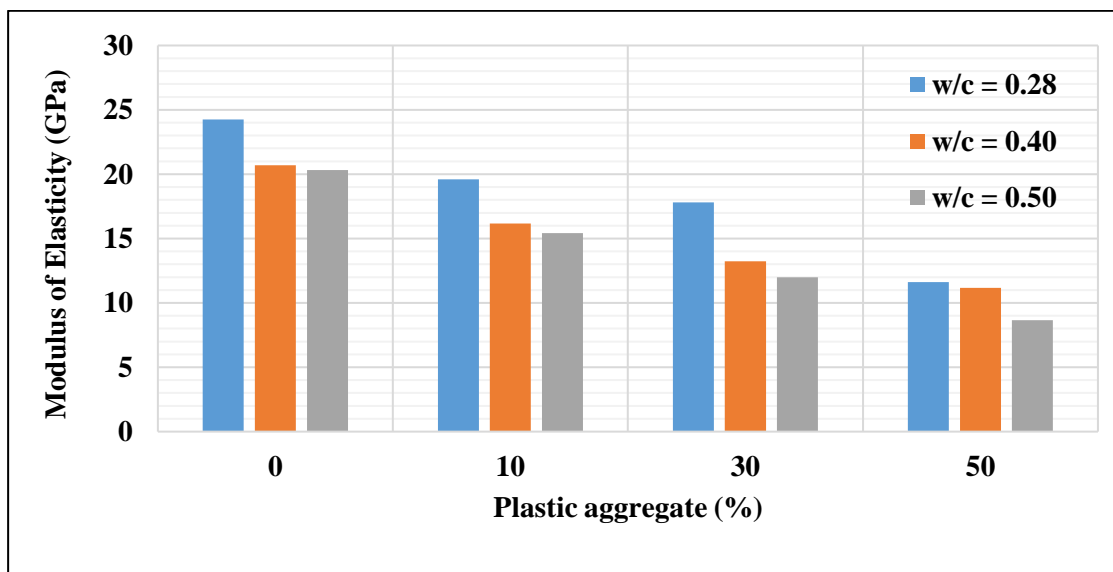
Figure 2.15 Evaluation of modulus of elasticity (Al-Manaseer and Dalal, 1997)

21

From the above discussion, it can be concluded that the utilisation of plastic as aggregates in concrete has led to the decrease in the bulk density by 2.5 to 13 %, compressive strength by 34 to 64 % by using recycled plastic aggregates ranging from 10 to 50 %. Similar trend observed for split tensile strength but there was increase in the toughness index and ductility of concrete. Use of discrete reinforcement derived from shredded mixed plastic, milled plastic particles and melt processed plastics resulted in significant gain in impermeability and shrinkage cracking. Metallic fraction which constitutes of copper, aluminium, iron, lead, zinc etc. can be used to make conductive cementitious composite which can be used in cathodic protection and ground-earthing. The use of metals from e-waste is advantageous as it has a massive energy savings when compared to the used virgin materials and other benefits listed in Table 2.5.

Table 2.5 Energy savings of recycled materials over virgin materials (Cui and Forssberg, 2003)

Metals	Energy saving (%)
Aluminium	95
Copper	85
Iron and steel	74
Lead	65
Zinc	60
Paper	64
Plastics	> 80

2.7 Corrosion in RC Structures

Usually, the destructive interaction between environment and RC structures which leads to the decrease in the service life by degradation of materials is called corrosion. The major causes of corrosion are inefficient design, poor construction techniques, inadequate materials selection, and exposure to more severe environmental conditions than expected (Broomfield, 2007).

2.7.1 Significance of Corrosion

Concrete is the most adaptable, economical and most widely used construction material and Reinforced Concrete (RC) structures are an integral part of infrastructure of any country which is essential to the quality of life, industrial productivity, international competitiveness and security. RC is also one of the most durable material when compared to steel, timber etc. performing adequately throughout its service life. But, in certain cases RC structures do not perform adequately as expected up to its service life. Generally, structural and non- structural

22

factors that can adversely affect are considered during design stages. Structural factors mainly includes mechanical loading conditions, abrasion, erosion and the type of loads that can come over a structure during its life time. Non-structural factors includes mainly the interaction of structures with the surrounding environment which may influence the durability of the structure by chemical and physical action (Neville, 2013).

The serious consequences of corrosion has made it a problem of great significance. Apart from the problems that we encounter daily due to corrosion, it might cause plant shut downs, waste of valuable resources, materials and energy, contamination of product, reduce in efficiency, increased maintenance cost, expensive design and can also imperil safety, inhibits technological progress and have negative impact on health and environment (Roberge, 2000; Javaherdashti, 2000). However, in many studies impact of corrosion is often described in terms of economic loss. The financial losses can be grouped in two categories namely direct losses and indirect losses. In a financial corrosion study (Broomfield, 2007), the direct losses on US highway bridges was estimated to be $12 billion involved in capital cost and maintenance of super and sub-structures. Indirect costs that mainly considered delays of traffic were calculated to be more than ten times of direct costs. Corrosion leads to direct and indirect economic losses. The economic cost of corrosion losses is estimated to be 3 % of the world's GDP i.e. USD 2.2 trillion (Hays, 2010). In the Indian context so far there was no corrosion auditing but it is reported in CORCON – 2015 (International Conference on Corrosion held in Chennai) that around Rupees 6 lakh crores is lost in India every year due to corrosion in terms of energy, resources and life. Out of the total loss, ₹ 2 lakh crores is lost due to corrosion of infrastructure (Press Trust of India, 2016). Also it can be said, corrosion causes loss of almost 6% of the India's GDP annually which equalizes to the revenue generated by the Indian railways (Bhargav, 2014). Therefore, corrosion is a serious issue that should be taken care of with the ageing of the RC structure (Apostolopoulos and Papadakis, 2008).

2.7.2   *Corrosion of Steel in Concrete – An Electrochemical Process*

Corrosion is a complex electrochemical phenomena which requires flow of current from cathodic region to anodic region through the electrolyte. The three necessary elements for setting up of a corrosion cell are anode, cathode and electrolyte. The anodes and cathodes are connected by the steel bar itself through which electronic current flows. The anodic and cathodic region can be on the steel reinforcement bar and the electrolyte is concrete. Concrete is alkaline in nature due to the formation of portlandite ($Ca(OH)_2$) and other alkaline

hydroxides of Na, K etc. which leads to high pH of pore water (12.6-13.5) in concrete (Neville,2013).

The alkaline environment leads to the development of a passive layer over the steel surface. This passive layer mainly consists of γ- Fe_2O_3 and few other oxides and oxyhydroxides tightly adhering to the steel surface (Neville, 1995). This passive film is only a few nanometers thick and is composed of hydrated ferrous (Fe^{2+}) and ferric (Fe^{3+}) oxides. Though, this passive layer is strong enough to resist mechanical damage of steel surface and it is destroyed when concrete gets carbonated or by ingress of chloride ions (Bertolini *et al.*, 2004). The destruction of the passive layer is termed as depassivation. The depassivation will lead to corrosion of steel reinforcement (Anwar *et al.*, 2014; Apostopoulos and Matikas, 2016).

Every metal has a tendency to go back to its native and more stable ore state in a suitable environment, leading to corrosion. The chemical reactions involved in corrosion of steel bar in concrete are almost similar whether corrosion occurs due to carbonation or chloride contamination. The steel dissolves in water present in pores of concrete and releases electron in the anodic reaction as shown below:

Anodic reaction (oxidation):

$$Fe \longrightarrow Fe^{2+} + 2e^-$$ ……………….. (2.1)
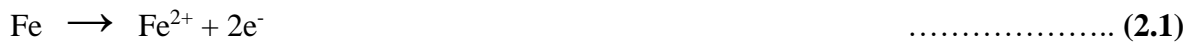
To maintain electrical neutrality, these electrons should be consumed at some other site making it a cathodic site. These electrons migrate through the steel bar to the cathodic site and combines with oxygen and water to form hydroxyl ions.

Cathodic reaction (reduction):

$$2H_2O + O_2 + 4e^- \longrightarrow 4OH^-$$ …………… (2.2)

These reactions do not lead to spalling or cracking of concrete. The ferrous ion reacts with hydroxyl ion to produce ferric hydroxide and is then hydrated due to presence of water to produce rust. The chemical equations involved are (Broomfield, 2007):

$$Fe^{2+} + 2OH^- \longrightarrow Fe(OH)_2$$ …………… (2.3)
<center>Ferrous hydroxide</center>

$$4 Fe(OH)_2 + 2H_2O + O_2 \longrightarrow 4 Fe(OH)_3$$ …………… (2.4)
<center>Ferric hydroxide</center>

$$2 Fe(OH)_3 \longrightarrow Fe_2O_3{\cdot}H_2O + 2H_2O$$ ……….…….(2.5)
<center>Hydrated ferric oxide (rust)</center>
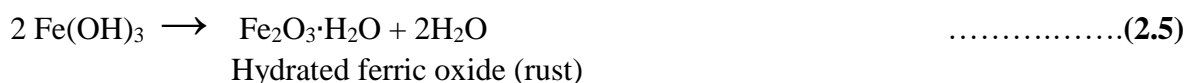
The corrosion process is sketched as shown in Fig. 2.16.
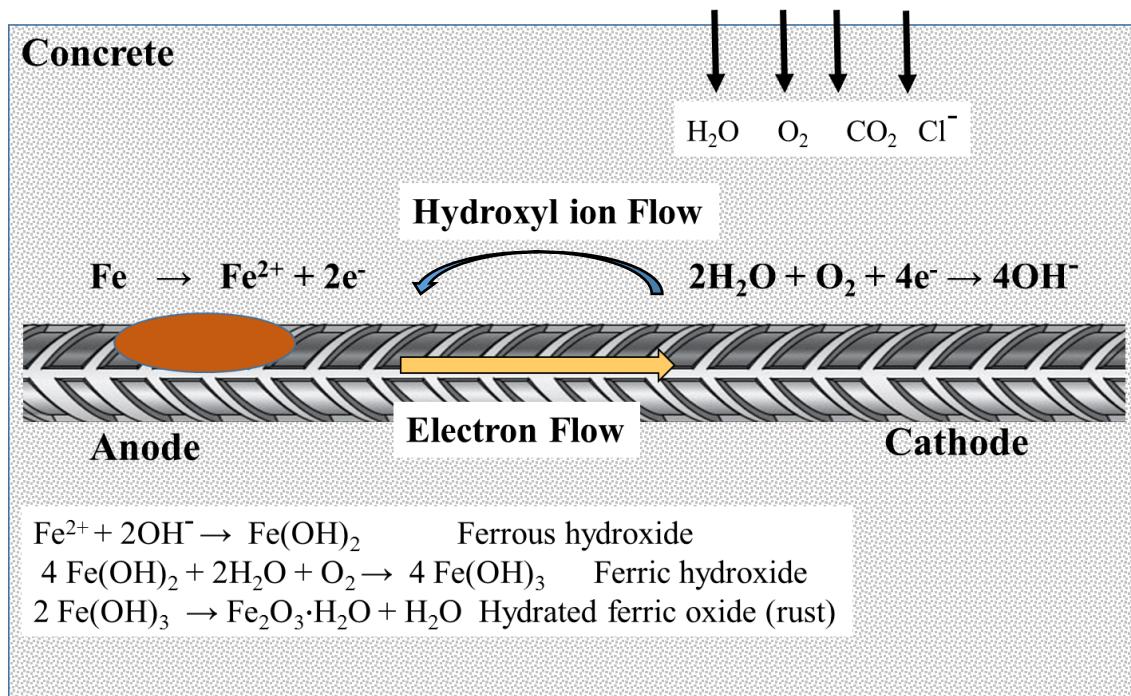
Figure 2.16 Schematic illustration of the corrosion of reinforcement steel in concrete as an electrochemical process (Ahmad, 2003)

Unhydrated ferric oxide usually occupies twice the volume of steel corroded. This volume can increase to six to ten times to that of the steel consumed when hydrates (Broomfield, 2007). Due to the increase in volume, tensile stress (radial stresses) will be exerted on the concrete and will lead to cracking and spalling. If corrosion rate is slow i.e. low current density, the production of corrosion products will be slow and the dissipation of corrosion products can take place with time reducing the radial stresses at concrete/steel interface in such cases (El Maaddawy and Souodki, 2003). Most of the times rust stains appear on the surface after cracking due to leaching of corrosion products.

The corrosion of steel embedded in concrete can be divided in to two main phases: initiation and propagation. In the initiation phase, the steel bar is still covered with passive coating but depassivation can start due to carbonation of concrete or ingress of chloride ions in concrete and near the steel concrete interface. The second stage is the propagation of corrosion on the steel surface to a limit where it cannot get passivated again and beyond it corrosion can have severe consequences. The corrosion initiation and propagation is shown in the Fig. 2.17.
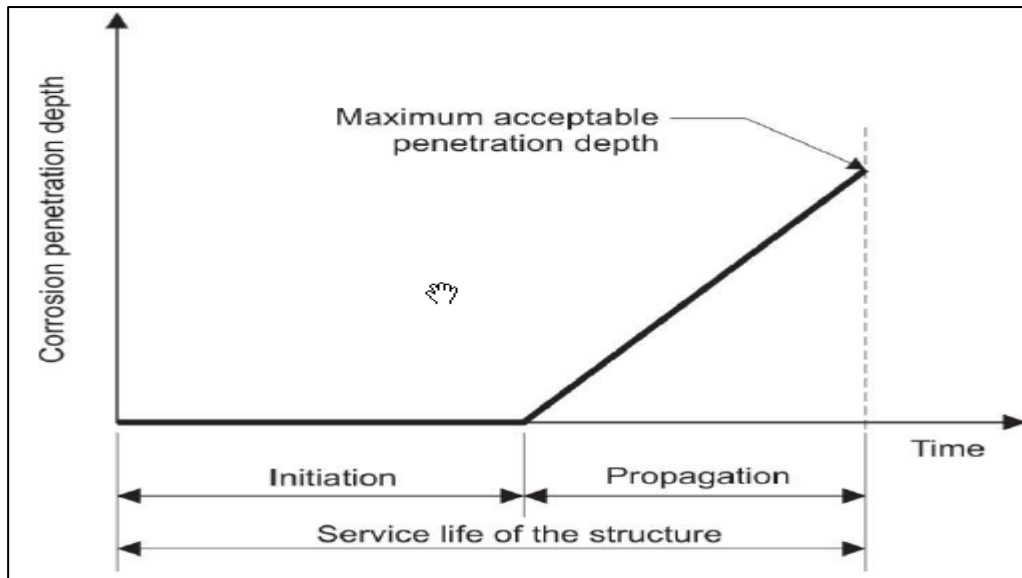
Figure 2.17 Initiation and propagation periods for corrosion in RC structures (Bertolini *et al.,* 2004)

2.9.1 Mechanism of Steel Corrosion in Concrete

The corrosion of steel in concrete occurs by two mechanisms. The two mechanisms are explained in the sections below.

2.9.2 Corrosion due to carbonation

Carbonation is the reaction of carbon dioxide gas present in the atmosphere with the alkaline hydroxides present in concrete pore water to produce carbonic acid and tends to neutralise the pH of concrete. Alkaline hydrates present in concrete like $Ca(OH)_2$, CSH gel, alkali hydroxides reacts readily with the carbonic acid produced. The reaction that occurring in concrete can be written as:

$$CO_2 + H_2O \rightarrow H_2CO_3 \text{ (Carbonic acid)} \qquad\qquad \text{……………} \textbf{(2.6)}$$
$$H_2CO_3 + Ca(OH)_2 \rightarrow CaCO_3 + 2H_2O \qquad\qquad \text{…………….} \textbf{(2.7)}$$

The productions of carbonic acid leads to lowering of pH generally < 9.5 and can approach to neutrality (Bertolini *et al.,* 2004; Broomfield, 2007). Carbonation can lead to lowering of pH and increase in the corrosion rate (Neville, 1995). A secondary effect of carbonation is freeing of the bound chlorides that were in form of calcium chloro-aluminate hydrate. The liberation of chloride can make the environment near rebars more aggressive (Bertolini *et al.,* 2004). The effect of carbonation on a reinforced structural element is depicted in (Fig. 2.18).

26
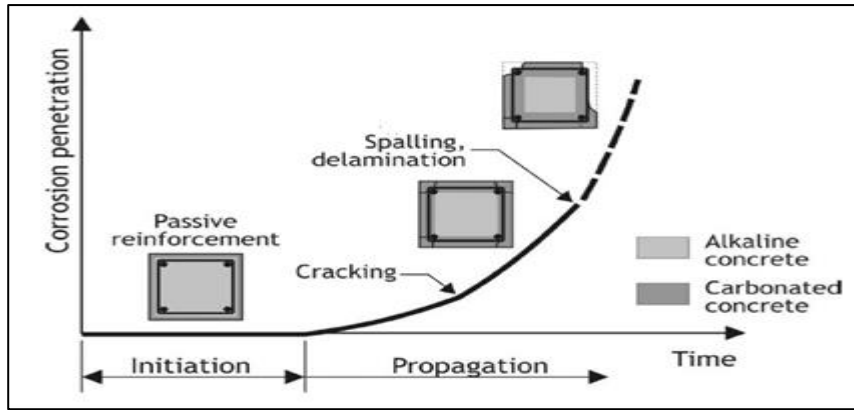
Figure 2.18 Schematic diagram showing the effect of carbonation on life of reinforced structural element (Bertolini, 2008)

2.9.3 Chloride attack mechanism

During carbonation, the pH of concrete is lowered and the passive layer gets destroyed. But, in case of chloride ion, they directly attack the passive layer and destroys it at a particular point where corrosion starts (Neville, 2013; Apostopoulos and Matikas, 2016). There is no neccarily drop in pH of water present in pores of concrete away from the steel. There is a particular level under which there is no danger of corrosion to steel reinforcement called chloride threshold. If the concentration of chloride ions exceeds this threshold value, the passive layer gets locally destroyed and it leads to localized pitting corrosion (Bertolini *et al.*, 2004).

Chloride ions activate the surface of the steel to form an anode, the passivated surface being the cathode. The reactions involved are as follows:

$$Fe^{2+} + 2Cl^- \rightarrow FeCl_2 \qquad \text{................... (2.8)}$$

$$FeCl_2 + 2H_2O \rightarrow Fe(OH)_2 + 2HCl \qquad \text{................... (2.9)}$$
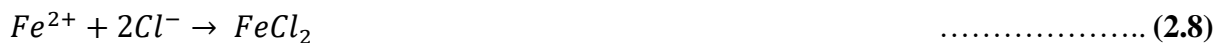
Total chloride content is not relevant to corrosion. Some of chlorides are acid soluble chloride which is equal to the total amount of chloride present in the concrete or that is soluble in nitric acid, others are bound chloride which is the sum of chemically bound chloride with hydration products of the cement, such as the C_3A or C_4AF phases, and loosely bound chloride with C–S–H gel. It is only the remaining chlorides, namely, free or water-soluble chloride which is the concentration of free chloride ions (Cl^-) within the pore solution of concrete, and is extractable in water under defined conditions and are available for the aggressive reaction with steel (Ahmad, 2003).

Chloride ingress can lead to localised corrosion, also called pitting. During pitting, a very aggressive environment is produced near to the steel bars and due to current flowing in to the pits, more chloride ions migrate towards the pit and lowering the alkalinity. Severe localised corrosion can occur if oxygen contents are low inside concrete (Apostopoulos and Matikas, 2016). A schematic representation of pitting corrosion is given in Fig. 2.19.
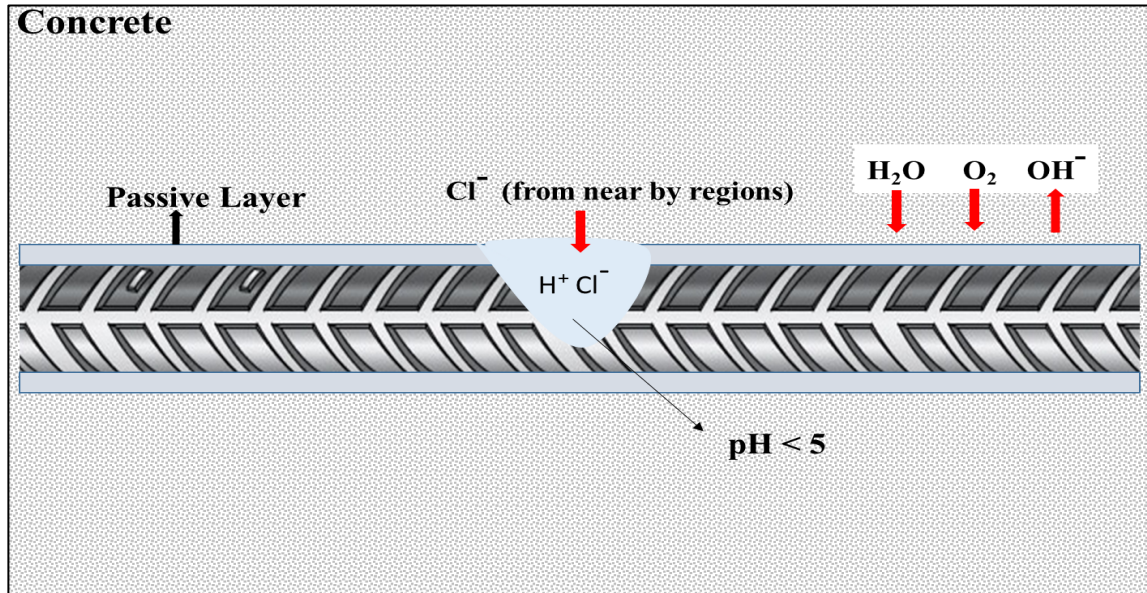
Figure 2.19 Pitting corrosion due to chloride ions (Broomfield, 2007)

BS 8110: Part 1(1997) and BS 206 (2000) gives acceptable levels of total chloride as 0.4% by mass of cement. While, ACI 318(2014) has recommended to consider water-soluble chloride ions only and has limited them to 0.15% by weight of cement. IS 456 (2000) has prescribed the limit of total acid soluble content of chloride ions to 0.6 kg/m^3 by weight of cement at the time of placing.

There can also be a synergistic action of carbonation and chloride attack. This can release the bounded chloride by breaking of chloro-aluminates and thus increases the concentration of chlorides ahead of carbonation front. This increase in chloride concentration can cause increase in corrosion (Broomfield, 2007).

Corrosion may lead to loss of strength and ductility of the steel bars which is a matter of concern for areas having high level of seismicity (Cairns *et al.*, 2005; Du *et al.*, 2005; Apostolopoulous and Papadakis, 2008; Lee and Cho, 2009).

2.8 Techniques for Corrosion Control in RC Structures

Different techniques that are used to control corrosion and repair of RC are categorised into two classes. They are conventional repair methods and electrochemical methods. Conventional repair methods involve removal of affected concrete and replacement with new alkaline concrete, patching, coatings, sealers, membranes and barriers, encasement and overlays, use of corrosion inhibitors, using alternative corrosion resistant reinforcing bars. These are generally a local solution to corrosion and can lead to acceleration of corrosion in the nearby repaired areas. After a serious damage, these are generally a costly and less-effective methods. Electrochemical repair techniques includes cathodic prevention, cathodic protection, electrochemical chloride extraction, and realkalisation (Roberge, 2000; Bertolini *et al.*, 2002; Broomfield, 2007).

In electrochemical techniques, the chemical reactions and current flow due to corrosion is suppressed by application of an external DC supply with the help of an anode (temporary or permanent), along with a monitoring and control system.

2.8.1 Conventional Techniques

Conventional repair techniques are very expensive and time consuming. In case of chloride affected structures, often large amount of contaminated concrete needs to be removed to prevent the further initiation of the corrosion. Patch repair is one of that conventional techniques used as a short-term remedy against corrosion. Once patch repair is done, the chloride ions can be present in the surrounding area of repair. This causes accelerated corrosion of the surrounding reinforcement bars. Hence further periodical repair needed for the structure to attain the required service life. Electrochemical incompatibility between the repair material and the old concrete is also a concern. Epoxy bar coating is also used to isolate the steel bar from the moisture, chlorides and oxygen. It is very difficult to attain 100 % coverage in this treatment, also it contaminates the adjacent concrete surfaces with epoxy and accelerated corrosion can takes place if the bars are only partially coated (Chess *et al.*, 1998).

Conventional repair techniques uses heavy machinery, is labour intensive and costly, and provides momentary protection (Polder and Peelen, 2014).

2.8.2 Electrochemical Techniques

The current review concentrates on electrochemical techniques which are used for repair in the corrosion affected RC structures. Various methods are in practice for corrosion prevention and

protection like cathodic protection, cathodic prevention, electrochemical chloride extraction and electrochemical realkalisation. Although, out of these cathodic protection and prevention is the best suited technique for RC structures which are carbonated and contaminated with chlorides. So, this review mainly focuses on cathodic protection and prevention of steel in RC structures.

2.8.2.1 Cathodic Protection (CP)

Cathodic protection is a reliable, relatively economical and most effective way of protection and controlling corrosion in RC structures which are contaminated with chloride and carbonated (Pedeferri, 1996; Jing and Wu, 2009; Polder and Peelen, 2014; Byrne *et al.*, 2016;). Cathodic protection is cheaper, easier, can treat a larger area simultaneously and most importantly does not give rise to incipient anode problems. Therefore, it is most suited repair technique to be employed in chloride contaminated structures (Broomfield, 2007).

2.8.2.2 History of Cathodic Protection

The development of cathodic protection over the years can be divided into three phases: pioneering phase, developmental phase and maturity phase (Polder and Peelen, 2014).

a) Pioneering Phase (1970-1990)

It started when Stratfull showed the effectiveness of the technique and the applications started on bridges in America in the year 1974 (Stratfull, 1974). This phase mainly emphasised on development of new feeding and monitoring systems. Also, the design and protection criteria were defined for concrete structures and it was proved that cathodic protection could be the effective solution to the corrosion problem in concrete (Pedeferri, 1996). In mid-80s, CP was introduced in Europe and a similar revolution broke out supporting development of different meshed anodes based on conductive polymeric materials, mixed metal oxide titanium anodes and overlays like conductive paints etc. Anodes were made of polymer cables with a copper wire, activated titanium mesh or conductive coatings were used as anodes (Polder and Peelen, 2014).

b) Developmental Phase (1991-2004)

In 90s, the development of Cathodic Prevention (CPrev) took place with the establishment of the fact that CP can not only control the corrosion but can also improve the resistance to corrosion and can delay the onset of corrosion (Pedeferri, 1996). This phase also addressed the development of techniques for infrastructures other than bridges. It was consequently applied to about 500000 m^2 of concrete as cathodic protection and cathodic protection was employed to about 140000 m^2 of new concrete structures and almost all prestressed structures in Italy despite of the fact that it can lead to hydrogen embrittlement

(Pedeferri, 1996). Maaddawy and Soudki (2003) tested the effectiveness of the ICCP technique. The design of the ICCP systems were discussed by Bertolini *et al.* (2004).

c) Maturity Phase (2005 – present)

In this phase, CP has been accepted worldwide as a method that can provide long term protection of RC structures. Commercialisation of CP was started. More and more companies whether big or small showed immense interest and joined hands with researchers to make a collaborative effort for fighting corrosion. Extensitve research on anodic systems were being carried out throughout the world (Broomfield, 2007). Glass *et al.* (2008) introduced a hybrid system for cathodic protection.

2.8.2.3 Principle of Cathodic Protection

The basic principle of all the cathodic protection systems is to provide an external DC supply current or a source of electrons which can supress or completely eliminate the anodic reactions on steel. Principle of ICCP is to apply current and drive steel to a potential so that it lies in passivity zone or immunity zone of Pourbaix diagram (Pourbaix, 1974). It can also be said that the principle is to polarize the metal using an external source so as to make the steel bar equipotential and eliminating potential gradient along the steel bar which would however lead to formation of macrocells leading to corrosion (Bhuiyan *et al.*, 2014). The potential of steel is taken in to the range of E_{pit} to E_{pro}, so that the initiation of pits will stop and corrosion current will reduce (Fig. 2.20). Potential path $4 \rightarrow 6 \rightarrow 5$ shows cathodic protection and $1 \rightarrow 2 \rightarrow 3$ shows cathodic prevention.
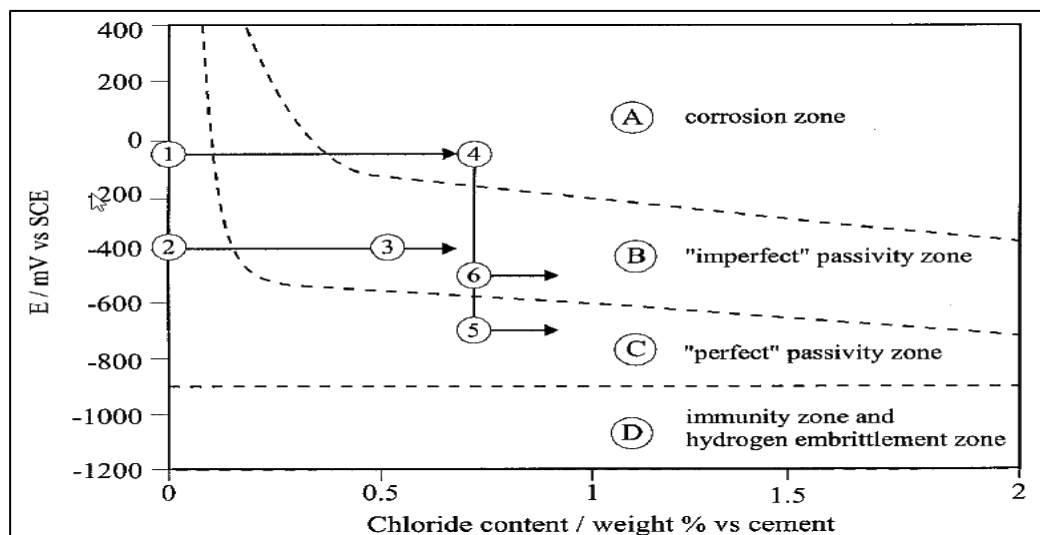
Figure 2.20 Steel behaviour in chloride contaminated concrete. Evolution paths of CPrev and CP (Bertolini *et al*., 1998)

31

2.8.2.4   Types of Cathodic Protection

Cathodic protection is enforced in two ways, Sacrificial Anode Cathodic Protection (SACP) and Impressed Current Cathodic Protection (ICCP), and more recently a new system with the properties of both the systems has been introduced called hybrid system (Glass *et al.*, 2008).

2.8.2.5   Sacrificial Anode Cathodic Protection (SACP)

Sacrificial cathodic protection is generally used for the protection of underground pipelines and submerged structures. In SACP less noble metals than steel like zinc or aluminium is connected with the steel bar and the dissolution of this anode metal provides current instead of an external power supply (Darowicki *et al.*, 2003) (Fig. 2.21). Its advantages are simplicity, cost savings, availability of wide range of anodes and low maintenance (Nikolakakos, 1999). Disadvantages with the SACP are requirement of periodic replacement of anodic metal due to its dissolution in the process, limited control over the system and driving voltage is low and may be inadequate to provide full cathodic protection in all situations (Chess *et al.*, 1998).
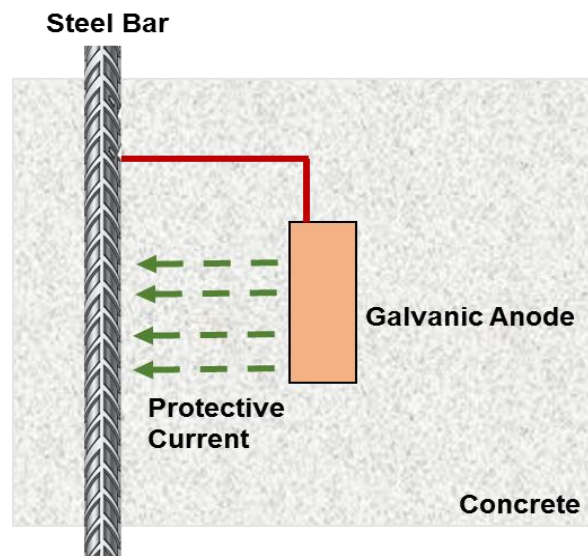
Figure 2.21. Sacrificial anode cathodic protection

Alloys made from zinc, aluminium and magnesium are generally used as sacrificial anodes (BS 7361, Part 1, 1991). But, during use Al and Mg oxides can attack concrete (Parthiben *et al.*, 2008). Monitoring of the sacrificial anodes for long periods helped the researchers to come up with an inference that the 100 mV depolarisation criterion, which applies to cathodic protection systems, is not appropriate for the cathodic protection systems involving sacrificial anodes (Sergi, 2011). Sacrificial anodes are more effective in preventing corrosion initiation by providing cathodic prevention than in controlling ongoing pitting corrosion. Need of new monitoring criteria instead of 100 mV decay criteria due to its

unreliability in sacrificial protected structures is pointed out even though it remains as the most acceptable monitoring criteria in field situations (Bertolini *et al.*, 2002) .

Whiting *et al.* (1996) evaluated various materials to identify the most suitable sacrificial anode. Aluminium anodes are found to give maximum current outputs and dissolution of the metal than Mg and Zn anodes. 100 mV decay criteria is found to be matching with all the selected anodes and finally conformed that the Al and Zn perform better than Mg anodes for the application in concrete. SACP is limited to small targeted repairs and short life time (Wilson *et al.*, 2013). Kean and Davies (1981) stated that SACP is less liable to cause interaction with adjacent structures and unconnected metal parts in same structures.

2.8.2.6   Impressed Current Cathodic Protection (ICCP)

In this method, a small direct current (DC) is supplied from a permanent anode which can be fixed at the top or into the concrete to the steel bars (Fig. 2.22). The current passed should be sufficient enough to halt the anodic reactions and cathodic reactions that can occur at steel surface to produce hydroxyl ions. The production of hydroxyl ions will increase the alkalinity and repassivation of the steel bar or strengthening of passive layer will take place (Bertolini *et al.*, 1998).The potential of steel is brought to a value more negative than the corrosion potential and thus steel bars become a cathode. A schematic diagram of ICCP systems is shown in Fig. 2.22.
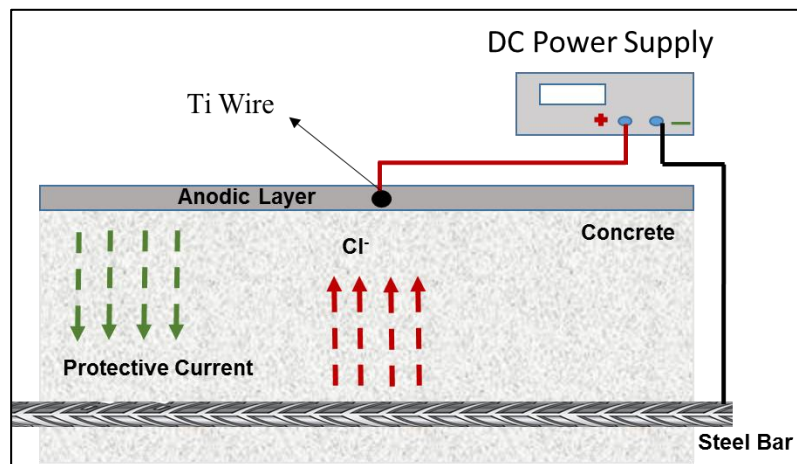
Figure 2.22. Impressed current cathodic protection

The current density applied varies from $1 - 2$ mA/m^2 for cathodic prevention and $5 - 20$ mA/m^2 with respect to steel surface. After application of CP or CPrev on a structure, it should be operated throughout the service life of the structure (Bertolini *et al.*, 2004). Typically, life span of these systems ranges from 5 to 25 years depending on the anode used. The anode system

should be able to perform according to the design parameters and should not result in performance degradation either of concrete-anode interface or the anode during the design life. The different types of anodes which are used worldwide are listed and discussed below:

i.   Conductive coating anode systems (surface mounted)
ii. Activated Titanium anode systems (embedded)
iii. Platinised Titanium or Niobium wires (embedded)
iv. Conductive overlays

a) Conductive Coating anode systems (surface mounted)

These mainly includes organic coatings and thermally sprayed metallic coatings. Organic coating systems shall include an organic conductive coating (carbon based) which can be water or any other solvent based and an array of primary anodes joined to the coating system (BS 12696, 2012). These conductive coatings are carbon based which uses spherical carbon or graphite fibres mainly. Orlikowski *et al.* (2004) stated that coatings having a graphite content of about 45 to 50% have shown low resistance and stability at higher potentials but higher porosity. All conductive coatings are black in colour owing to the presence of carbon, and so are coated with a decorative and compatible top coat. Organic coatings can usually deliver current up to 20 mA/m^2 and are maintenance free up to 10 years of service. These have generally 10 to 15 years of service life (Broomfield, 2007). BS: 12696 (2012) specified the thickness of coating shall be of 0.25 to 0.50 mm applied by brush, roller or air sprayed. The primary requisite for conductive coatings is to have a low volume electrical resistivity, typically less than 10 Ω-cm (Chess *et al.*, 1998). These should not be used on wetted surfaces or where probable water exposure can occur. The coatings should have a good adhesion property throughout its service life and will cost £20 – £40/m^2 (₹1800/- to 3500/- per m^2) (Broomfield, 2007). Failure can occur by loss of adhesion or flaking, acidification due to anodic reaction and wetting.

Thermally sprayed metallic coatings uses metals sprayed as coatings of Zn, Al-Zn, Al-Zn-In, Ni and Ti as anodic material. These can be directly applied to steel rebar if exposed or over the concrete. A coating may also be applied over these to avoid atmospheric corrosion (BS 12696, 2012). After a few years of use, the resistance between the coating and concrete surface might rise due to the formation of corrosion products between them. Sprayed zinc is more effective when used in ICCP than in SACP (Anwar *et al.*, 2014). Catalysts may be required for enhancing current supply. The thickness of these coatings are of order 200 to 400 nm and are 0.10 mm to 0.40mm when arc sprayed and would be serviceable for a 10 to 15

years of design life (Chess *et al.*, 1998). For the application of coatings, bulky devices are required and also have a safety and health hazard. The cost of these coatings ranges from £60 – £100/m^2 (₹5000/- to 9000/- per m^2) (Broomfield, 2007).

These are mainly used as secondary anodes to distribute current uniformly over the structure that is coming from primary anode.

b) Activated titanium anode systems (embedded)

The anodes system consists of titanium substrate and a catalytic coating of oxides of platinum group metals, iridium, ruthenium or platinum along with oxides of titanium, zirconium and tantalum which are embedded in a concrete overlay ((BS 12696, 2012). Titanium in anodes act as a stable base while coating acts as the anode (Sohangpurwala, 2009).These are very robust in nature and have a theoretical life up to 100 years but service life of about 25 years is estimated when used in ICCP systems (Christodoulou *et al.*, 2010). These are commercially available in form of meshes, ribbons, and rods or tubes which are embedded in holes drilled in the concrete. These anodes were initially developed for chlorine generation. These can supply large currents but are restricted to a maximum of 110 mA/m^2 of anode surface to reduce lowering of pH because of production of acid at anode (Chess *et al.*, 1998). Titanium mesh overlay systems are costly and heavy in nature as compared to other anodes, but are most reliable and have high tolerance (Polder *et al.*, 2009). The failure of these anodic systems typically is due to debonding from the concrete substrate, which can be credited to improper surface preparation and application (Byrne *et al.*, 2016). These are used as primary anodes in concrete. These generally cost £40 – £100/m^2 (₹3500 to 9000 per m^2).

The anodes used are always at a risk of corrosion themselves when used in chloride environments if operated potential difference of metal/electrolyte exceeds 8 V (BS 12696, 2012).

c) Platinised Titanium or Niobium wires (embedded)

These are the most frequently used primary anodes in ICCP systems in conductive coating systems, titanium meshes and strips. These are very thin in diameter i.e. smaller than 5 mm. Titanium wires are coated with platinum and copper cored wires are coated with niobium and can vary in diameter form 0.8 mm to 10 mm or more (Chess *et al.*, 1998). These primary anodes are also available in form of thin plates.

Uncoated titanium wires or strips can also be used as primary anodes. An oxide layer is formed on the anodes and remains unharmed during its service life till the applied voltage does not exceed the threshold voltage of operation.

d) Conductive Overlays

Conductive asphalt overlays were the first ones used in ICCP systems in the late 1970s. These were not commercially encouraged, so were unable to find place in commercial cathodic protection systems (BS 12696, 2012).

Different types of cementitious overlays are developed and are effectively tested in laboratory but are not commercialised to great extent except few proprietary systems.

Conductive cementitious anodes are modified mortars by use of polymers like acrylic and styrene butadiene rubber (SBR), carbon particles, conductive fibres etc. These generally can operate at a current density of 20 mA/m^2 for a short period of time while these can also be used to supply current up to 30 mA/m^2 momentarily (BS:12696, 2012). Application of a current density more than 50 mA/m^2 showed the destruction of cementitious matrix near the primary anode due to the acidity created by anodic reactions. It was recommended to keep the spacing between primary anodes to 1 m and maximum current density of $10 - 15$ mA/m^2 of steel surface for the safe design of cathodic protection systems with cementitious mortar (Bertolini *et al.*, 2004). The average bond strength (pull-off strength) between the concrete substrate and the overlay shall be greater than 1.5 MPa and the minimum shall be greater than 1 MPa (BS 2012). These are commercially available as proprietary anodes and cost around £30 – £70/m^2 (₹2600 to 5000 per m^2).

The electrical conduction in cementitious conductive overlays made using fibres is mainly due to pore solution and tunnel effect of fibres a shown in Fig. 2.23 (Chu and Chen, 2016). Wu *et al.* (2005) explained the bridging effect of fibres in the anodic overlay that can increases the number of paths of current flow in the system and thus increases conductivity. At the optimized content of fibres or conductive particles, the current follows the path of lowest resistance. The decrease in current density and resistance will reduce the throwing power required and the system would become economically efficient.
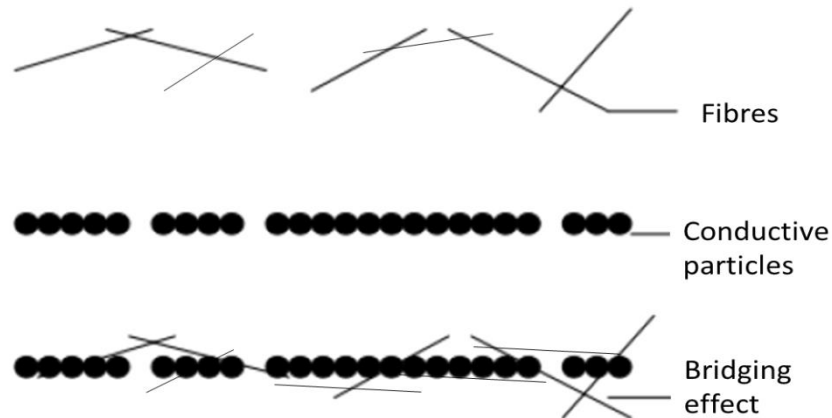
Figure 2.23 Conduction in Cementitious overlays. (Wu *et al.,* 2005)

Newer materials that can help in developing conductive cementitious overlays are being explored and testing is being carried out. Chung (2004) explained the multi-functional uses of such conductive cementitious materials and has conducted a comparative study of steel fibres, steel dust, coke powder, nano-carbon fibres and graphite powder. In recent years, development and laboratory testing of cementitious overlays containing carbon fibres has taken place. Jing and Wu (2011) used carbon fibres in cementitious anode for cathodic protection and optimized caron fibres (CF) content at 0.5% to 0.6%. Yehia and Host (2010) applied the conductive cementitious overlay developed using steel fibres and shavings to the surface of slabs of varying dimensions and checked the suitability for cathodic protection. The electrical resistance of the slab is found to be increasing with increase in time. Higher voltage is required for the specimens in order to keep same amount of polarization and effective cathodic protection (Tuan and Yehia, 2004). Carbon fibres improves mechanical strength, increases toughness and electrical conductivity providing combined properties of mesh anodes and conductive coatings of durability and robustness (Jing and Wu, 2011) with less addition to the dead load of the structural members (Polder *et al.*, 2011). Anwar *et al.* (2014) worked towards making the anode light weight by using pumice aggregate. Use of higher percentage of carbon fibres or other carbon based materials in conductive mortars can cause deterioration of electrical properties due to presence of chloride ions and oxygen and chloride liberation in the anodic layer (Jing and Wu, 2009). The resistance of cementitious anode with carbon fibre increases with increase in strain because carbon fibres cementitious anode shows peizoresistive effect (Chu and Chen, 2016; Reza *et al.*, 2004). The main research carried out on cementitious materials has concentrated in improving the mechanical properties, developing certain properties with specific use integrated with basic structural functioning of the material.

37

However, recently moving away from basic materials with specific functional use and structural use, development of materials with multi-functional properties has taken attention of the researchers (Chung, 2004).

Cementitious overlays are supposed to deliver current uniformly between the protected steel bars and decrease the contact resistance between the anode and the substrate. The steel bars near to the anodes receives greater current density than the steel bars away from the anodic layer. Moreover, even the steel bars which were at the same level received different current densities as observed by Jing and Wu (2009). The non-uniform current distribution was observed due to the non-homogeneous resistance distribution of concrete (Hassanein *et al.*, 2002; Jing and Wu, 2009).

Use of cement based anodes for realkalisation and electrochemical chloride extraction is relatively less explored area. Carmona *et al.* (2015) and Durstewitz *et al.* (2012) demonstrated the use of cementitious anode for electrochemical chloride extraction and realkalisation, respectively. The anodes were made using graphite powder and chloride removal efficiency of overlay was found to be similar to titanium mesh anodes (Perez *et al.*, 2010).The list of various conductive particles and fibres in making conductive mortar or concrete are listed in Table 2.6.

Table 2.6 Electrical resistivity with conductive admixture

Researcher	Conductive admixture	Vol. %	Resistivity (Ω-cm)
	None	0	10^3 to 10^{11}
Wen and chung (2001)	Steel fibre (8 μm dia.)	0.09	4.5×10^3
Wen and chung, (2000)	Steel fibre (60 μm dia.)	0.10	5.6×10^4
Wen and chung (2001)	Carbon fibre (10 μm dia.)	0.36	1.3×10^4
Cao and Chung (2003a)	Coke powder (< 75 μm)	0.51	6.9×10^4
Cao *et al.* (2003b)	Graphite powder (< 1 μm)	0.92	1.6×10^5
Chu and Chen (2016)	Carbon fibre (7.2 μm dia.)	0.90	1.7×10^5
Carmona *et al.* (2015)	Graphite powder (< 45 μm)	50*[(by mass)]	1.5×10^2
Eldho (2014)	Graphite powder	20*[(by mass)]	4×10^3
	Coke breeze	40*[(by mass)]	9×10^3
	Carbon fibre	0.6	3×10^3

2.8.2.7 Beneficial Effects of CP

Christodoulou *et al.* (2010) indicated that steel which is cathodically polarised during the application of CP and CPrev remains passive as a result of residual effect of polarisation and suggested use of intermittent ICCP systems. Similar tests were carried out by Bhuiyan *et al.* (2014) and interrupting ICCP current was found beneficial. CP can completely stop corrosion and can sustain passivity. ICCP leads to production of hydroxyl ions and drive chloride ions away from steel thus transforming the environment around steel. Byrne *et al.* (2016) stated that CP can drive chloride ions at least 100 µm away from steel bars. The current density required for CP reduces drastically once the steel bar is repassivated (Christodoulou *et al.*, 2010). CP leads to increase in chloride threshold for steel corrosion in concrete (Bertolini *et al.*, 2009). CP obstructs local acidification and stops pitting initiation called buffer effect. Also, reduction in chloride content near the steel bar and reduction in diffusion of chloride ions into concrete (chloride barrier effect) was also observed during CP application (Pedeferri, 1996).

2.8.2.8 Negative Effects of CP

Negative effects of ICCP are damage to concrete due to ASR where reactive aggregates are present, reduced anode efficiency with time, adhesion loss or bond degradation of steel/concrete interface and hydrogen embrittlement in high strength steels (Pedeferri, 1996; Bhuiyan *et al.*, 2014).

2.9 Patents Search

Cathodic protection of steel in RC structures remains as a hot topic for research all around the world. Analysis of patents shows that researchers are working both on the sacrificial anode cathodic protection and impressed current cathodic protection development (Fig. 2.24). The major research area is developing newer anodes for both techniques. Patent search engine PATENT-INSPIRATION (AULIVE, 2016) was used for the patent search. The keywords used were "Cathodic protection, anodes, concrete" for search and analysed results are shown in Fig. 2.24.

Application of cement based anodes in cathodic protection is very less explored area since there are not many patents filed under this category, but there are a number of patents on conductive cementitious compounds. Some of the patents in this area are reviewed.
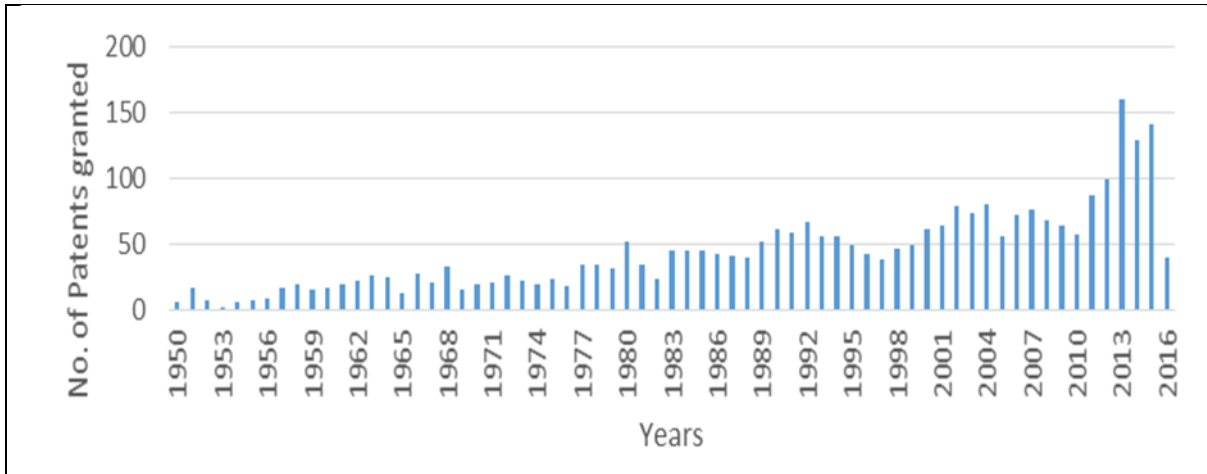
Figure 2.24 Trends of patents for cathodic protection anodes worldwide

Concrete is a poor conductor of electricity, especially in dry conditions. Electrical resistivity of concrete varies from 10^{11} Ω-cm for oven dried to less than 10^3 Ω-cm for very wet conditions (Lopez, 1993). Development of a good conductive concrete with high mechanical properties is necessary for the growing needs of the concrete industry. Concrete having good mechanical properties and good electrical conductivity can be used in various applications.

It can be used in the cathodic protection system, for the de-icing of roads and for the electrical grounding purpose. Researchers around the globe worked for decades for the making of conductive concrete and mortar. Barnard (1965) patented electrically conductive concrete. It was made by incorporating conductive materials like iron filings and carbon black with the Portland cement mixture. Electrical conductivity depends on the amount of carbon black used and by using 10 % by weight of carbon black a resistivity of less than 0.1 kΩcm was achieved. The Marcony Company Limited filed a US patent (Freeman *et al.*, 1976) on electrically conductive concrete in 1986. Westhof *et al.* (1993) patented a type of anodic overlay which can be used in the cathodic protection system with the name modified cementitious system. This cementitious system contains Portland cement binder, siliceous filler like sand with low clay content, anti-foaming agents, plasticizer and a water soluble base. This base neutralizes hydrogen ions formed in the anode layer and prevents the deterioration of anode and ensures long life for the cathodic protection systems.

Xie *et al.* (1995) invented conductive cement based compositions exhibiting both good electrical conductivity and mechanical strength. Proper dispersion of conductive phase in the mixture is necessary for the preparation. Both slurry infiltration technique and conventional mixing is done depending on the target properties. Conductive phase includes conductive fibers and conductive particles. Composition is developed by ensuring the threshold fiber content and

40

uniform dispersion of the fibers throughout the volume of the composite both before and after hardening. Composite with compressive strength of 30 MPa and electrical resistivity of 43 Ωcm was achieved. Bennet and Schue (1999) developed an electrically conductive building material which can be used for the shielding against the electromagnetic waves. It is composed of binder, a mixture of graphite, amorphous carbon and sand. It is observed that simultaneous use of both graphite and amorphous carbon will create a synergic effect and resultant product will be more efficient in terms of conductivity. Ramme *et al.* (2002) awarded a patent for the invention of an electrically conductive concrete and controlled low strength materials. This invention has got application in the protection of electrical equipment from the lightning. It is developed from high carbon content fly ash. The product has achieved an electrical resistivity of 1.5 k.Ω-cm and compressive strength of 13.8 MPa.

Pye *et al.* (2003) developed a conductive concrete composition which is able to give a compressive strength of 30 MPa and electrical resistivity of 78 Ω-cm. It is composed of coke breeze and carbon fiber as the conductive phases. This concrete is less dense than the conventional concrete due to the presence of porous materials (Pye *et al.*, 2003). It is important to keep the w/c ratio as low as possible to make the concrete durable and to achieve high compressive strength.

There are only three patents filed around the world in the field of use of e-waste in concrete and building materials. Wang and Tengfei (2011) developed a concrete by using 33.4% (by weight of cement) PCBs powder with a compressive strength of 51.6 MPa. Liang *et al.* (2014) developed a radiation resistant concrete using lead containing CRT glass to make concrete with normal density ranging from 2380-2450 kg/m^3 which can replace thick concrete in nuclear plants having same radiation resistance. Yunchun *et al.* (2014) claimed to have used 45% of PCBs powder to make concrete which can be used to make kerbstones and paving bricks.

2.10 Research Status of Cathodic Protection in India

A little amount of work has been carried out in India on cathodic protection. There are around 30 patents in Indian patent database. Most of the patents are filed by foreign companies and CSIR from India focussing on sacrificial anodes. No patent were found on cementitious anodes for ICCP systems. Parthiban *et al.* (2008) studied the application of magnesium anodes for sacrificial cathodic protection of steel in concrete. It was observed that magnesium anodes shift the potential of steel bars in to more negative values at the beginning and performance reduces as the time passes (Pye *et al.*, 2003). Reduction in the concentration of the chloride ions in the

vicinity of steel bars was also observed. Cementitious anodes have been developed at CSIR-CBRI by using carbon fibres, graphite powder and coke breeze (Eldho, 2014; Karade 2016). The developed anodes have been used to control corrosion in concrete made using sea-water (Karade and Goyal; 2016). Cathodic protection is not a commercially popular technique in India because of its high cost and lack of expertise in this field.

2.11 Research Gaps Identified

The following areas are identified, where there is not enough information is available in the literature and need further studies:

i. Limited literature is available on use and effect of e-waste on concrete properties.

ii. No literature is available on use of metallic powder from e-waste as conductive fillers to make conductive cement composite.

iii. Limited information is available on multifunctional use of cementitious anode for both electrochemical chloride extraction and cathodic protection.

iv. Risk of debonding of cementitious overlays from the concrete substrate needs further studies.

v. No specific guidelines are available for use cathodic protection systems in Indian context.

vi. There is a need of development of a newer anode system, which is cost-effective, highly efficient and light-weight.

2.12 Summary

In the literature review, a wide range of sources journals, reports, patents, internet etc. were thoroughly searched with a focus on use of e-waste and its potential for using it in making mortar or composite. Although, there is limited literature available on use of e-waste in concrete or mortar, there seems to be a possibility of utilisation e-waste in concrete. Few important observations are summarized in the section below:

i. Use of plastic from e-waste reduces the bulk density of mortar or concrete and rendering a light weight composite material.

ii. Use of e-waste reduces the mechanical strength of mortar or concrete when used as replacement for aggregates.

iii. The metallic fraction of the e-waste shows potential to be used as conductive fillers in making conductive mortar.

iv. There is a need of cost effective cementitious overlay with high efficiency and improved durability.

CHAPTER 3

EXPERIMENTAL WORK

3.1 Introduction

The main aim of this study is to explore the possibility of using metallic extracts from the e-waste as conductive fillers to prepare conductive cement composite which could provide a cost-effective solution as an anode to be used in cathodic protection of reinforced concrete structures for controlling corrosion of the steel reinforcement in reinforced concrete. Keeping this in view, various experiments were planned and conducted. This chapter explains the experimental procedures followed to assess various properties of the raw materials, prepared anodes and the evaluation of anodic overlay applied to the concrete substrate.

3.2 Raw materials

3.2.1 Cement

The cement used throughout the studies was OPC 43 grade, Ultratech cement complying to IS 8112 (2013). The chemical characterisation of the cement was done using X- ray fluorescence (XRF) analyser. Consistency, setting time and compressive strength of cement were found as per IS: 4031 (2013) Part-4, Part-5 and Part-6, respectively.

3.2.2 Aggregates

For preparing concrete specimens, locally available coarse sand with a specific gravity of 2.64 and coarse aggregates of size under 12.5 mm and under 20 mm were used. The coarse sand was falling under Zone II as per IS 383 (2016). The testing of coarse and fine aggregates was carried out as per IS 2386 (1963). The coarse sand was sieved through 4.75 mm sieve before use to remove coarser material. To obtain acceptable workability of concrete, a third generation polycarboxylic ether based superplasticiser (SP) (Gelenium 51 BASF make) was used. The specific gravity of the SP was 1.05 and the dosage of 0.2% by weight of cement was decided after conducting a few trials to obtain the desired slump of 75±5 mm.

3.2.3 Conductive Fillers

3.2.3.1 e-Waste Metallic Powder

The metallic extract of the e-waste was obtained after milling of printed circuit boards (PCBs) taken out from TVs, mobiles, refrigerators, washing machines etc. It has a specific gravity of 5.09 and used during this study. The metallic extract was procured from Auctus E-Recycling Solutions Pvt. Ltd., Greater Noida (U.P.) and a sample is shown in Fig. 3.1. The physical properties of e-waste metallic powder were found using the same methods as used for finding out the properties of fine aggregates and given in IS 2386 (1963). The aspect ratio of the e-waste metallic powder was found using the image analysis system comprising of a microscope, a high resolution digital camera and an advanced image analysis software. The digital camera is mounted on the inverted microscope. The camera captures and transfers the images to the computer for analysis. The particle size analysis was carried out using a Laser Particle Analyser.

Figure 3.1 e-Waste metallic powder

The chemical composition of the metallic extract was determined using inductively coupled plasma atomic emission spectroscopy (ICP-OES) (Fig. 3.2). For this purpose, the metallic powder was first digested in aqua regia (HNO_3: HCl; 1:3) for 24 hours as most of the metals are digested in due time. The ratio between metals and aqua regia was kept 1:20 (Park and Fray, 2009). The liquid was then filtered through a filter paper for removal of unwanted plastic particles i.e. impurities. The filtered liquid was then diluted 10 times and was used for determination of dissolved metals.

Figure 3.2 Inductively coupled plasma optical emission spectrometer

3.2.3.2 Graphite Powder

Another low-cost conductive filler used was graphite powder with a mean particle size of 44.56 μm and a fixed carbon content of 62 % (by mass of the powder). The fixed carbon content influences the conductivity of the carbonaceous materials. The specific gravity of the graphite powder was found using Le Chatelier's flask according to IS: 4031 Part-11 (1988). The graphite powder used was black in colour and a small sample is shown in Fig. 3.3.
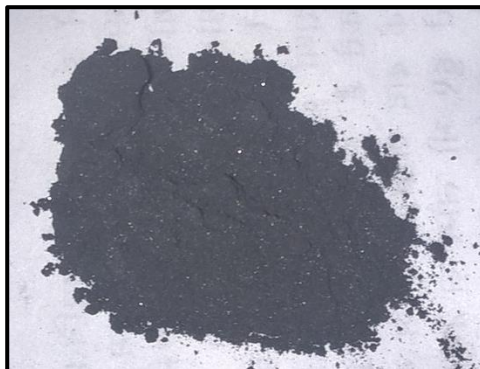
Figure 3.3 Graphite powder

3.3 Mix Proportion, Casting and Curing

3.3.1 Conductive Cement Composite

The experimental investigations were conducted in two parts - conductive cement composite study and corrosion monitoring and control on RC slab specimens. The preliminary studies were conducted on the conductive cement composite prepared using e-waste metallic powder only and then in combination with graphite powder. The combination of conductive fillers was optimised by use of the Design of Experiments (DOE) approach. The details of the experimental plan followed is explained in this section.

3.3.1.1 Conductive Cement Composite Mix Proportioning

For preliminary studies, the content of e-waste metallic powder was kept as 0%, 1%, 2%, 5%, 15% and 20% by volume of the composite which equals 0%, 3.14%, 6.28%, 15.71%, 47.13%, and 62.84% by weight of cement. An OPC 43 grade cement was used and the water-cement ratio was 0.3. Response Surface Method (RSM) was used for planning the experiments and mix design of the composite as a part of the Design Of Experiments (DOE) approach. It helps to optimize the variables depending on the responses. In this study, the responses were compressive strength and resistivity.

3.3.1.2 Design of Experiment Approach (DOE)

Response surface method was used to find the optimal mix design to achieve the peak performance with responses as resistivity and compressive strength of the composite. The main variables in design were the content of e-waste and graphite powder.

A central composite design (CCD) was adopted with two numeric factors (e-waste metallic powder content and graphite powder content) which were varied over five different levels, $+\beta$ and $-\beta$ ($\beta = 2$) as axial points, $+1$ and -1 as factorial points and the centre point as shown in the figure below (Fig. 3.4).
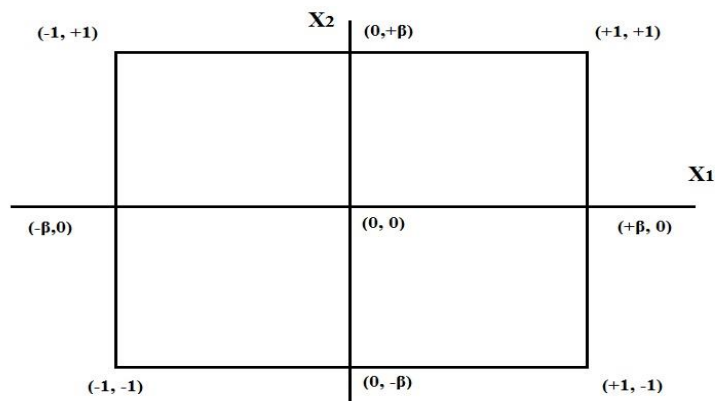
Figure 3.4 CCD with two factors varied over five levels

The different levels and parameters for CCD of two variables are shown below (Table. 3.1) which would finally help in obtaining and optimising the mix design of the conductive cement composite. The e-waste metallic powder was varied from 5% to 25% (at equal intervals) by volume of the wet cement paste in the composite and the graphite powder was varied from 0% to 40% by mass of cement. The resulting combinations are listed in Table 3.1.

Table 3.1 Parameters for RSM (central composite design)

Conductive Fillers	Levels				
e-Waste Metallic Powder (% by vol.)	X1	X2	X3	X4	X5
	5 (15.7*)	10 (31.4*)	15 (47.1*)	20 (62.8*)	25 (78.5*)
Graphite Powder (% by vol.)	Y1	Y2	Y3	Y4	Y5
	0	10	20	30	40

*By weight of cement

The mix design prepared with the help of CCD is presented in Table 3.2.

Table 3.2 Mix design according to CCD

Mix Designation	e- Waste Metallic Powder (% by volume)	Graphite Powder (% by weight)
CC1	5 (15.7*)	20
CC2	10 (31.4*)	10
CC3	10 (31.4*)	30
CC4	15 (47.1*)	20
CC5	15 (47.1*)	0
CC6	15 (47.1*)	40
CC7	20 (62.8*)	10
CC8	20 (62.8*)	30
CC9	25 (78.5*)	20

*By weight of cement

3.3.1.3 Mixing and Casting of Conductive Cement Composite Specimens

Two major tests for conductive cement composite are resistivity and anodic polarisation of the specimens. For casting the specimens for these tests, the moulds were cleaned and a thin layer lubricating oil was applied so as to make them air tight and to ease the demoulding. Preparation of the conductive cement composite was done with a laboratory digital mortar mixer (Fig. 3.5) having a capacity of 5 litres.

Cement and conductive fillers were dry mixed for 2 minutes and then, water was added according to the water-cement ratio and also to compensate for the apparent water absorption of the graphite powder. After the addition of water, the wet mix was further mixed for another 2 minutes to ensure uniform mixing.

(a) Digital Mortar Mixer

(b) Prepared specimens for resistivity test
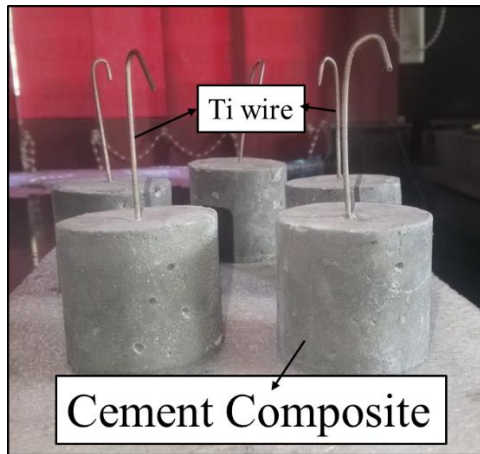
(c) Prepared specimens for polarization test

Figure 3.5 Preparation of conductive cement composite specimens

The casting of composite specimens in the moulds was done in three different layers each of depth one-third of the moulds. For the 25 mm sized cubes, the casting was done in two layes. Each layer was well compacted using the vibrating table and the excess material was removed using a trowel.

The surface of the cast specimens was given a smooth finish. The cast specimens were stored in the laboratory for 24 hours and were covered with a wet cloth to minimise water evaporation from the surface. For compressive strength testing of cement composite 25 x 25 x 25 mm^3 size

cubes were cast. Cylindrical specimens of 50 mm diameter and 50 mm height were cast to study the anodic behaviour of the prepared cement composite.

3.3.1.4 Curing of Composite Specimens

The specimens were demoulded after 24 hours after casting and then immersed in water in curing tank for next 27 days (Fig. 3.6. The curing was done using potable tap water as used for mixing.

Figure 3.6 Curing of Samples in tap water

3.3.2 Concrete

The concrete was mix proportioned and used to cast RC specimens for the corrosion monitoring & its control. The cast specimens were overlaid by an anodic layer to uniformly distribute the supplied current over the concrete surface. The details of the mix proportioning, casting and curing are discussed below.

3.3.2.1 Mix Proportioning of Concrete for Slab Specimens

In this study, M30 grade of concrete was used and proportioned in agreement with the Indian Standard IS: 10262 (2009). The mix proportioning was checked using various trial mixes and the mix proportion was finalised having a slump of 75±5 mm. M30 grade was chosen for this study as corrosion is a major problem in areas where concrete can get contaminated with chloride and at least M30 grade of concrete is to be used in such areas as specified by the IS: 456 (2000). For the concrete mix, common salt at 3.5% by weight of cement was added to

prevent the formation of the passive layer on the steel reinforcement and to ensure corrosion of steel in the hardened concrete. The mix proportioning details are given in Table 3.3.

Table 3.3 Mix proportion of concrete

Sr. No.	Components		Quantity (kg/m³)
1	Cement		400
2	Fine aggregates		710
3	Coarse aggregates	Under 12.5 mm	820
4		Under 20 mm	350
5	Water (l/m³)		180
6	Superplasticiser (l/m³)		0.8
7	Salt		14
8	Proportion C: FA: CA		1: 1.78: 2.93

3.3.2.2 Mixing, Casting and Curing of Concrete

Mixing of components to obtain a homogeneous mix was done in a rotating drum type batch mixer as shown in Fig. 3.7. The mixing process comprises of the loading method of constituents, the discharge method, mixing time and the mixing energy. Firstly, the coarse aggregates were loaded into the mixer and mixed for one minute, thereafter cement and fine aggregates were loaded and dry mixed for about 2 minutes. After the completion of dry mixing, 60% of the water was added to the dry mix and further mixing is done for another 2 minutes. To ensure proper dispersion of superplasticiser, the superplasticiser and common salt were mixed with the remaining water and was then loaded into the mixer. The concrete mix was discharged after mixing for another 2 to 3 minutes so as to obtain a homogeneous wet mix.

Figure 3.7 Drum type concrete batch mixer and cast specimen

For testing compressive strength of the concrete, cube moulds of 100 x 100 x 100 mm^3 were used. For monitoring the corrosion and electrical behaviour of steel reinforcement embedded in the concrete, slabs of 300 x 300 x 50 mm^3 were cast. A ribbed steel rebar of diameter 10 mm was concentrically inserted before pouring concrete into the mould with exposed embedded length of 24 cm and remaining 6 cm of the rebar was taped with an electrical insulating tape. The interior surface of the moulds was coated with a thin layer of oil in order to facilitate demoulding and to avoid adhesion of concrete to the mould surface. Concrete was poured in three layers into the cube moulds and each layer was compacted by using a vibrating table. The concrete was poured into the slab moulds in single layer and compaction was done using needle vibrator. Excess material was removed and the surface was smoothened out using a trowel.

The specimens (slabs and cubes) were demoulded after 24 hours from addition of water to the mix and were then immersed in water in a curing tank for the next 27 days (Fig. 3.8). The curing was done using potable tap water as used for mixing.

Figure 3.8. Curing of concrete specimens

3.3.3 Experimental Methods

The testing program and experiments were planned to find out the electrical, mechanical and electrochemical behaviour of the prepared specimens. This was planned to cover the objectives of the study in three parts which were the mechanical behaviour of the composite, its electrical behaviour including resistivity and polarisation of the anodic composite, and finally monitoring of the electrochemical behaviour of the steel bar embedded in the concrete during acceleration of corrosion and controlling the corrosion.

3.3.7.1 Compressive Strength Test

The compressive strength of the cement composite and concrete was tested on a servo controlled universal testing machine (UTM) of 1000 kN capacity. The testing of the specimens was carried out in the saturated surface dry (SSD) conditions. The rate of loading was kept at 0.23 MPa per second or 140 kg/cm^2/min. During the testing, it was made sure that the load had been distributed uniformly by placing the specimens at the centre of the loading platens (Fig. 3.11). Eq. 3.1 gives a formula for the calculation of compressive strength of the specimens.

$$f_{ck} = \frac{P}{A}$$ …………………. (3.1)

Where,

f_{ck} = compressive strength (MPa)

P = ultimate load (N)

A = cross sectional area of specimen (mm^2)

(a)   (b)

Figure 3.9 Compressive strength testing of concrete cube

For each specimen i.e. concrete and conductive cement composite, 3 specimens were tested at 3, 7 and 28 days and mean value of the three for each period was reported as the respective strength of the specimen.

3.3.7.2 Electrical Behaviour of the Conductive Cement Composite

The most important parameter for a material to be used as an anode for cathodic prevention of steel in reinforced structures is its electrical resistivity. Similar to concrete, cement composite is dielectric in nature and have high resistivity but can be polarised by application of DC current.

The higher the resistivity, higher is the energy, current and time required to polarise the cement composite. To decrease the time of polarisation and resistivity of the cement composite, conductive fillers were added to the cement composite whose effectiveness is tested by electrical resistivity test and anodic polarisation test. Both of these tests are described below.

Electrical Resistivity of Conductive Cement Composite

The electrical resistivity of the conductive cement composite can be measured by using alternating and direct current (DC). The use of alternating current (AC) techniques is advantageous as the direct current polarises the dielectric material and thus it will not provide true resistivity. Wenner probe was used for measuring the resistivity of the cement composite, which is most widely used for determination of resistivity (ASTM G57, 2012; Anwar *et al.,* 2014). The two outer electrodes facilitate the current flow and the inner two electrodes measure the potential difference in the electric field across the specimen. For measurement using direct current, the measurement method given in RILEM TC 154-EMC (2000) and ASTM G-57 (2012) was used, the connections were made using cast in copper electrodes of thickness 0.2 mm were used for measurement by application of direct current. The schematics of the sample and the applied technique is shown in Fig.3.10. As the resistivity of copper electrodes is very low as compared to the conductive cement composite, it has a negligible effect on the measurements made.
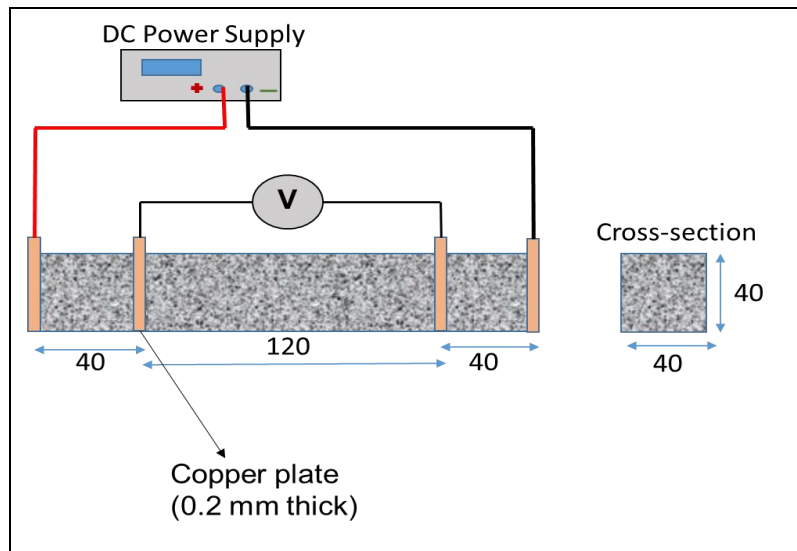
Figure 3.10 Schematics of DC resistivity test

For resistivity measurements using direct current, a rectifier or a DC power supply is used to provide current and the current and potential drop across the inner electrodes is measured using a Fluke 17B+ high impedance (>1 MΩ, <100 pF) multi-meter as shown in Fig.3.11. All the measurements were taken at a low current density (<300μA) and as soon as the power supply i.e. current starts flowing in order to reduce the effect of polarisation of the cement composite.
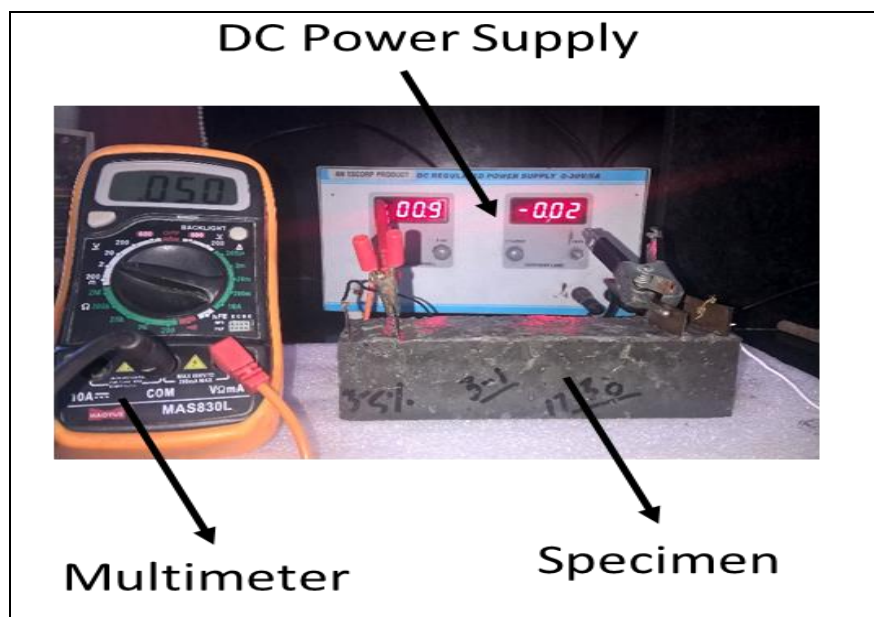
Figure 3.11 Measurement of DC resistivity

Measurements using AC are made using commercially available resistivity meter (Resipod™) with an AC current supply with a frequency of 40 Hz. The probe spacing was 38 mm. The specimens which were used for resistivity measurements by direct current supply were used for AC resistivity measurements as well. This could be done as the depth of the samples used were not exceeding 5% of the minimum separation of the inner electrodes

(ASTM G57, 2012). The probe was pressed against the surface of the specimen along the longitudinal axis of the specimen on all the surfaces and average of all the three readings were taken as the resistivity of the specimen (Fig. 3.12).

Figure 3.12 Measurement of AC resistivity

Accelerated Galvanostatic Test (AGT) of the Conductive Cement Composite

To study the dissolution behaviour of the anodic cement composite, the galvanostatic test was performed on cylindrical specimens of 50 mm diameter and height. A titanium wire of diameter 1.5 mm was cast axial into the specimens. The upper and lower surfaces of the anodes were masked with epoxy to make the surfaces non-conductive. The test was conducted by immersing the specimens in saturated $Ca(OH)_2$ solution (pH = 12.8) with and without 3% NaCl. For preparing the saturated $Ca(OH)_2$ solution by adding 3 g/l $Ca(OH)_2$ to water (ASTM C511, 2013). The anodic current density of 200 mA/m^2 referring to the surface area of the anodic composite in contact with the electrolyte i.e. saturated $Ca(OH)_2$ solution was applied using a DC power source. The cumulative charge passed during the test was 24,200 kC/m^2, which is equal to 28 years of charge passed across the anode when the current density is 10 mA/m^2. The titanium wire was used as the primary electrode and was connected to the positive terminal of the power source, whereas the steel bar was connected to the negative terminal immersed in the electrolyte (Fig. 3.13). The test was conducted for 14 days in the ambient laboratory conditions and was monitored regularly. The anodic potential was measured periodically with reference to copper-copper sulphate electrode. After the test, the probes were examined visually for any cracks on the outer surface and the probes were broken wide open for examining the embedded titanium wire for any rust spots and damages using SEM.
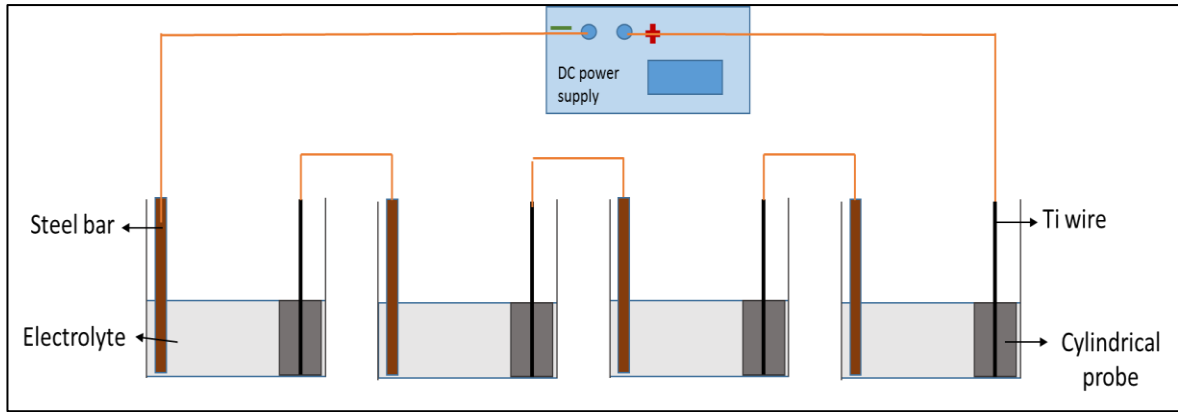
Figure 3.13 Test setup for AGT

Anodic Polarisation Test

After conducting of accelerated galvanostatic test for 7 days and 14 days, to study the consumption of anodes in the test with respect to time the polarisation test was performed on all the cement composite specimens. The I_{corr} values were then obtained from the $E - \log I$ plots. The potential of polarisation of the anodes was kept in the range of -3.5 V to 7.5 V. The test was performed using two electrodes method using IVIUMSTAT of Ivium Technologies (UK). The parameters for polarisation test are tabulated below (Table 3.4):

Table 3.4 Test parameters for anodic polarisation

Parameters	Values
E_{start}	7.5 V
E_{end}	-3.5 V
E_{step}	10 mV
Scan rate	0.1667 mV/s

3.3.7.3 Microstructural Studies

The FE-SEM/EDAX analysis were conducted on different specimens in order to identify the changes in microstructure as a result of the addition of conductive fillers and due to the movement of current through the conductive cement composite (Fig. 3.14).

Figure 3.14 SEM analyzer for obtaining micrographs

3.3.7.4 Performance Evaluation of Anodes

The performance of anodic composite is evaluated by application of an anodic layer over the slab surface and applying impressed current cathodic protection (ICCP) technique to control corrosion. The slab specimens prepared were applied with an anodic layer of 3 mm thickness and the primary anode i.e. titanium wire was placed on a 3 mm groove made over the concrete surface (Fig. 3.15). Corrosion was induced in the steel bars by applying impressed current for 3 days at a current density of 200 mA/m^2 of the steel surface. The total charge passed was 51,840 Coulombs. After acceleration, ICCP was applied by means of applied mortar. The ICCP was applied on the slabs as shown in Fig. 3.15. The schematics of the diagram are shown below (Fig. 3.16).

Figure 3.15 Application of anode layer on concrete slabs

57
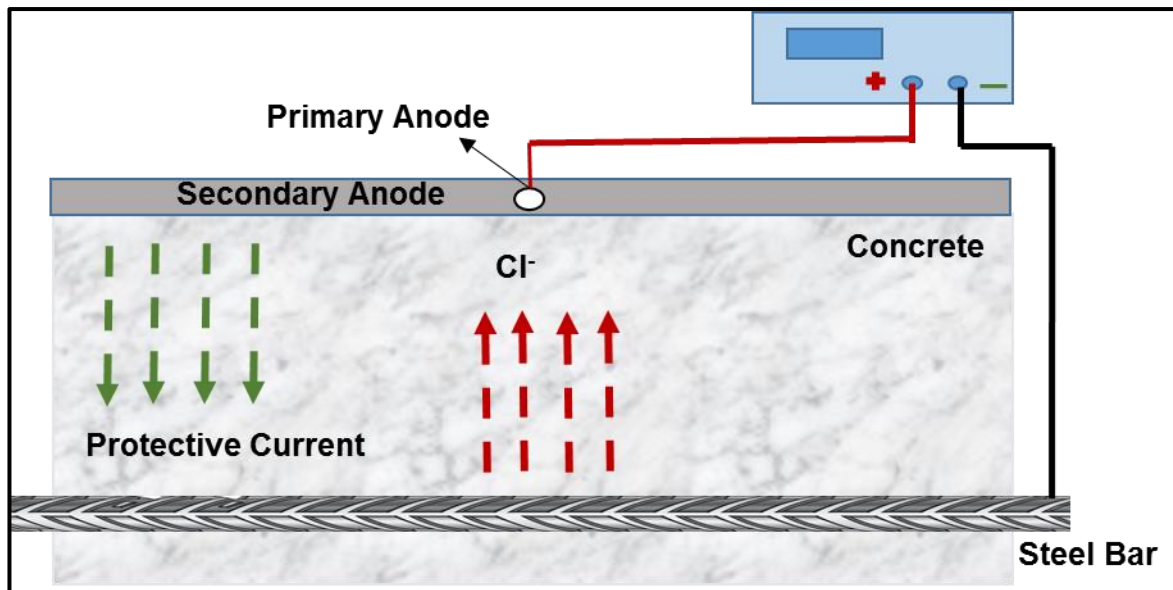
Figure 3.16 Schematics of cathodic protection

The details of the ICCP technique are as follows:

a) The steel bar was connected to the negative terminal of the rectifier and the positive terminal to the titanium wire. A current density of 10 mA/m^2 with reference to the surface of the steel bar initially and was regulated accordingly. The protection with a current density of 10 mA/m^2 was applied for 7 days and then the current density was increased to 20mA/m^2.

b) Corrosion of the steel reinforcement was periodically monitored at an interval of 7 days and the current was regulated accordingly in order to improve protection and not to reach -850 mV with reference to Cu/CuSO$_4$ to avoid hydrogen embrittlement of steel (BS EN 12696, 2016).

For testing and monitoring of corrosion and the prevention technique, non-destructive testing of slabs by means of half-cell potential measurements, linear polarisation resistance measurements and cyclic sweep were used whose details are provided in the sections below.

Half-cell Potential Measurements

Each and every metal has a tendency to return to its native state in which it is more stable in the surrounding environment. The reactions thus starts occurring on the surface of the metals to achieve a more stable configuration. In a similar process, the steel bar embedded in concrete starts to corrode and develops a potential. This developed potential is measured using a reference electrode which has a constant potential. In this study, copper/copper(II) sulphate reference electrode was used having a potential of +0.314 V with respect to hydrogen electrode. The schematic diagram of the measurements are shown below (Fig.3.17).
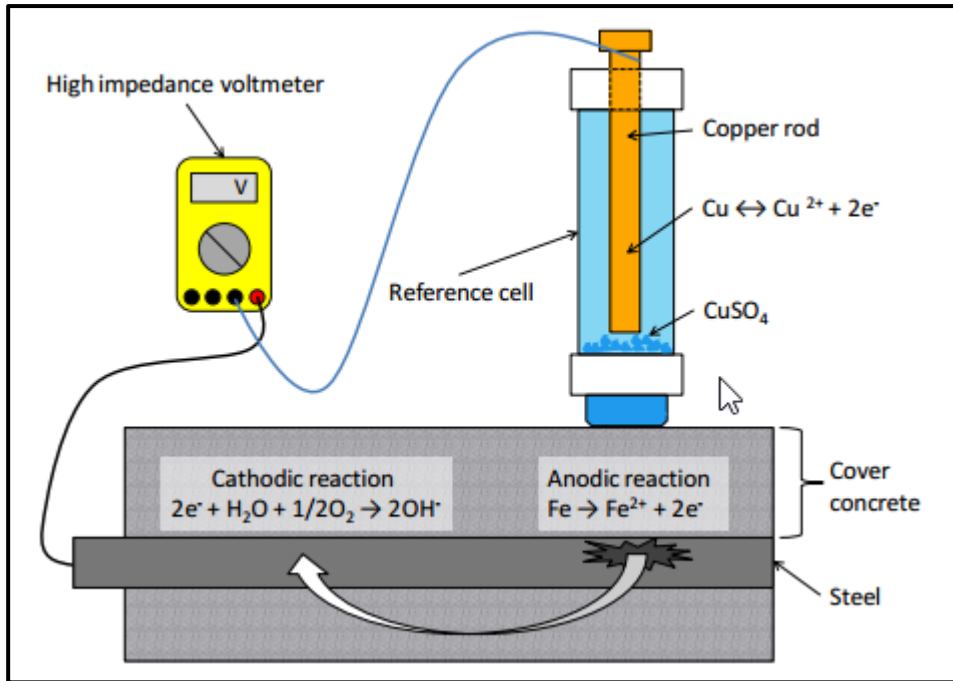
Figure 3.17 Schematics of HCP measurements taken on slab (Broomfield, 1997)

The results of the half-cell potential measurements were interpreted according to ASTM C876 (2009) and Concrete Society Technical Report 60 (2004). A sample measurement of the half-cell potential is shown in the Fig. 3.18.

Figure 3.18 HCP measurements taken on slab

Cyclic Sweep

Cyclic sweeps were performed over the steel bars embedded in the slabs to obtain the polarisation curves (Fig. 3.19). The Tafel slopes obtained were used to calculate the Stern-Geary constants which are in turn used to calculate the corrosion rate of steel. The sweep was performed using IVIUMSTAT equipment from IVIUM Technologies (UK). The parameters used for performing cyclic sweep are tabulated below (Table 3.5).

Table 3.5 Cyclic sweep parameters

Parameters	Values
Start Potential	-700 mV
Stop Potential	+700 mV
Sweep Rate	100 mV/min
Cell Settle Time	10 sec

*start and stop potentials were taken wrt to open cell potentials

Linear Polarisation Resistance (LPR) Measurements

LPR measurements are widely used to measure the corrosion and quantifying it as corrosion rate. LPR measurements were performed using IVIUMSTAT equipment from IVIUM Technologies (UK). The parameters for conducting LPR measurements are listed in Table 3.12. The arrangement of the LPR test using guard ring is shown in Fig. 3.6.

Table 3.6 LPR measurement parameters

Parameters	Values
Start Potential	-20 mV
Stop Potential	+20 mV
Sweep Rate	6 mV/min
Cell Settle Time	10 sec

*start and stop potentials were taken wrt to open cell potentials

The results of the LPR measurements were interpreted according to Concrete Society Technical Report 60 and the amount of steel dissolving to form ferrous oxide is measured using Stern-Geary equation (Equation 3.2).

$$i_{corr} = \frac{B}{Rp}$$

.... (**3.2**)

Where,

B = constant relating to the electrochemical behaviour of the metal under the testing environment

ΔE = potential shift (mV)

ΔI = current flow (mA)

$Rp = \Delta E/\Delta I$ (ohm)
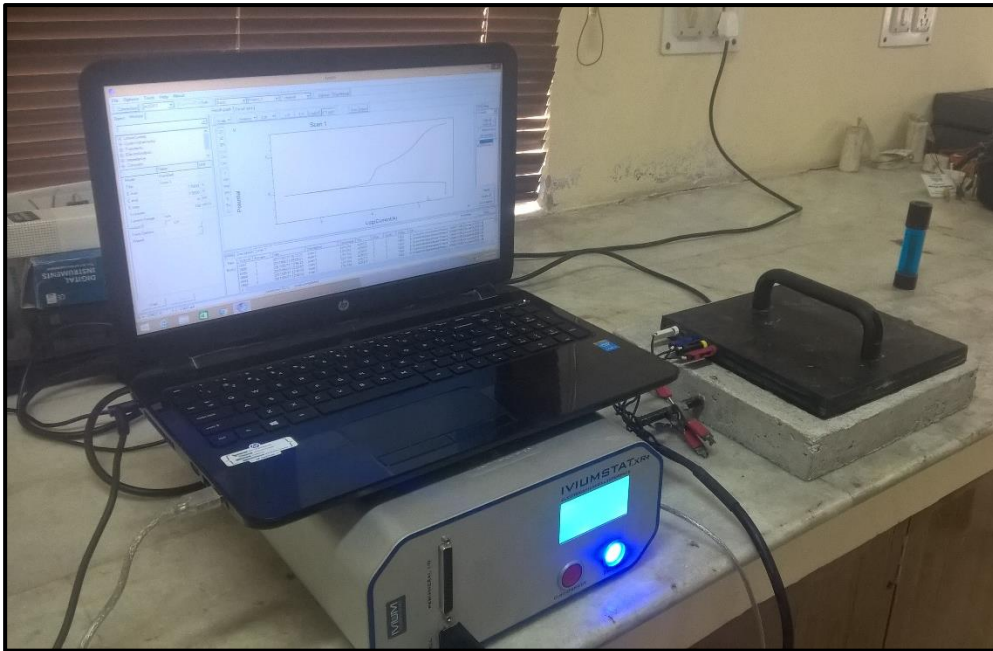
Figure 3.19 Specimen and connections for LPR measurements

Electrochemical Impedance Spectroscopy (EIS)

The electrochemical processes occurring during corrosion of steel embedded in concrete is a complicated process and EIS helps in developing a better understanding of what is happening inside the concrete. As every electrochemical process can be modelled using basic electrical elements, so is the corrosion of steel rebars. By using EIS and modelling the electrochemical process using basic electrical elements, these processes can be well understood and can give the information which other monitoring techniques are unable to provide. Testing was performed using ACM Field Machine from ACM Instruments, UK as shown in Fig. 3.20.

The testing parameters for EIS are listed in Table 3.7.

Table 3.7 EIS test parameters

Parameters	Values
Start Frequency	100 kHz
Stop Frequency	100 Hz
Amplitude	10 mV/RMS
Cell Settle Time	10 seconds
Readings per test	100
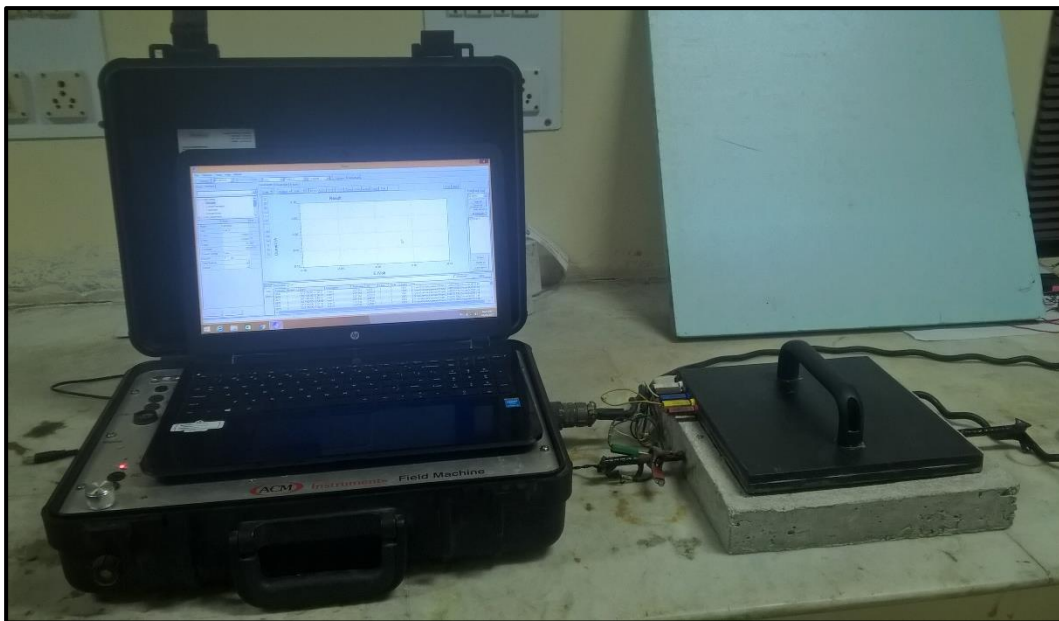
Figure 3.20 Specimen connection for EIS measurements

The response of test performed was in the form of Nyquist and Bode's plots which were studied using EIS analysis software ZMAN 2.2. An electrical circuit using ohmic resistance, charge transfer resistance and double layer capacitance was used to model and analyse the obtained impedance plots.
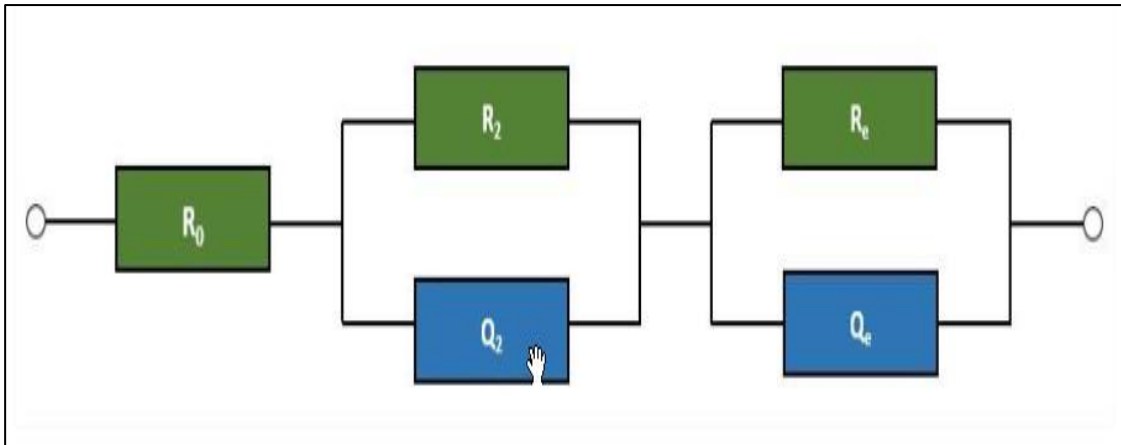
Figure 3.21 Equivalent circuit for analysis of impedance spectra

The equivalent model selected for the corrosion process is shown in the Fig. 3.21 consisting of offset resistance (R_o) having a minor relevance to the process is obtained at higher frequencies and can be neglected, R_b is the bulk concrete resistance surrounding the rebar which is obtained at medium frequencies. Q_b is the capacitance developed between concrete and the passive layer of steel when steel bar is passivated. The electrode charge transfer resistance (R_e) and the double layer capacitance (Qe) are obtained at lower frequencies which give a clear idea of the process and changes occurring at the steel bar surface (Jing and Wu, 2010).

CHAPTER 4

RESULTS AND DISCUSSION

4.1 Introduction

This chapter discusses the results obtained by conducting various tests to achieve the objective of the study. Firstly, the characteristics of various materials used in the study are discussed. Then, the mechanical and electrochemical properties of the anodic cement composite evaluated through the investigation are discussed. The efficacy of the applied CP technique using newer kind of anode is examined and discussed.

4.2 Characterisation of materials

4.2.1 Cement

The physical properties and chemical composition of cement is listed in Table 4.1 and Table 4.2 respectively. The results obtained are found to be complying to IS 8112 (2013).

Table 4.1 Characteristics of cement

Parameters		Results	Limits (IS 8112:2013)
Standard consistency (% of water by wt. of cement)		28	Not specified
Setting time (min.)	Initial	122	30 (min.)
	Final	240	600 (max.)
Fineness (m²/kg)		242	225
Soundness (mm)		1.5	10 (max.)
Specific gravity		3.15	Not specified
Compressive strength (MPa)	3 days	25.10	23 (min.) at 3 days
	7 days	36.25	33 (min.) at 7 days
	28 days	46.10	43 (min.) at 28 days

Table 4.2 Chemical composition of cement

Chemical Composition		Range (Shetty, 2005)
Compounds	**XRF results (%)**	
CaO	64.30	60-68
SiO_2	19.30	18-25
Al_2O_3	5.85	3-8
Fe_2O_3	5.03	0.5-6
MgO	0.83	1-4
$Na_2O + 0.6 K_2O$ (Total alkali)	0.81	0.4-1.3

4.2.2 *Aggregates*

Physical characteristics of fine aggregates and coarse aggregates are shown in Table 4.3 and 4.4, respectively. The grading curve for sand is shown in Fig. 4.1.

Table 4.3 Physical properties of fine aggregates

Physical Properties	Observation	IS:383:2016 Recommendations
Appearance	Dark Grey	
Specific gravity	2.64	2.60-2.70
Water absorption (%)	1.30	-
Moisture content (%)	0.35	-
Grading	Zone II	-
Fineness modulus	2.31	2.00-3.50
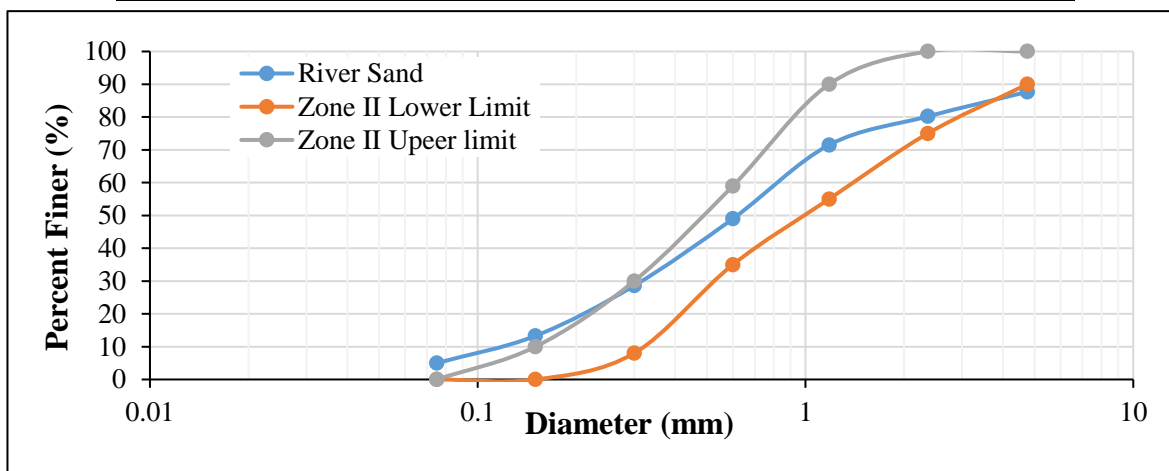
Figure 4.1. Gradation curve for sand

65

The sand was found to be lying in Zone II according to IS 383 (2016). The specific gravity of the sand was found to be 2.64 and fineness modulus of 2.31.

Table 4.4 Physical and mechanical properties of coarse aggregates

Test Parameters	Aggregate size		Limits in accordance to IS standards
	< 20 mm	**< 12.5 mm**	
Specific gravity	2.69	2.68	2.60 - 2.70 (IS 383)
Water absorption (%)	1.47	0.52	Not specified
Dry rodded density (kg/m^3)	1590	1575	
Loose bulk density (kg/m^3)	1472	1435	
Voids (%)	45.20	45.64	
Crushing value	18.56	16.54	45 (max.) (IS 2386)
Impact value (%)	23.00	11.52	45 (max.) (IS 2386)

The specific gravity of coarse aggregate was found to be 2.69 and 2.68 for 20 mm down and 12.5 mm down, respectively. Other properties of the aggregates were found to be in accordance with the limits provided in various IS standards.

4.2.3 Conductive Fillers

4.2.3.1 e-Waste Metallic Powder

The physical properties of the e-waste metallic powder are listed in Table 4.5 and chemical composition is shown in Fig. 4.2.

Table 4.5 Physical properties of e-waste metallic powder

Parameters	Values
Specific gravity	5.089
Bulk density (kg/m^3)	2340
Fineness modulus	3.13
Aspect ratio	1.0 to 2.2
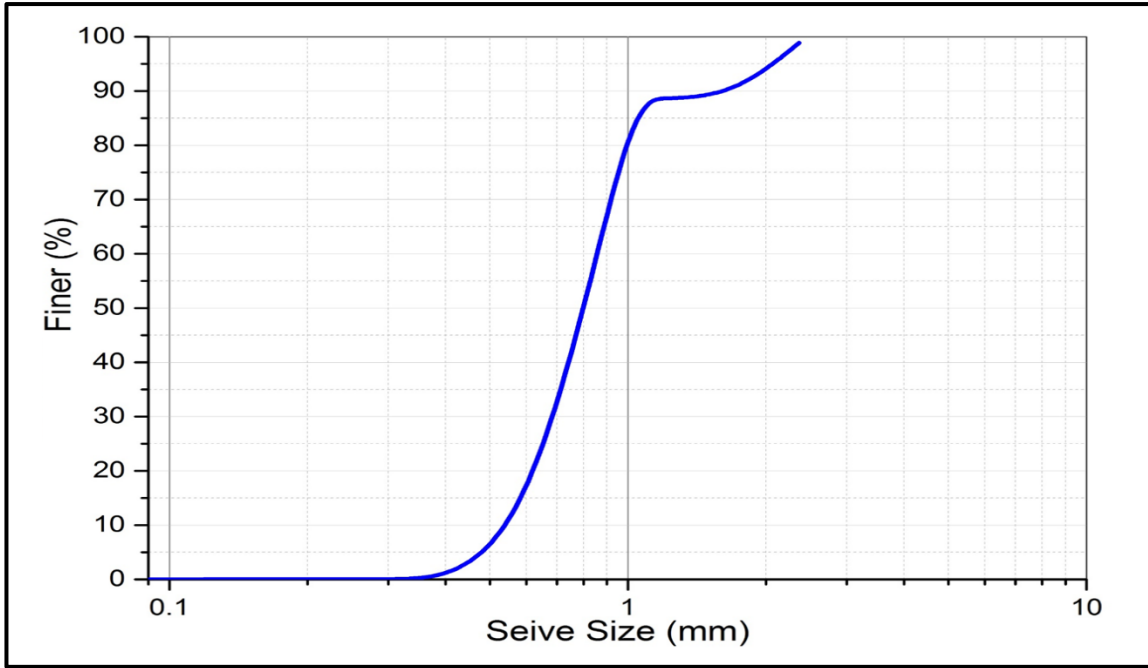
Figure 4.2 Gradation curve for e-waste metallic powder

The size of the maximum particles was between 600 μm and 850 μm as the weight percent of the particles passing through 850 μm and retained over 600 μm sieve was maximum.
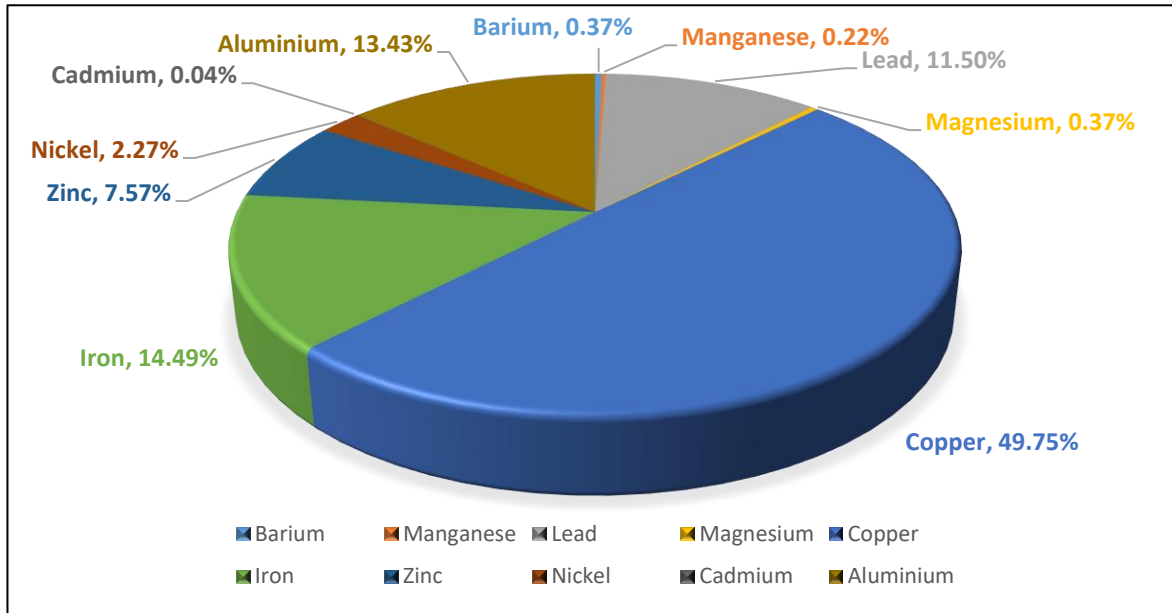
Figure 4.3 Chemical composition of e-waste metallic powder

The chemical composition of e-waste metallic powder is shown in the Fig. 4.3. The specific gravity of the e-waste metallic powder was found to be 5.089 and a bulk density of 2340 kg/m^3 which is very high as compared to other aggregates and cement. It can be observed from Fig. 4.3 that Copper constitutes almost 50% by weight of the e-waste metallic powder, Iron, Aluminum, Lead, Zinc and Nickel were found to be 14%, 11.5%, 7.57%, 2.27%, respectively

and other metals like Cadmium, Barium, Magnesium, and Manganese were found in very small quantities (<0.37%). The presence of heavy metals like Zinc, Cadmium, Lead and Barium makes the metallic powder hazardous. Thus, the use of metallic powder should decrease the resistivity of the cement composite as Copper is highly conductive in nature and is present in large amount in e-waste metallic powder.

4.2.3.2 Graphite Powder

The specific gravity of the graphite powder was found to be 0.8. The other properties of graphite powder are listed in Table 4.6 and the particles gradation curve is shown in Fig. 4.3.

Table 4.6 Properties of graphite powder

Parameters	Values
Specific gravity	0.8
Bulk density (kg/m^3)	555
Water content by mass (%)	0.5
Ash by mass (%)	23.0
Fixed carbon by mass (%)	62 .0
Volatile matter by mass (%)	14.5
Water absorption (%)	72
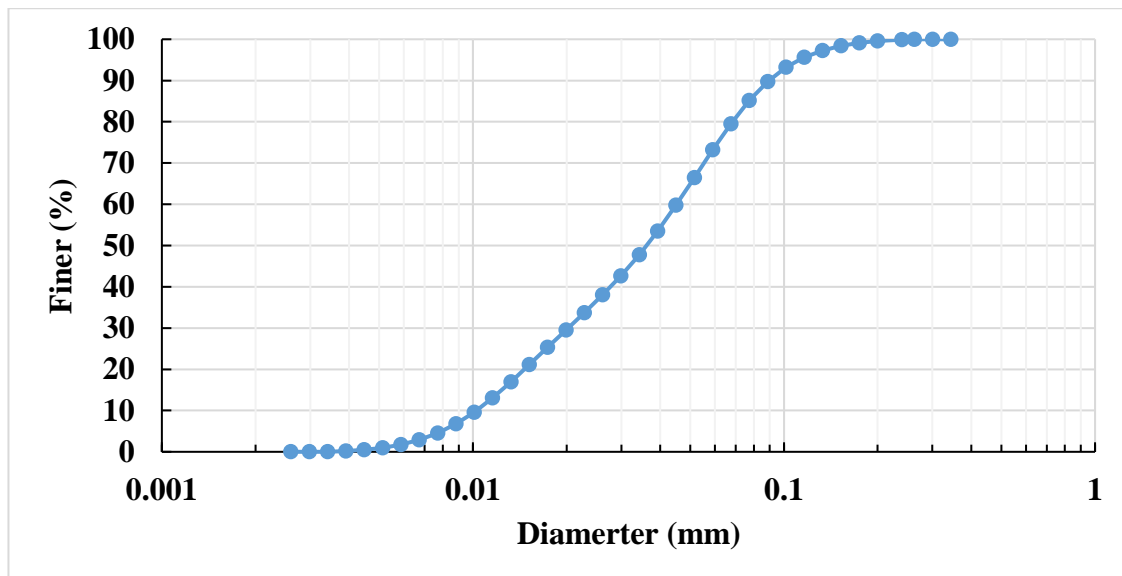
Figure 4.4. Gradation curve for graphite powder

The mean size (D_{50}) of the graphite powder was found to be 44.56 μm and the specific gravity was found to be 0.8 due to its porous nature with a bulk density of 555 kg/m^3 and a high water absorption of 72%.

4.3 Properties of Conductive Cement Composite

A cementitious composite should have a sufficient compressive strength besides the functional properties. So, a high compressive strength is desirable for the anodic cementitious mix. To ascertain this, compressive strength tests for different mixes were done and the results are presented.

4.3.1 Compressive Strength

The compressive strength of the conductive cement composite with e-waste metallic powder content of 1%, 2%, 5%, 15%, and 20% by volume was tested and the results are shown in Fig. 4.5.
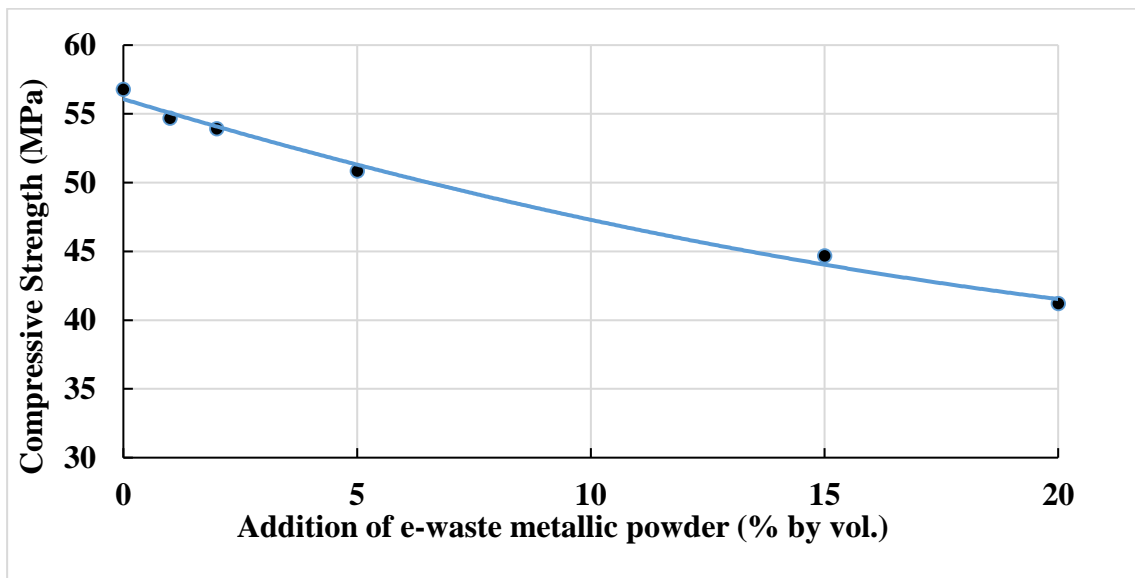
Figure 4.5 Change in compressive strength with content of e-waste metallic powder (at 28 days)

It can be observed from the Fig. 4.5 that the compressive strength of the cement composite decreases with increase in the content of metallic powder. The reason for the decrease of the strength can be due to increase in the porosity of the mix owing to the chemical reaction occurring between aluminium, water and hydroxides in wet composite. This can also be attributed to the weak bond between cement paste and metal particles due to the smooth surface and hydrophilic nature of the metals.

The effects of addition of graphite powder on compressive strength of the composite are shown in Fig. 4.6.
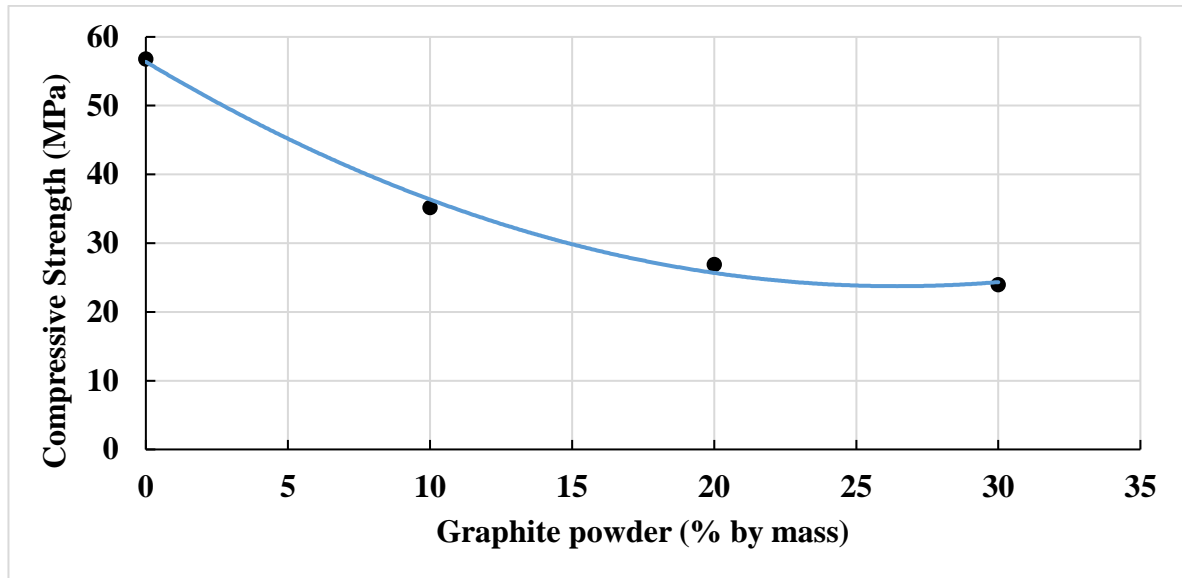
Figure 4.6 Change in compressive strength with addition of graphite powder (at 28 days)

It can be observed from the Fig. 4.6 that the compressive strength of the composite decreases with increase in the graphite powder content. This is because of the difference in the specific gravity of the cement paste and graphite powder and also due to the flaky nature of the graphite particles which lie dormant in the composite. Another reason can be the porous nature of the graphite powder, poor bond with the cement paste and lower compressive strength of the graphite particles.

4.3.2   *Electrical Resistivity of Conductive Cement Composite*

The resistivity of the anode is the most important parameter for an anodic system, so the changes in resistivity were comprehensively examined. The effect of increasing content of the conductive fillers on DC resistivity for the composite 1%, 2%, 5%, 15%, and 20% of e-waste metallic powder by volume of wet cement paste are shown in the Fig. 4.7.
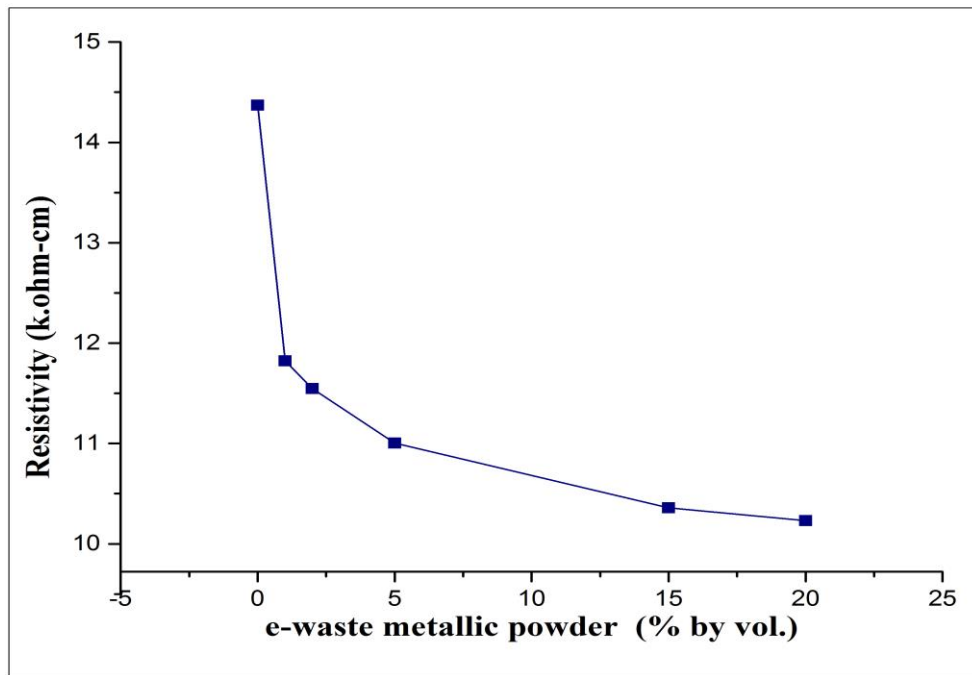
Figure 4.7 Effect of addition of e-waste metallic powder on resistivity (at 28 days)

It can be observed that the resistivity of the cement composite is reducing with increase in the e-waste metallic powder content. However, the reduction in the resistivity was not very high. The resistivity of a cementitious composite depends on the size of the conductive fillers, thickness of the cement composite film around the filler. The resistivity can either be improved by reducing the size of the fillers or by increasing the filler content. The reason for the observed behavior can be the lower content of e-waste metallic powder and a larger size of the metal particles as compared to other conductive fillers. So, to decrease the resistivity and to avoid increase in the bulk density, graphite powder was chosen to be used in combination with e-waste metallic powder. The graphite powder was chosen as it is easily available, cheap and has a smaller particle size as compared to other conductive fillers.

The effect of addition of graphite powder to the cement paste was also studied and is shown in the Fig. 4.8. The content of graphite powder was taken as 5%, 10%, 20% and 30% by mass of the cement.

71
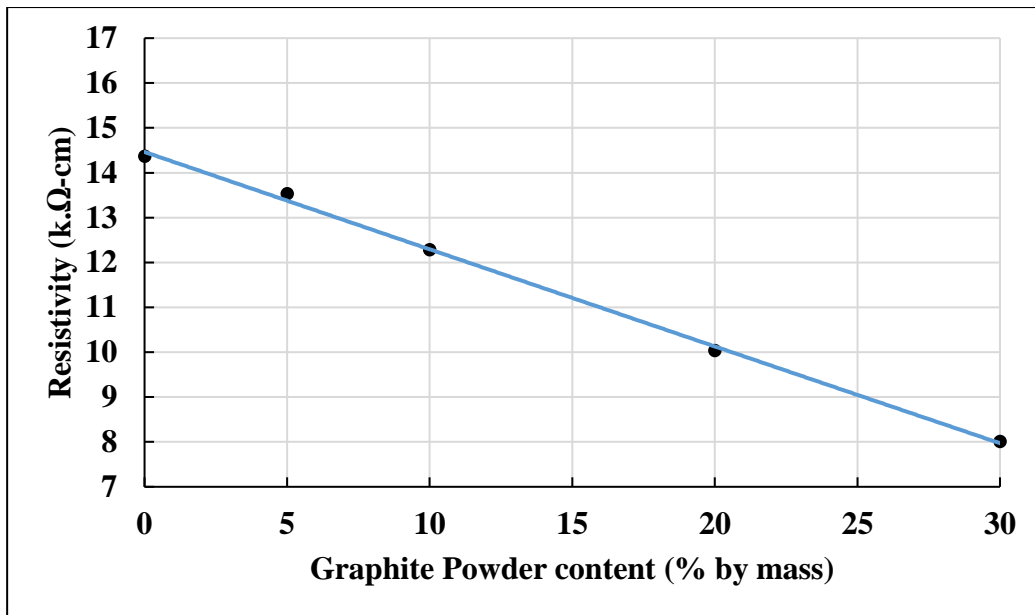
Figure 4.8 Effect of addition of graphite powder on resistivity (at 28 days)

It can be observed from the Fig. 4.8 that the decrease in resistivity is higher as compared to the decrease when e-waste metallic powder was added. This can be due to the smaller size of the graphite particles and a uniform dispersion of the graphite particles across the composite.

When both of the fillers are used in combination, the mix was designed on the basis of RSM the relationships between the content of various conductive fillers and the response variable properties i.e. compressive strength and resistivity of the composite were obtained using DOE approach.

4.4 Mechanical Properties of Cement Conductive Composite Anodes with Conductive Fillers in Combination

4.4.1 Compressive Strength of Composite

The influence of addition of conductive fillers on the compressive strength of the composite mix proportioned by DOE approach was studied. The compressive strength of the composite was tested during the study and was found that the compressive strength of the composite decreases with increase in the conductive filler content. The obtained mean compressive strength for three specimens during the detailed study is plotted with the curing age in Fig. 4.9.
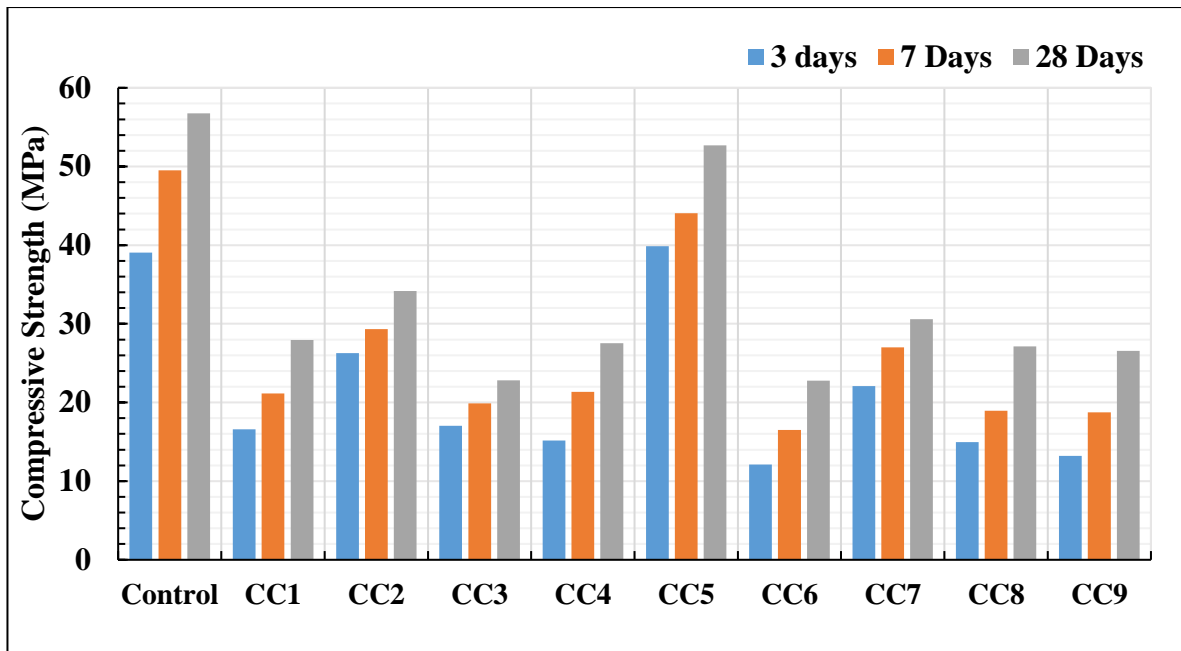
Figure 4.9 Effect of addition of conductive fillers on compressive strength with age

The presence of conductive fillers reduces the compressive strength of the conductive cement composite when compared with the control cement mix. It can be observed that for the mix CC5 i.e. without graphite powder and 47.1% e-waste metallic powder by mass, there is only a change of 5% in the compressive strength at 28 days. The mix CC6, with the presence of 47.1% (by mass) e-waste metallic powder and 40% graphite powder shows the highest decrease of 69%, 71% and 66% at 3,7 and 28 days, respectively.

For a better understanding of the dependence of compressive strength on both fillers used in the mix, RSM is used to obtain the compressive strength with a change in the content of different fillers content. The dependence of compressive strength on the each of the factors (e-waste metallic powder content and graphite powder content) was found using DOE approach and is shown in Fig. 4.10.
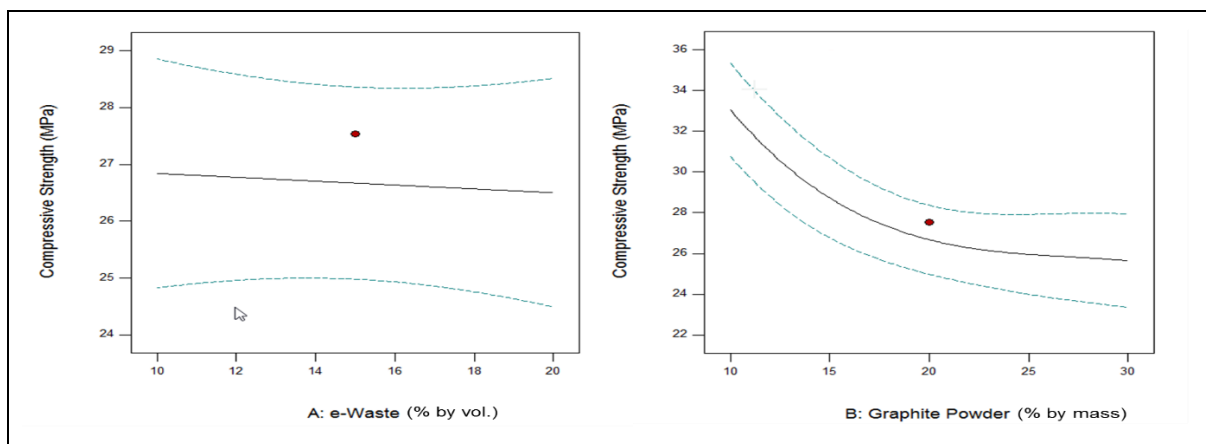
Figure 4.10 Effect of conductive fillers on compressive strength

It is evident that the addition of graphite powder reduces the compressive strength to a larger extent as compared to the e-waste metallic powder. This could be attributed to the smaller particle size and flakiness of the graphite powder as compared to the other component.

The effect of the combination of the fillers on the composite cement composite is shown in the Fig. 4.11.
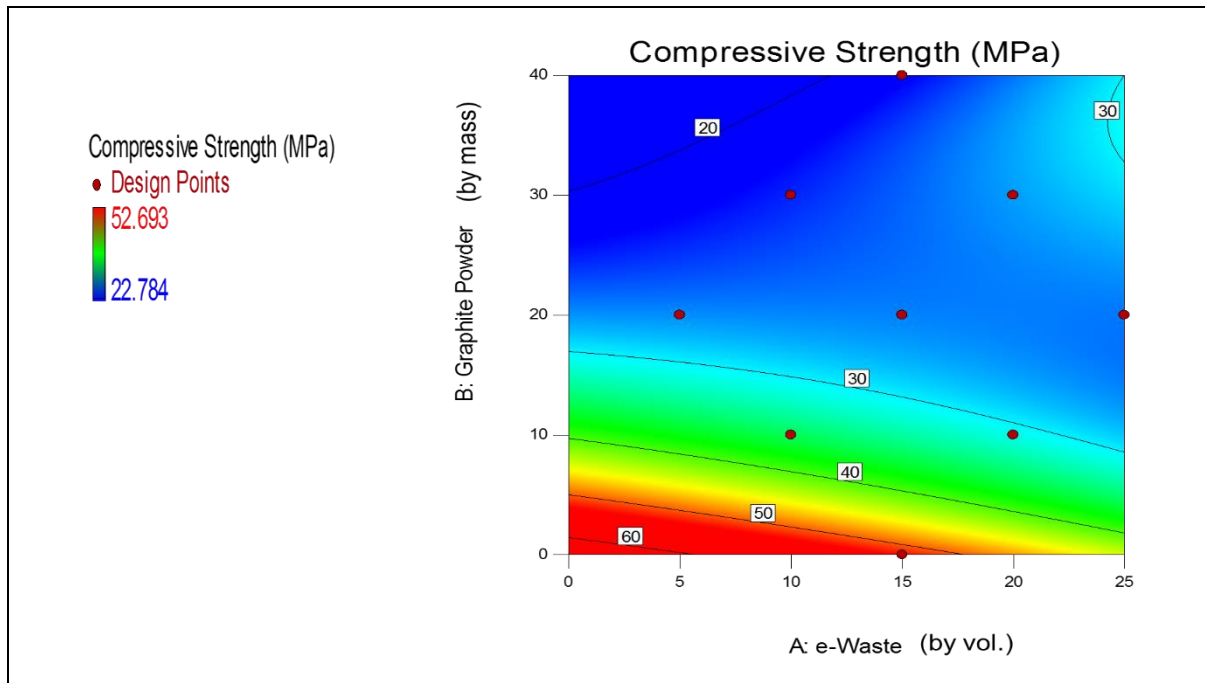
Figure 4.11 Contour plot for effect of conductive fillers on compressive strength (at 28 days)

It can be observed from the contour plot that the compressive strength of the composite reduces with increase in the filler content. This is happening because the cement particles are substituted by the graphite particles and e-waste metallic particles which do not have any binding capacity and have a lower specific gravity as compared to cement particles. This can also be attributed to the reduction in the amount of cement present in a fixed volume of the cement mix on the addition of the fillers. An equation for prediction of compressive strength on the basis of statistical analysis of the results obtained is given in equation 4.1.

$$Comp. Strength = 64.73158 - 0.82494 * eW - 3.41969 * GP + 0.039548 * eW * GP + 0.10233 * GP^2 - 0.0012566 * GP^3 \quad ………………….... \textbf{(4.1)}$$

Where,

    GP = graphite powder content (% by weight of cement)

    eW = e-Waste metallic powder content (% by vol. of the composite)

The relation between predicted and the observed compressive strength is shown in Fig. 4.12.

It can be observed that the predicted and actual compressive strength shows high linear dependency. From the analysis of variance at 0.05 significance level, it can be said that the proposed model is highly significant as R^2 value obtained is 0.9937 and adjusted R^2 value is 0.9831.
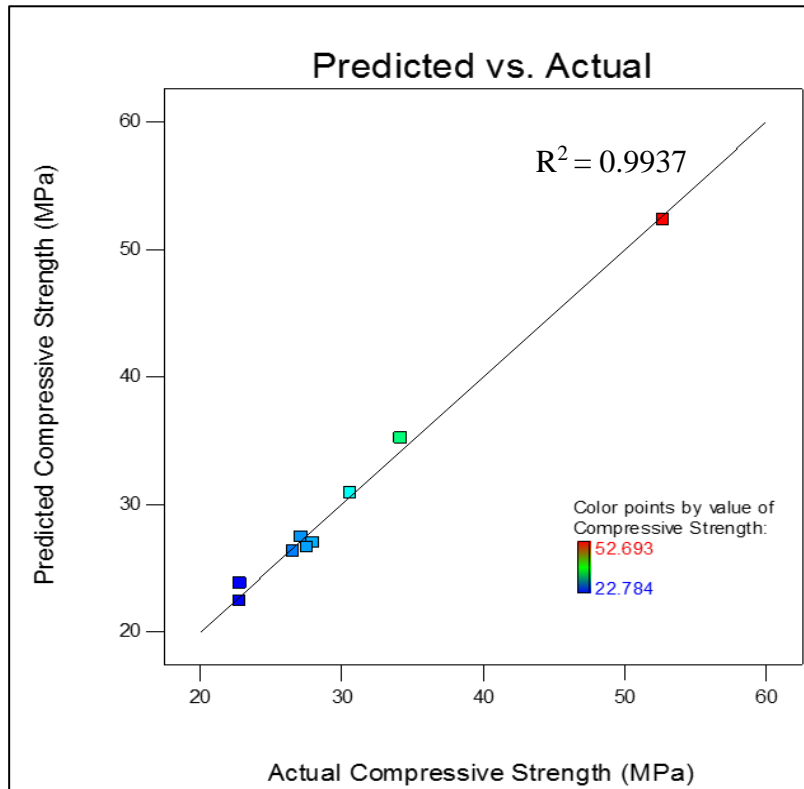
Figure 4.12 Predicted and actual - compressive strength

A 3D plot of dependence of compressive strength on content of conductive fillers is shown in Fig. 4.13.
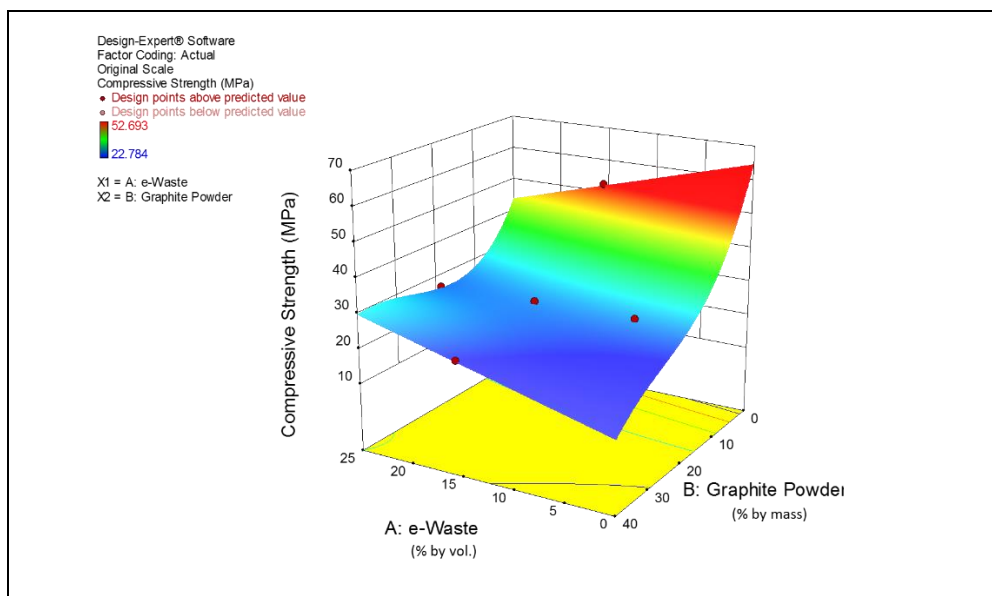
Figure 4.13 3D contour plot of compressive strength with filler content

It can also be observed from the 3D plot that greater reduction in the compressive strength is obtained on the higher percentage of the graphite powder as compared to the e-Waste metallic powder. The highest observed strength was of the composite CC5 containing (15% by vol.) 47.1% e-Waste metallic powder and no graphite powder and the lowest was of the mix CC6 having 47.1% by mass e-waste metallic powder and 40% by mass graphite powder.

4.4.2 *Bulk Density of Conductive Cement Composite*

The bulk density and the dry density measured for different mixes are shown in Table. 4.1.

The bulk and dry bulk density of the CC5 is the highest as no graphite powder is present in the composite and the lowest bulk density is of the CC6 with 47.1% (15% by vol.) e-waste metallic powder (by weight) and 40% graphite powder (by weight). The bulk density is decreasing with increase in the graphite content as the specific gravity and bulk density of graphite powder is much lower than that of the cement and e-waste metallic powder.

Table 4.7 Density of different composites

Mix Designation	Saturated Density (kg/m^3)	Dry Density (kg/m^3)	Water absorption (%)
Control	2285	1996	14.48
CC1	2104	1819	15.67
CC2	2247	1969	14.11
CC3	2074	1756	18.11
CC4	2137	1848	15.68
CC5	2506	2287	9.56
CC6	2013	1714	17.45
CC7	2301	2035	13.06
CC8	2187	1892	15.56
CC9	2252	1948	15.58

The lowest dry density was of the CC6 with highest water absorption of 17.45%. The lowest dry density and highest water absorption can be attributed to the presence of high graphite powder content of 40% (by mass) in the composite which is porous in nature and have a higher water absorption.

4.4.3 Compressive Strength of Concrete

The mix for M30 concrete was proportioned and samples were cast for the study of rebar corrosion and its control. The compressive strength at 28 days was found to be 37.53 MPa with a standard deviation of 0.8822 MPa which is acceptable according to the mix design of M30 grade of concrete.

4.5 Electrochemical Properties of the Conductive Cement composite

4.5.1 Resistivity

The electrical resistivity of the conductive cement composite was measured by using alternating current (AC) and direct current (DC). The DC resistivity of the combination or different mixes is shown in the Fig. 4.14.
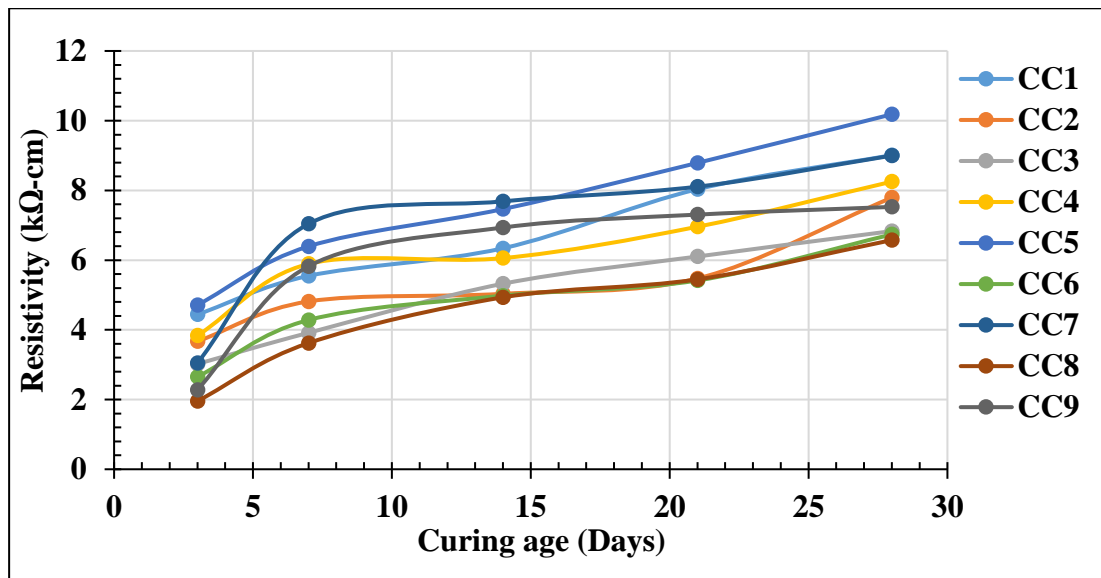
Figure 4.14 Effect of addition of conductive fillers on DC resistivity with age

The highest DC resistivity is exhibited by the CC5 similar to what was observed in case of AC resistivity. Whereas, the lowest DC resistivity was displayed by the CC8 which is 6.57 k.Ω-cm. The changes in the AC resistivity with the age of anodic composite is shown in the Fig. 4.15.
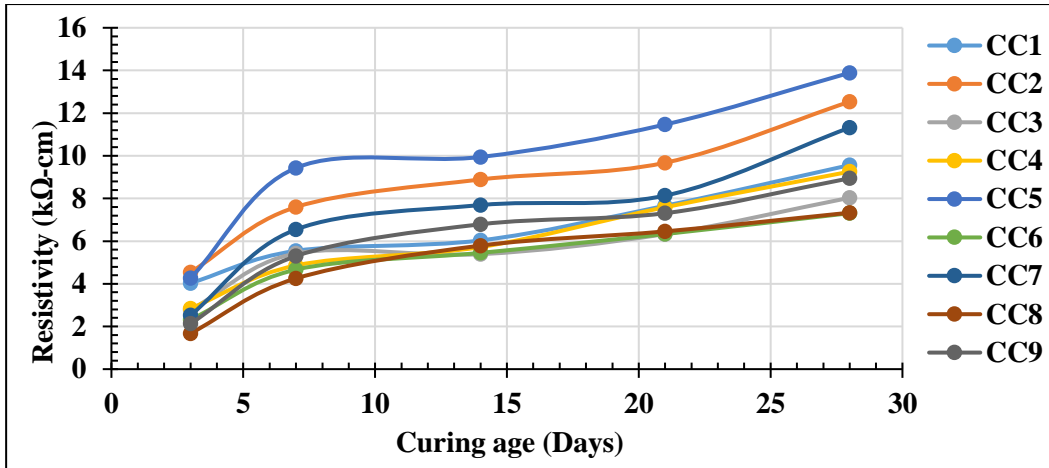
Figure 4.15 Effect of addition of conductive fillers on AC resistivity with age

For the optimization of the mix, AC resistivity is used as it is more reliable than the DC resistivity because of the polarisation effect of the cement paste in the composite. It can be observed from the plot that the highest AC resistivity is of CC5 i.e. having a value of 13.89 k.Ω-cm and it does not have graphite powder but contains 47.1% e-Waste metallic powder by weight of cement and the lowest AC resistivity is catered by the CC6 and CC8 which are nearly same at the values of 7.31 k.Ω-cm and 7.33 k.Ω-cm, respectively.

A correlation between AC and DC resistivity can be drawn by the obtained data and is shown in the Fig. 4.16.
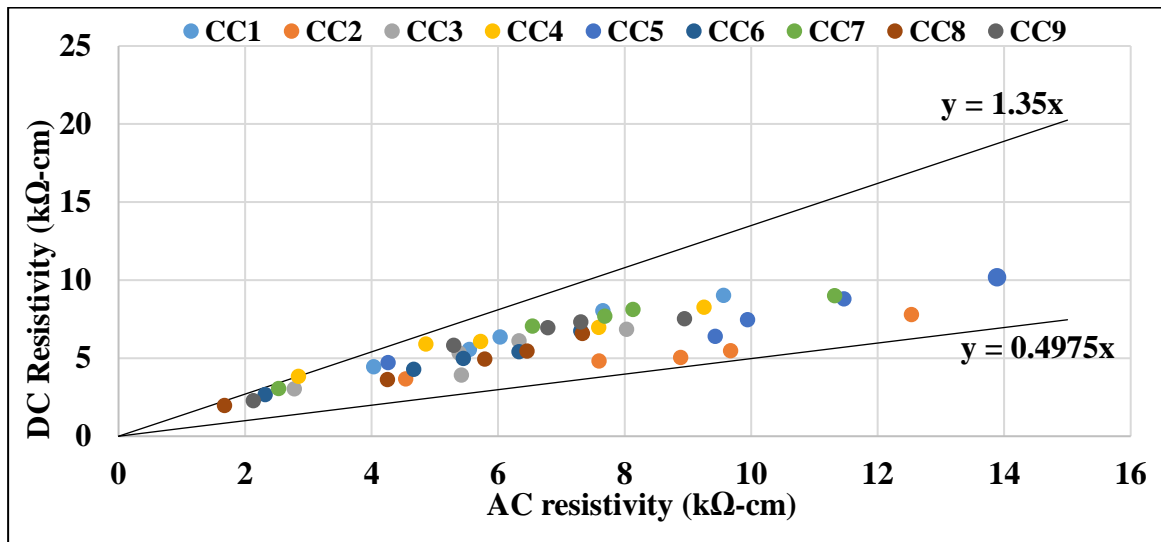
Figure 4.16 Correlation between AC and DC resistivity of anodic cement composites

A shadow zone between $y = 0.50x$ and $y = 1.35x$ is created due to the polarisation of the cement composite during the recording of test data. The polarisation has occurred as cement paste is a dielectric medium and charge starts accumulating as soon as the current start flowing through the system. To reduce the extent of polarisation of the cement composite, the test was

78

conducted at a very small current (<300 μA) and readings were taken as soon as the current is switched on.

The increase in resistivity of the specimens follows a similar trend with age as that of the compressive strength of the composite due to the hydration of the cement composite and increase in the hydrated products which are highly resistive as compared to the added fillers and are governing the increase in resistivity of the sample. The increase in the resistivity is also due to the reduction of pores as the hydration proceeds and the water present in the pores is replaced by the hydration products. This leads to reduction in porosity and an improved microstructure causing an increase in the resistivity.

For a better understanding of the dependence of resistivity on both fillers used in the mix, RSM is used to obtain the resistivity with change in the content of different fillers content. The dependence of resistivity on both conductive is shown in Fig.4.17.
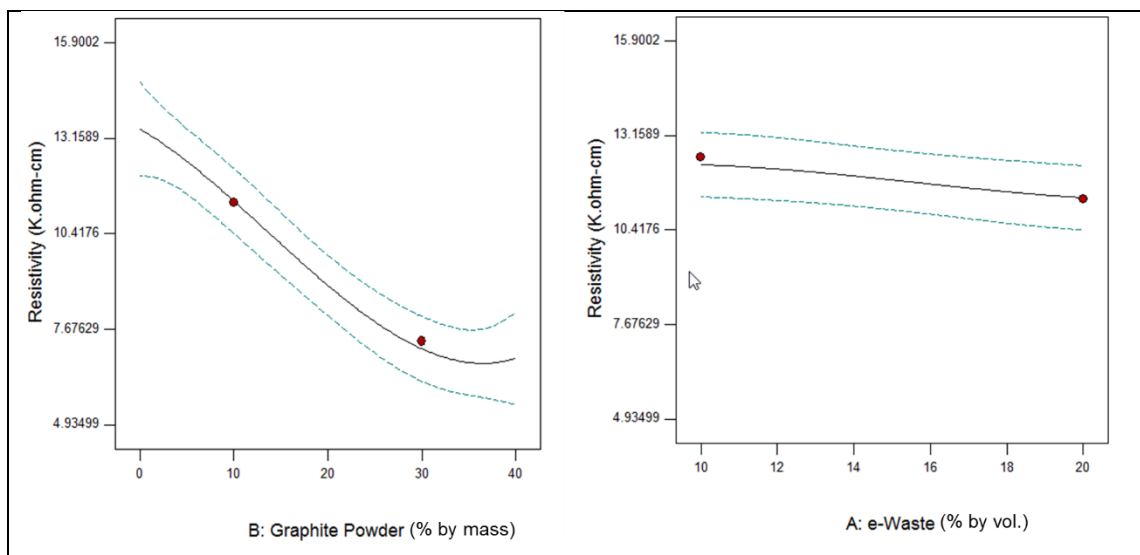
Figure 4.17 Effect of conductive fillers on resistivity of composite

It can be observed from the above plot that with an increase in the content of the e-Waste metallic powder, there is a constant decrease in the resistivity of the composite but the effect is more prominent due to presence of graphite powder.

It is observed from the above plot that the resistivity decreases with increase in the graphite powder content and then becomes almost constant. The decrease in the resistivity is about 40% when the graphite powder is increased from 0 to 40%. After 35%, a further increase in the graphite powder does not significantly affect the resistivity as the percolation threshold for the graphite powder would have reached and volumetric percolation of graphite powder has occurred in the composite.

The effect of the combination of both the fillers on the cement composite is shown by the contour plot in the Fig. 4.18.
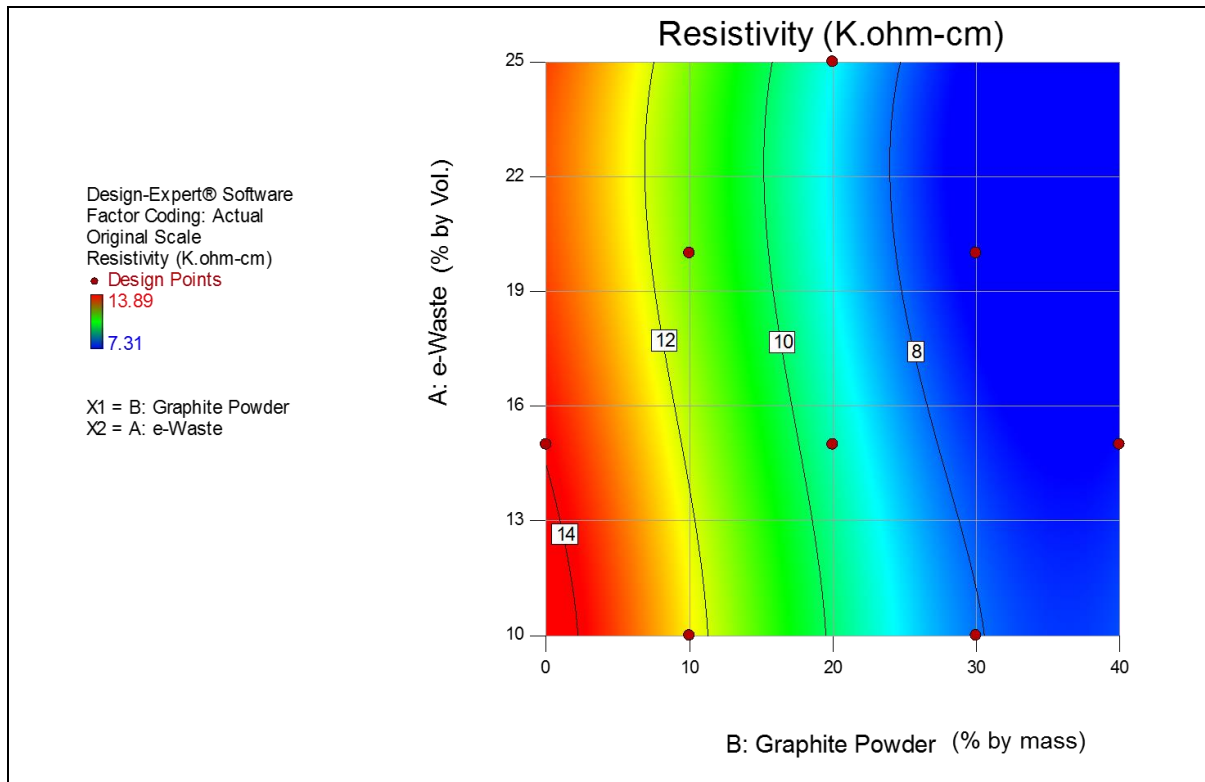
Figure 4.18 Effect of conductive fillers on resistivity

It is found from the contour plot that the resistivity of the composite reduces with increase in the fillers content up to a certain extent and further increase in conductive fillers content has an insignificant effect on the resistivity of the specimen. It can also be observed that the increase in the graphite powder content leads to greater decrease as compared to the e-Waste metallic powder as the volume of the fillers is less as compared to the graphite powder due to the smaller size of the graphite powder particles. The resistivity of the composite depends on the amount of the fillers present in the mix, size of the fillers and the thickness of the cement film around the fillers. A smaller size, thinner film and higher amount of fillers present will produce the lowest resistivity (Wu *et al.*, 2005). An equation for prediction of resistivity on the basis of statistical analysis of the results obtained is given in equation 4.2.

$$Resistivity = 12.45324 + 0.51003 * eW - 0.15739 * GP - 0.040389 * eW^2 -$$
$$0.00654 * GP^2 + 0.0008656 * eW^3 + 0.000159 * GP^3 \quad \ldots\ldots\ldots\ldots\text{(4.2)}$$

Where,

GP = graphite powder content (% by mass of cement)

eW = e-Waste metallic powder content (% by vol. of the composite)

The relation between predicted and the actual resistivity is shown in Fig. 4.19.
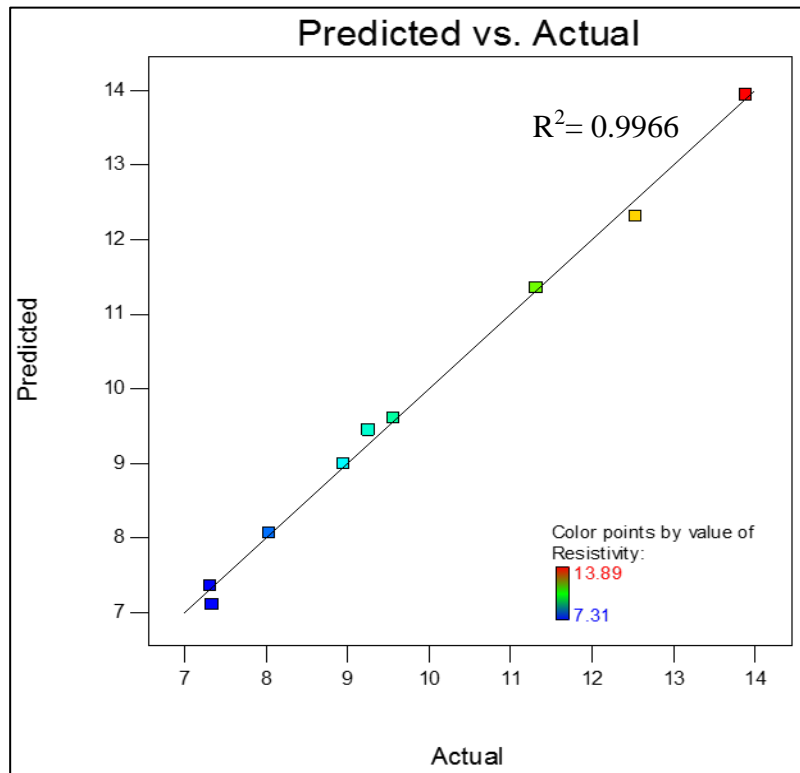
Figure 4.19 Predicted and actual -AC resistivity

A 3D plot for the dependence of compressive strength on the content of conductive fillers is shown in Fig. 4.16.
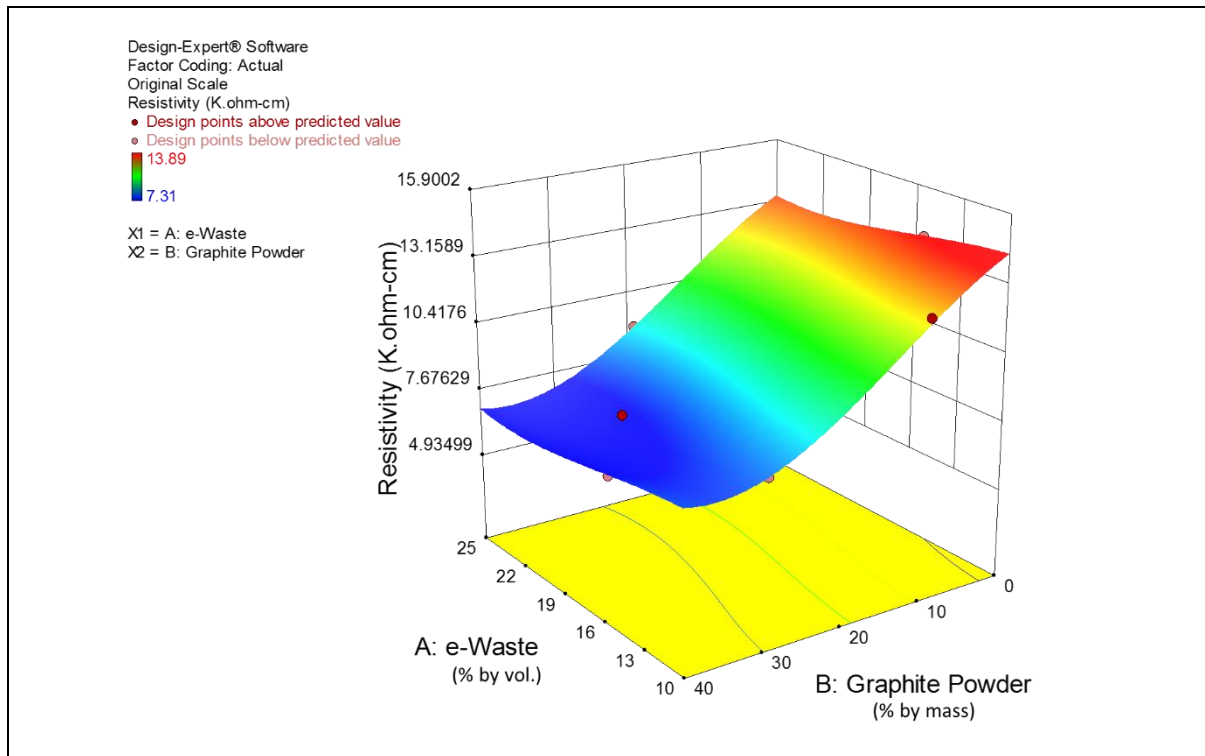
Figure 4.20 Effect of fillers content on resistivity

It is observed that the predicted values and the actual values show high linear dependency, which is also confirmed by analysis of variance at a 0.05 significance level. The R^2 value of the proposed model was found to be 0.9966 and adjusted R^2 was 0.9863 proposing the model to be highly significant.

A similar trend for both graphite powder and e-Waste metallic powder is observed. The increase in the filler content leads to increase in the resistivity of the conductive cementitious composite.

4.5.2 Accelerated Galvanostatic Test

4.5.2.1 In Saturated Ca(OH)$_2$ solution

The Fig. 4.21 shows the anodic potential shift of the cement composite specimens that has occurred due to the application of the constant current density of 200 mA/m^2 in saturated Ca(OH)$_2$ solution.

Figure 4.21 Anodic potential of the conductive cementitious composite as a function of exposure time in sat. Ca(OH)$_2$ solution

There was no stable potential observed for any of the mixes till 200 hours of exposure of the anodic probes. The variation of potential till 200 hours is listed in the Table. 4.7. It is to be noted that anodic potential is constantly changing throughout the test period which is due to the polarisation of the conductive cement composite samples and change in the resistance of the anodic probes. The widest range of potential rise and drop is observed for the anodic probes

82

with configuration CC5 and CC4 i.e. 12.2 V and 12.49 V, respectively. This may be attributed to the highest resistance of CC5 and CC4 and also to the absence of the graphite powder in specimen CC5 which enables a greater amount of cement composite in a fixed volume of composite. The presence of a greater amount of cement paste in the composite makes it hard to stabilise and polarise to a constant potential.

Table 4.1 Range of polarisation of different anodic probes till 200 hours of test

Specimen	Minimum E (V vs. CSE)	Maximum E (V vs. CSE)
CC1	4.25	9.4
CC2	4.64	12.98
CC3	6.11	13.12
CC4	3.77	16.26
CC5	5.43	17.63
CC6	5.36	14.58
CC7	5.19	14.8
CC8	5.11	12.93
CC9	6.57	16.98

After 200 hours of the test, further flow of current or polarisation leads to a comparative stabilised anodic potential of the specimens CC6, CC7, CC8 and CC9. The specimen CC6 was stabilised in the range of 5.9 V to 6.35 V, CC7 stabilised in the range of 5.35 to 6.58 V, CC8 was stabilised in the range of 5.1 V to 6.9 V and sample 9 was stabilised in the range of 9.56 to 12.23 V with reference to CSE. Whereas, the other specimens did not get stabilised and the resistance of the specimens would have been changing due to the polarisation of the cement composite. Further after 345 hours of the test, the probes got destabilised and the potential slightly increased. Specimen CC6 stabilised in the smallest range of potential that can be due denser microstructure and presence of highest amount of graphite powder which enables absorption of more $Ca(OH)_2$ into the system.

CC5 shows the highest potential shift from 5.43 V to 17.63 V which is due to its higher resistance and absence of graphite powder. This means, the higher the potential higher is the power consumption of the anode and thus the requirement of the output voltage from the rectifier increases, which is unfavourable for ICCP systems. It can be concluded that the presence of a high volumetric amount of conductive fillers in the system enables the anodic probes to stabilise at a nearly constant potential. The results showed that when a constant current density is supplied and anodic potential measured in various systems is mainly

influenced by the resistance of the probes and the presence of pores and the system constituents through which the electrolyte can enter the system. After the test, the anodic probes were visually examined, and no cracks were observed on any of the surface of the anodic probes. Hence, it can be concluded that there is no unusual dissolution of the constituents of the anodic probe.

4.5.2.2 In Saturated Ca(OH)₂ solution with 3% NaCl solution

The anodic potential shift of the conductive cement composite or the anodic probes with the application of constant current density of 200 mA/m^2 in saturated Ca(OH)$_2$ solution in presence of NaCl solution is shown in Fig. 4.22.

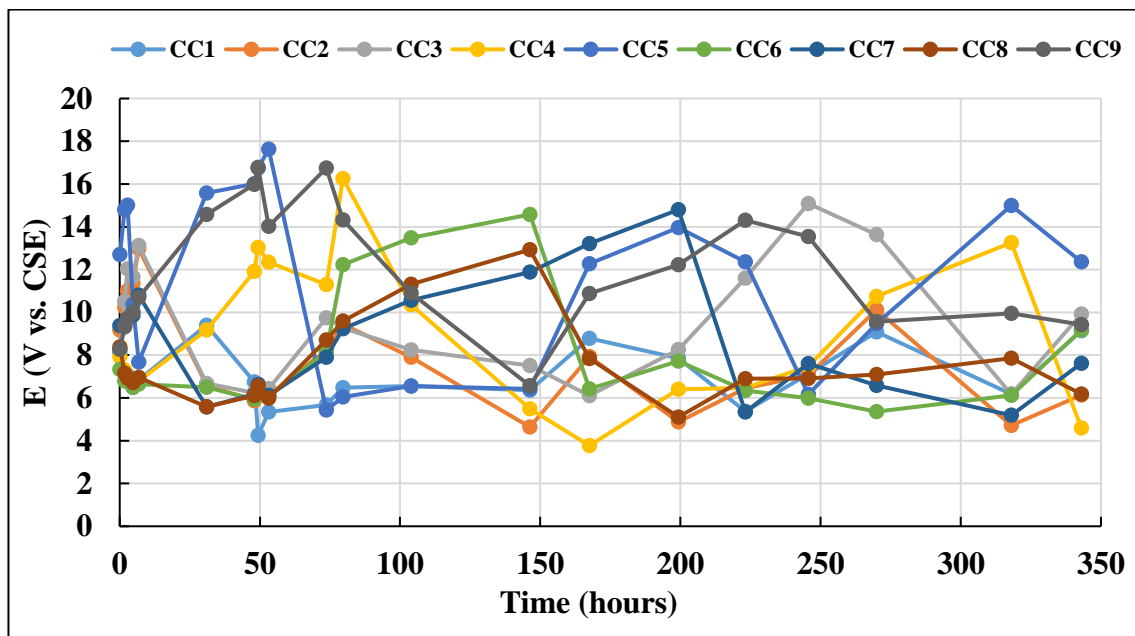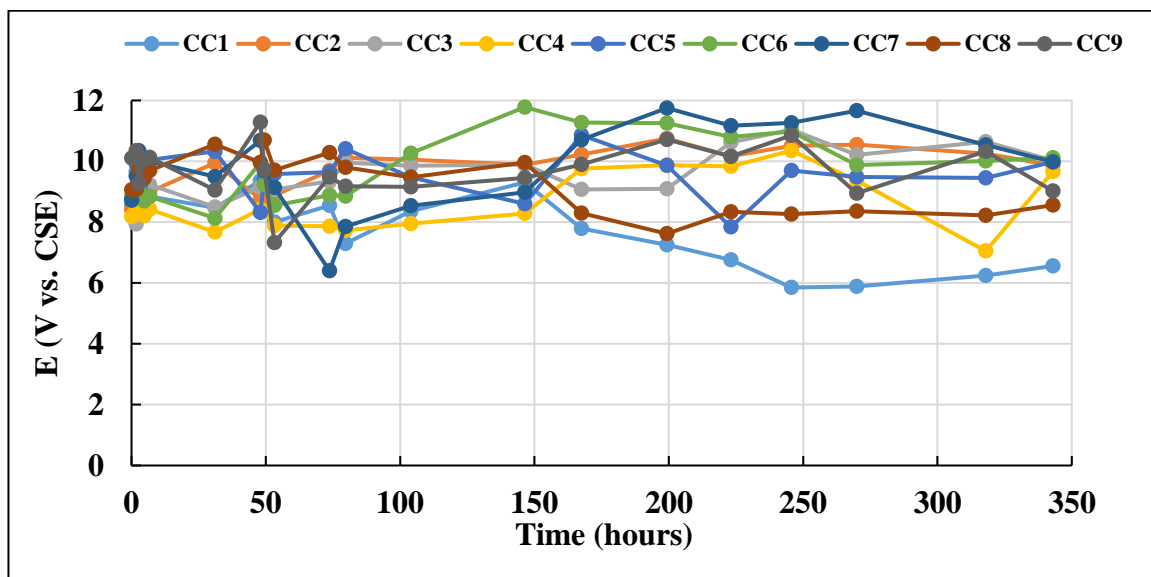**Figure 4.22 Anodic potential of the conductive cementitious composite as a function of exposure time in sat. Ca(OH)₂ solution with 3% NaCl solution**

Most of the specimens showed a stable behaviour or a more stabilised anodic potential shift. The anodic potential initially increases and then slightly reduces to stabilise at a constant potential. A constant or more stabilised configuration was observed only after 74 hours of the test duration. After another 72 hours i.e. about 146 hours of the test, a negative potential shift can be observed in all the specimens except CC4, CC7, and CC9.

The more stabilised configuration is due to the presence of chloride ions in the electrolyte which will start moving into the anodic probe towards the titanium wire as soon as the current starts flowing into the system. The stabilisation of anodic potential that took 146 hours of the test might be due to the saturation of the anodic probes with the chloride ions.

When comparing the anodic shift with the behaviour of anodic probes without chloride in the electrolyte solution, the anodic potential shift is reduced and a constant stabilised potential is achieved very soon.

From all the anodic probes, specimen CC1 is showing the most negative anodic potential shift, which might be due to higher permeation of the chloride ions into the probe due to its higher porosity as compared to other anodic probes. Whereas, the specimen CC8 also shows higher negative potential shift as compared to all other probes owing to its lower resistance as compared to all other cementitious anodic probes. The specimen CC8 is nearly stabilised at 8.26 V at the completion of the test. The highest potential shift is observed in the specimen CC7 at a potential of about 11.66 V wrt to CSE. The probable reason for the higher potential shift and stabilisation at high potential is due to the higher resistance offered by the anodic probe as can be observed from the Fig. 4.14 and Fig. 4.15.

Thus, it can be concluded that the shift in potential is reduced for all the specimens due to the presence of chloride ions in the electrolyte and permeation into the anodic probe and the anodic shift is dependent on the resistance of the anodic composite.

4.5.1 *Anodic Polarisation Tests*

After performing the electrochemical age test for 7 and 14 days by application of a constant current density of 200 mA/m^2, polarisation tests were performed on the various specimens to obtain E-logI plots. In order to find out the consumption of the anodic composite during the accelerated galvanostatic test, E-logI plots were analysed to obtain E_{corr} and I_{corr} values. E-logI plots for different anodes before application of the constant current density in saturated calcium hydroxide solution are shown in the Fig. 4.23 (1-9). Fig. 4.23(1) is for probe CC1, Fig. 4.23(2) is for probe CC2 and so on.

It is quite evident from the E-logI plots for various anodic mixes that the composite anode i.e. titanium wire and conductive cement composite are in the active region where the reaction rate of the anodic reactions increases with increase in the potential and the dominant reaction is the dissolution of anodic material. The active region of the anodic probes continues to a very high potential of +7.5 V and this is advantageous as the dissolution will ease the current flow through the anode. The active region is characterised by the oxidation reaction which will occur during the flow of current through the anode. E-logI plots for different anodes after application of the constant current density on the 7 and 14 days are shown in the Fig. 4.24 (1-9) and Fig. 4.25 (1-9), respectively.
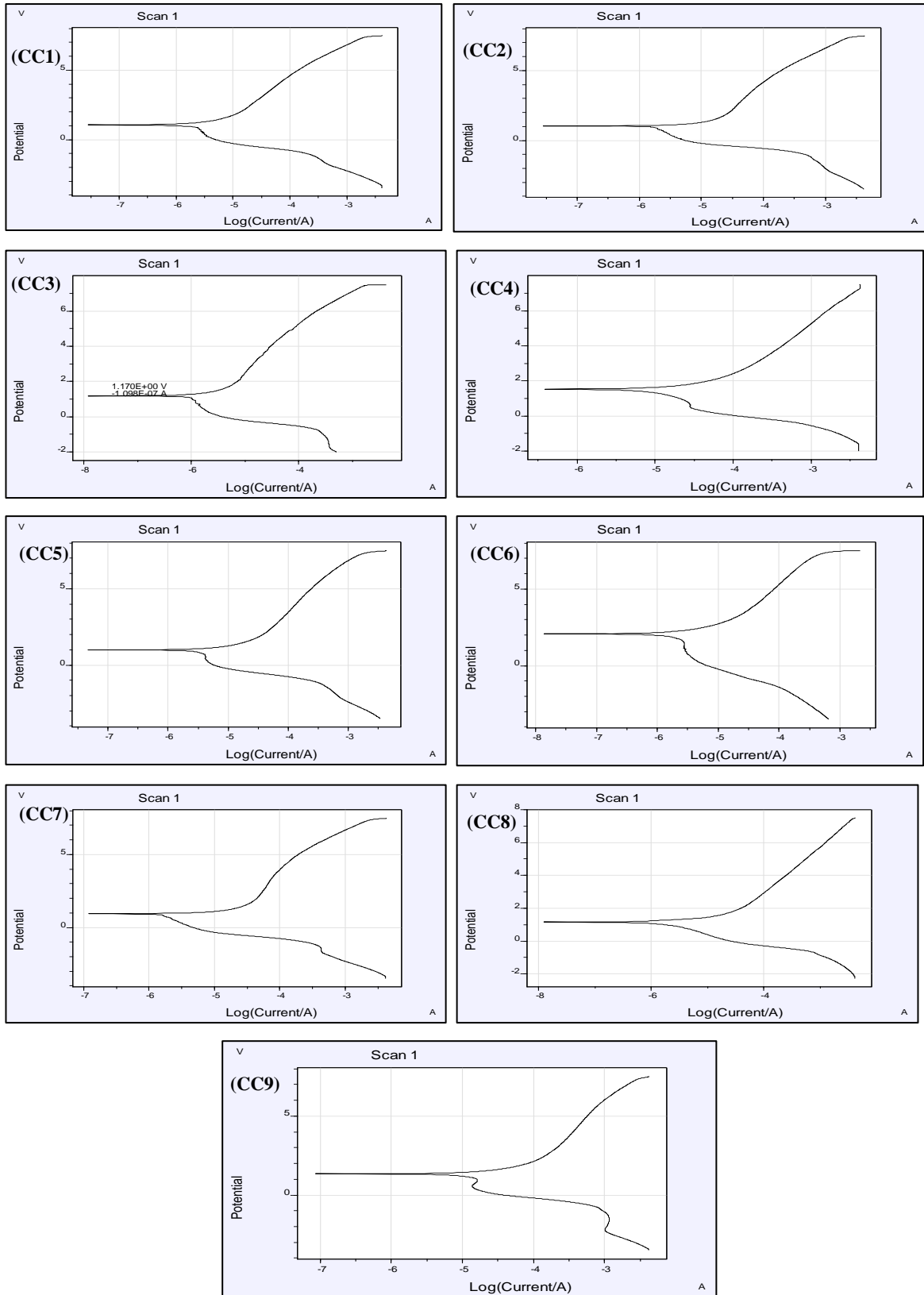
Figure 4.23 Polarization plots for different specimens before AGT in sat. Ca(OH)₂ solution
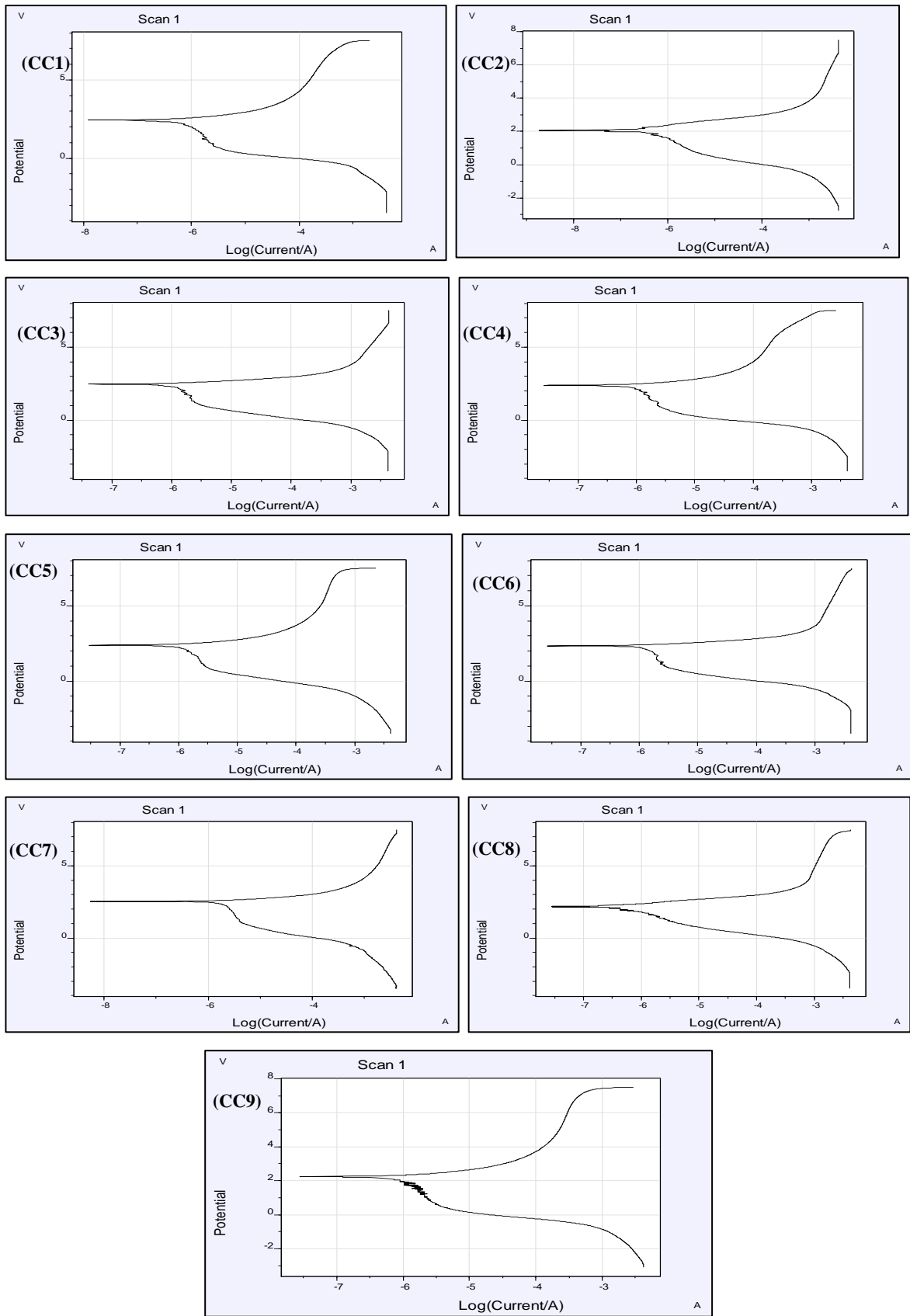
Figure 4.24 Polarization curves after 7 days of AGT in in sat. Ca(OH)$_2$ solution
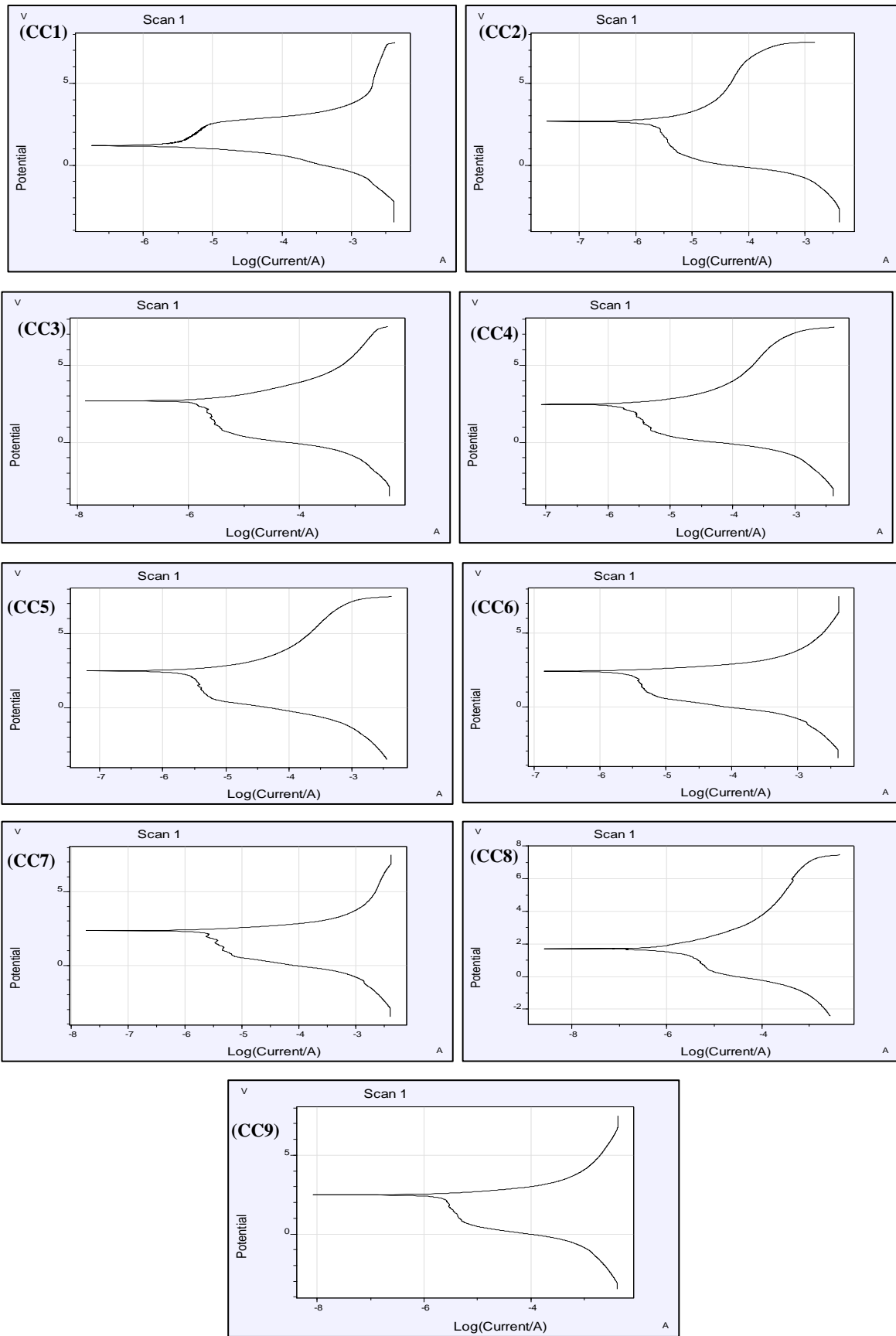
Figure 4.25 Polarization curves after 14 days of AGT in sat. Ca(OH)$_2$ solution

From the E-logI plots before initialising the accelerated galvanostatic test, the obtained E_{corr} values for the anodes ranges from -1.1176 V to 1.4314 V wrt CSE and the Icorr values ranges from 7.60E-08 V to 7.90E-07 V wrt CSE. It is to be noted that the composite anode probes along with titanium wire are in the active region and it will ease the consumption during ICCP technique.

It can be observed from the polarisation curves (Fig.4.24) that the behaviour of the anodic probes of specimens of CC2, CC3, CC6 and CC7 has changed with the application of current after 7 days. The potential shift due to accelerated galvanostatic test has compelled probes to enter into the passive region but at a higher potential greater than 6 V. All the other specimens still remain in the active zone and can be consumed easily as compared to others.

After 14 days of accelerated galvanostatic test, the anode probe specimens of CC1, CC6, CC7, and CC9 is showing passive behaviour at a high potential greater than 4 V, 6 V, 6.5 V and 6.5 V, respectively. All other specimens are displaying active behaviour which is most suited for an ideal anode. The E_{corr} and I_{corr} values obtained from these curves are plotted in Fig. 4.26 and Fig. 4.27, respectively.
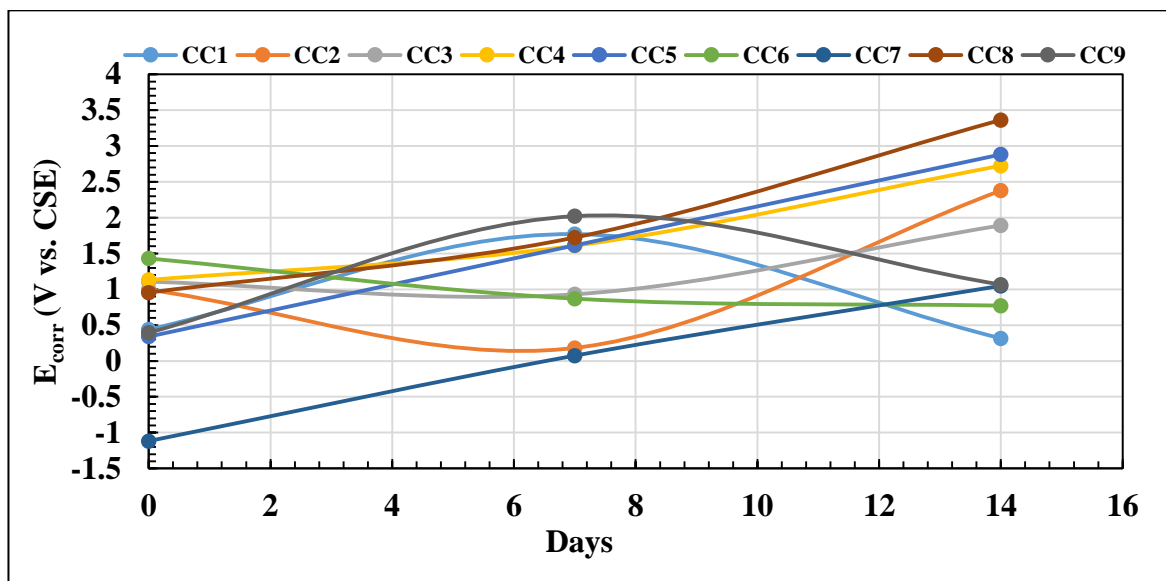
Figure 4.26 Effect of constant current density on corrosion potential of anodes in saturated Ca(OH)$_2$ solution

After 7 days of AGT, the E_{corr} values have increased for all the specimens except that for composites CC2, CC3 and CC6. This is due to the change of behaviour of the anodic probes which have entered the passive region from the active region with an increase in the anodic potential. As all the other specimens remained in the active region, thus the E_{corr} values have increased after 7 days.

It can be observed that for all the specimens except CC1, CC6 and CC9, the E_{corr} values have further increased with the increase in duration of AGT i.e. in 14 days. The reason for the unusual behaviour of CC1, CC6 and CC9 as compared to other specimens is due to the fact that they are showing passive behaviour at the end of 14 days but only at higher potentials. As the anode goes from active region to the passive region the anodic reactions start to slow down.
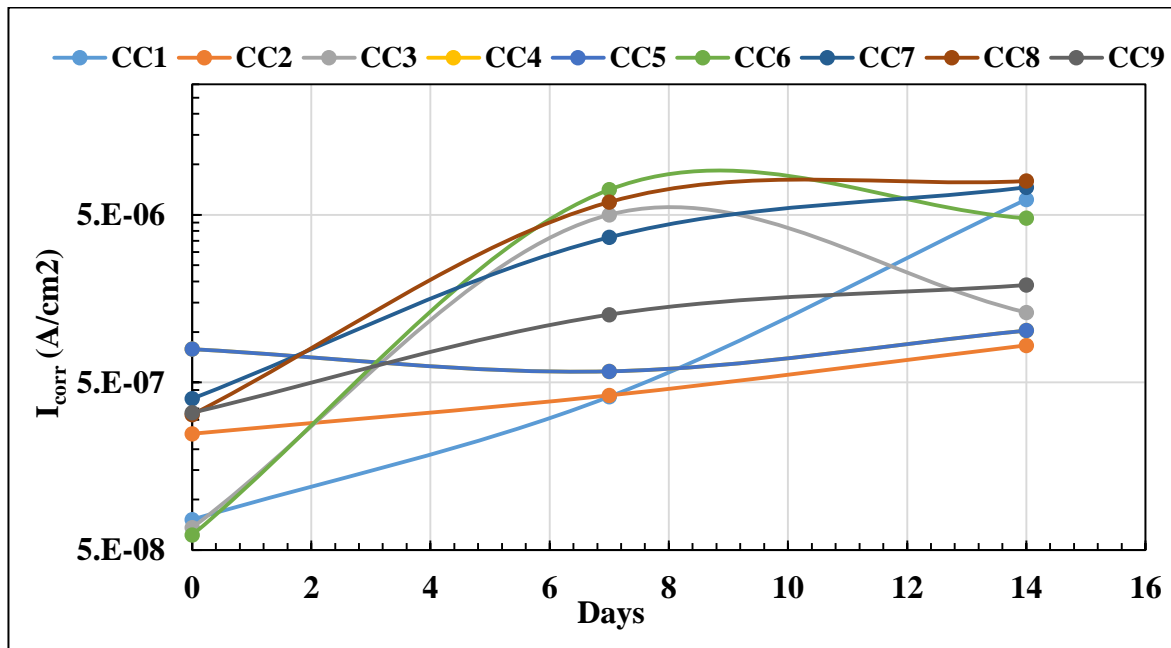
Figure 4.27 Effect of applied constant current density on corrosion current density of anodes in sat. Ca(OH)₂ solution

The I_{corr} values for all the specimens tend to increase with time when a constant current density is applied to the anode probes. This is due to the fact that the cumulative charge or the number of electrons flowing through the anode is increasing constantly with time and thus the rate of anodic or oxidation reactions would have been increasing. The rate of reactions might slow down when an anode enters from active region to the passive region. For the specimens which are exhibiting passive behaviour, the increase in the anodic current should be less when compared to the anodes showing an active behaviour.

The corrosion current of all the specimens has increased in the second half of the test (i.e. from 7 to 14 days) except specimens CC3 and CC6. The specimen CC3 shows an unusual behaviour while the probable reason for the decrease of I_{corr} values could be the passive behaviour of the anode due to which the anodic current decreases.

E-logI plots for different anodes before and after application of the constant current density in saturated calcium hydroxide solution with 3% NaCl solution are shown in the Fig. 4.28(1-9) – Fig. 4.30(1-9).
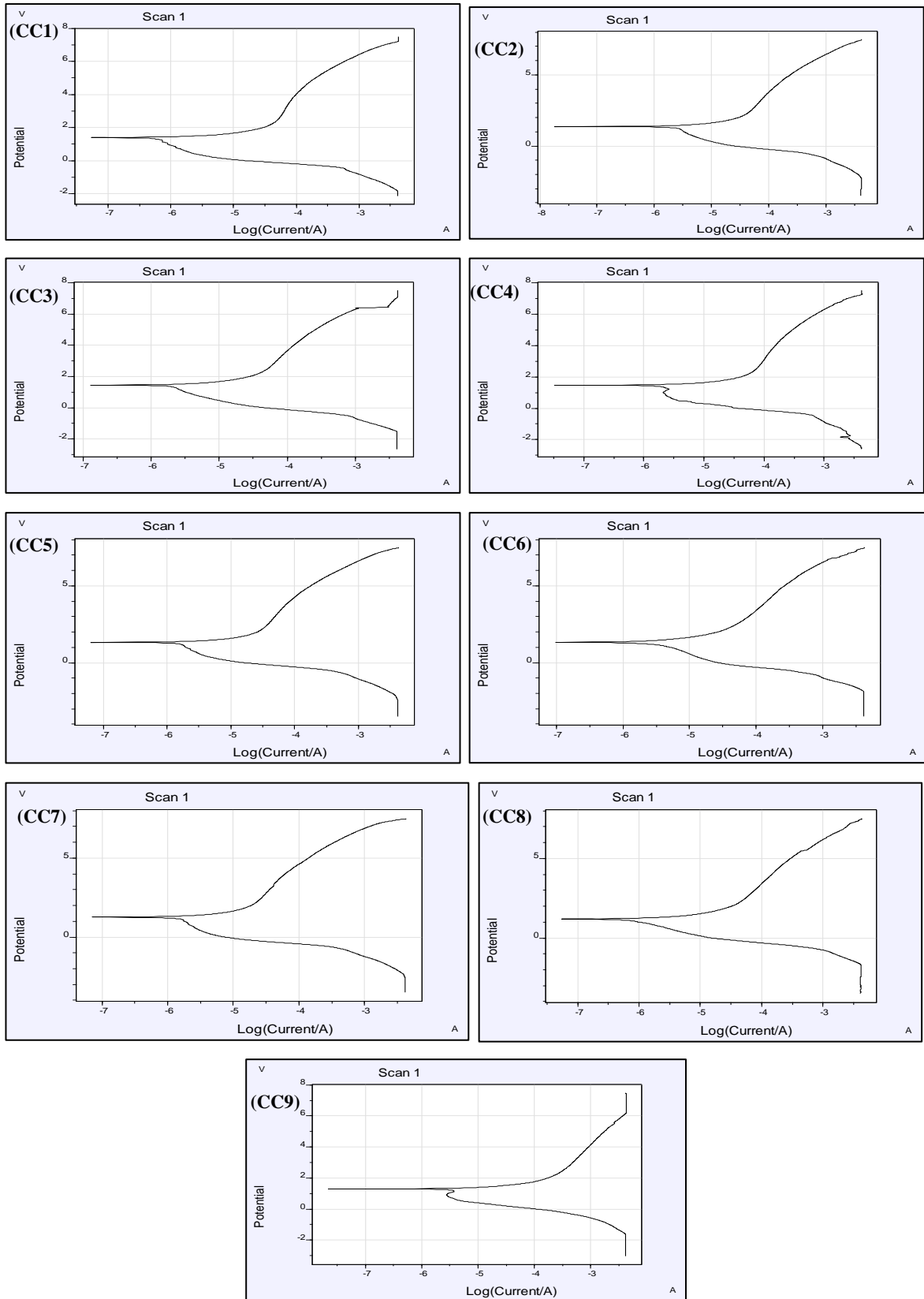
**Figure 4.28 Polarisation plots for different specimens before AGT in sat. Ca(OH)$_2$ soln. with 3% NaCl solution**
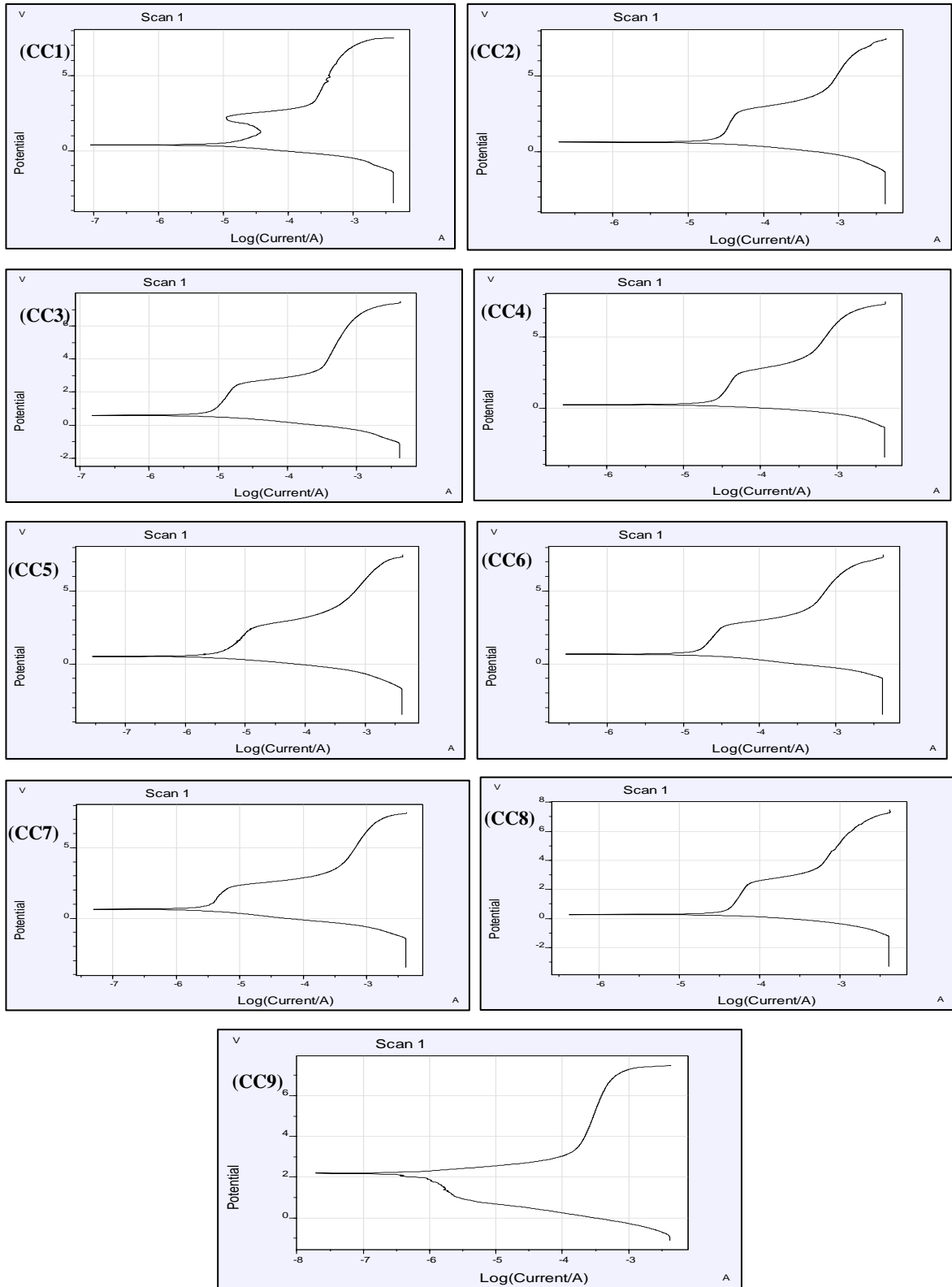
Figure 4.29 Polarisation plots for different specimens after 7 days of AGT in sat. Ca(OH)₂ soln. with 3% NaCl solution
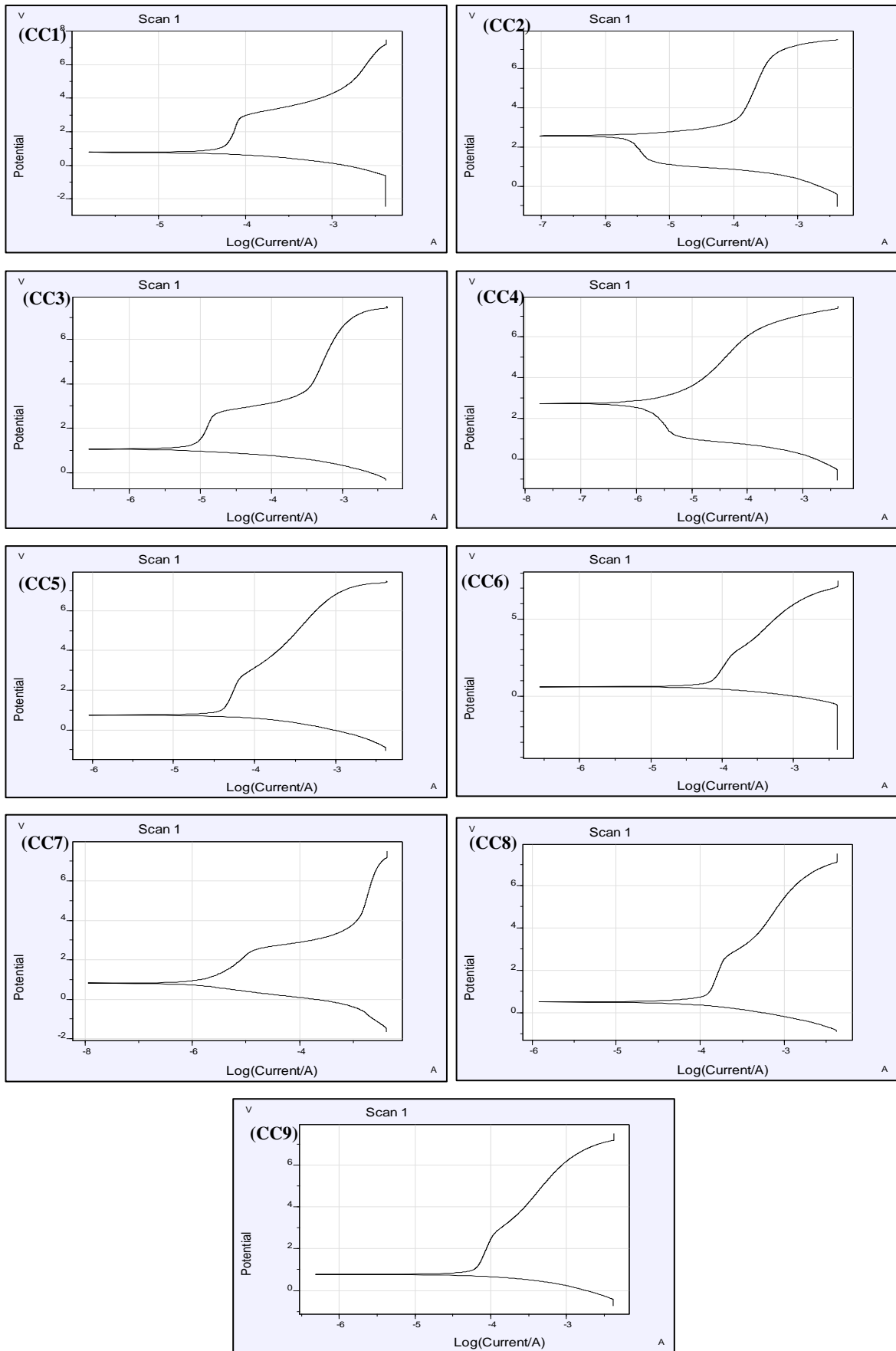
Figure 4.30 Polarisation plots for different specimens after 14 days of AGT in sat. Ca(OH)$_2$ soln. with 3% NaCl solution

93

Before application of AGT, it can be observed all the specimens are in an active state in the presence of chloride ions for the entire range of potential scan before application of current. Only the specimen CC9 exhibits presence of passive region after the potential reaches a high value of 6 V.

After 7 days of application of constant current density, the behaviour of anodic probes has changed in the same potential zone of testing. The specimens CC1, CC2, CC3, CC4, CC6, CC7 and CC8 displays slightly active – highly active – passive behaviour. The specimens CC1, CC3 and CC7 shows a relatively stable passive region as compared to others. Whereas, the anode specimens CC5 shows an active behaviour and specimen CC9 shows a highly active – passive behaviour.

After completion of the accelerated galvanostatic test, the polarisation curves were plotted and it was found that anode specimen CC3 still shows the passive – active – passive behaviour. The specimens CC4, CC5, CC6, CC8 and CC9 shows only active behaviour and are highly favourable for ICCP systems.

The specimen CC1 shows a presence of passive – active behaviour and specimen CC2 shows an active – passive behaviour with a presence of a stable passive region in the potential range of 3 V to 7 V. The specimen CC7 shows a highly active region till the potential value of 4 V and then a stabilised passive region after it till +7.5 V or end of the test. The E_{corr} and I_{corr} values obtained from these curves are plotted in Fig. 4.31 and Fig. 4.32, respectively.
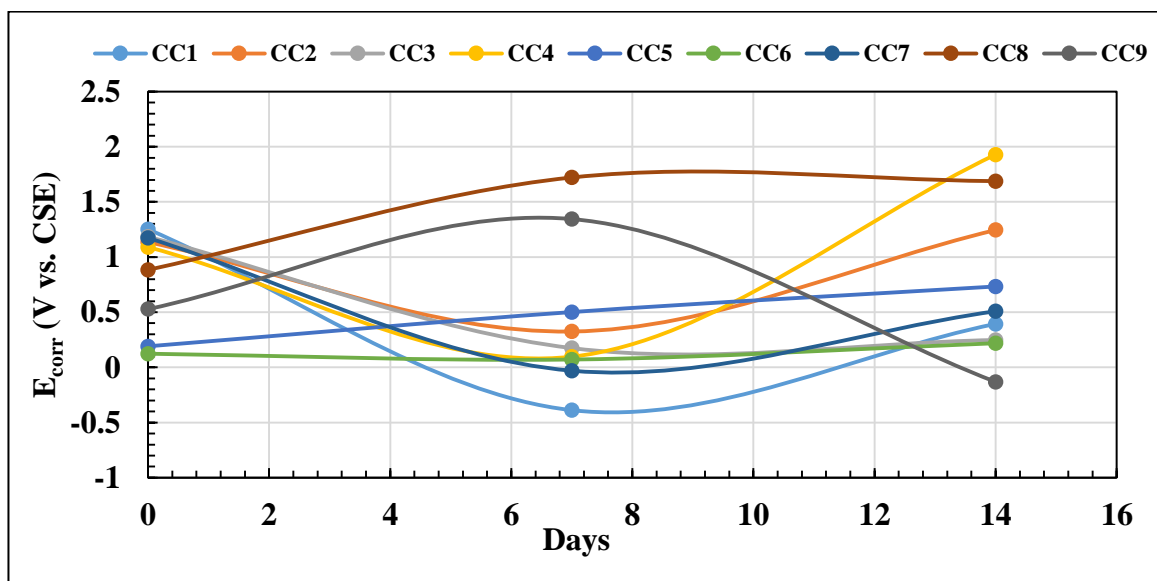
**Figure 4.31 Effect of applied constant current supply on the corrosion potential of anodic probes in sat. Ca(OH)$_2$ soln. with 3% NaCl solution**

After 7 days of AGT, the Ecorr values of the specimens CC1, CC2, CC3, CC4 and CC7 have decreased and the other specimens exhibited a considerable increase in the E_{corr} values. The decrease in the potential values can be explained by the change in the behaviour of specimens from the active state to a less active state in the region of smaller potential values. The increase in the E_{corr} values for the specimens CC5, CC6, CC8 and CC9 is due to the increase in the rate of anodic reactions of the anode probes which can be observed from the E-logI plots.

Furthermore, after completion of the AGT, the E_{corr} of all the specimens has either increased or remained almost constant. The reason behind this is the change in behaviour of most of the specimens to a more actively corroding state except for specimens CC3 and CC7 which have a significant passive zone.
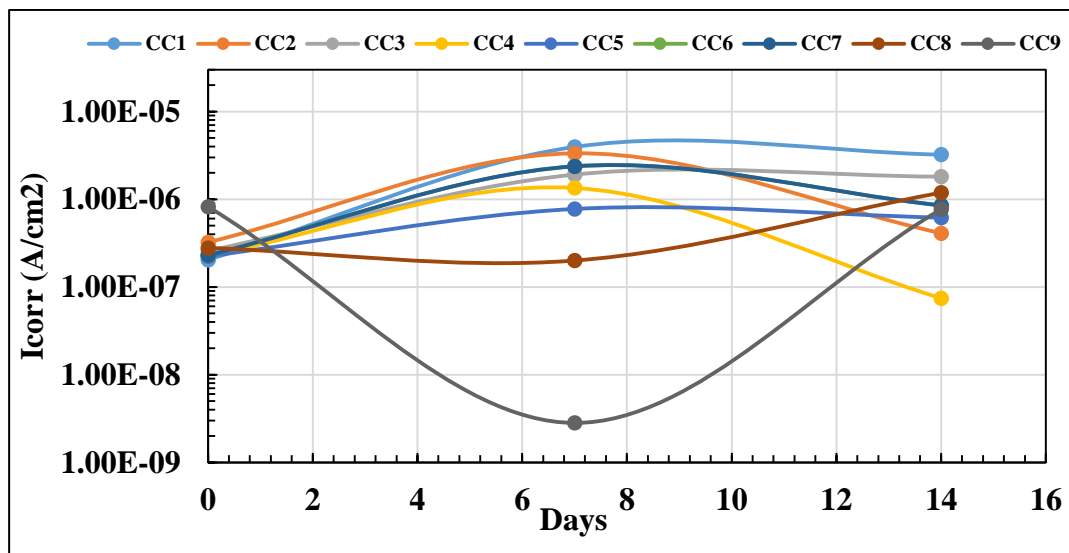
Figure 4.32 Effect of constant current supply on the corrosion current density of anodic probes in sat. Ca(OH)$_2$ soln. with 3% NaCl solution

The I_{corr} values for most of the specimens have increased with the duration of the accelerated galvanostatic test. The increase can be attributed to the change of the constant flow of current and the reduction in the resistance of the samples which is evident from the anodic potential plots of AGT. For the specimen CC9, as the resistance of the anode samples is increasing with time after 7 days which is clear from the anodic potential curve for the anode probes in calcium hydroxide solution with 3% NaCl solution.

The corrosion current density of the anodes has decreased for all the specimens except CC8 and CC9 after the completion of the AGT. The decrease of the corrosion current density might be due to the fact that the all the mixes are displaying a prominent presence of a passive region at lower potential values (at $E_{corr} \pm 2$ V). The increase in the corrosion potential of specimens

95

CC8 and CC9 can be explained by the E-logI plots (Fig. 4.30(8) and 4.30(9)), which exhibits absence of any passive region throughout the scanning potential which goes as high as +7.5 V from OCP. Also, the resistance offered by the specimens CC8 and CC9 is lower as compared to other mixes and stabilises much easily which can be inferred from the anodic potential curves.

On comparing E_{corr} and I_{corr} curves for electrolytic solution of saturated calcium hydroxide with and without NaCl contamination, it can be concluded that the corrosion potential decreases when the test is performed in the electrolyte contaminated with 3% NaCl solution.

It can also be said the corrosion current density of the anodic probes highly depends on the anodic polarisation behaviour and can reduce depending on the state of corrosion of the anode i.e. slightly active state, highly active state, slightly passive or perfectly passive behaviour.

4.6 Evaluation of Anodic Composite

The evaluation of the anodic composite was carried out by application of a 3 mm thick layer of anodic cement composite over the concrete slabs and monitoring of applied ICCP using the different electrochemical techniques such as half-cell potential measurements, linear polarisation measurements, polarisation studies and electrochemical impedance spectroscopy. The thickness of the anodic overlay was kept 3 mm in order to contain the biggest metal particle present in the composite i.e. under 2.36 mm.

4.7.1. *Half Cell Potential Measurements*

The half-cell potential measurements of steel embedded in concrete were taken at regular intervals for the protection period and are plotted in the Fig. 4.33.

The monitoring of half-cell potentials was started after the acceleration of corrosion was done by applying a current connecting steel reinforcement bar to the positive terminal of the battery and titanium wire was connected to the negative terminal. The current density after the acceleration was kept 200 mA/m^2 (10 times of the protection current) of the steel surface.
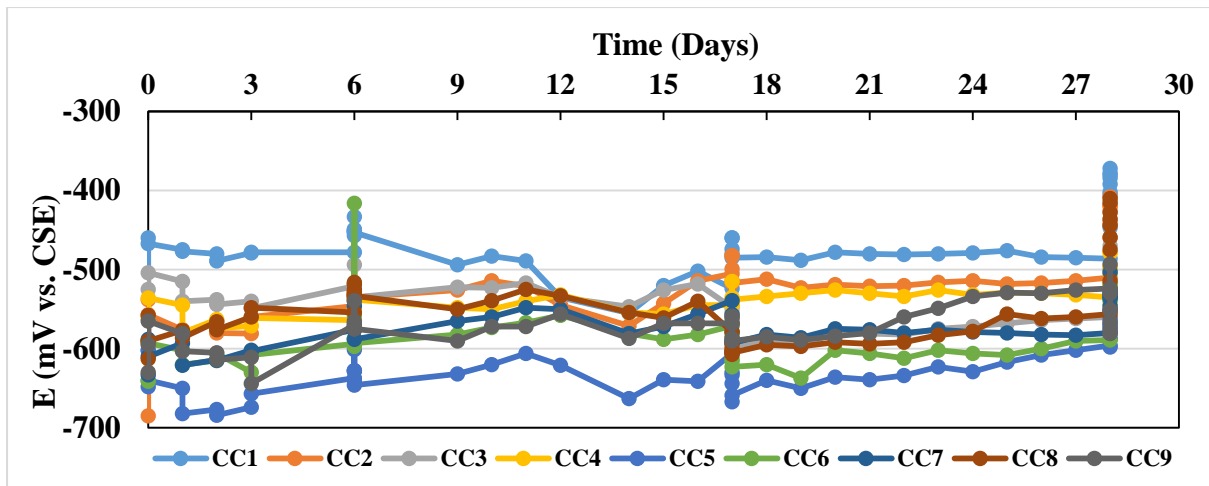
Figure 4.33 Change in half cell potentials with time durung ICCP

It can be observed that during acceleration period the half-cell potential values for all the specimens are more negative than 450 mV (vs. CSE) which implies that severe corrosion is occurring on the steel bar surface (ASTM C876-2015). According to the half-cell potential values measured, for the period of first 14 days even after application of cathodic protection, the half-cell potential values remained more negative than 450 mV (vs. CSE) and thus the state of corrosion over the rebar surface is of severe corrosion. The half-cell potential measurements after 28 days of protection has increased towards positive direction suggesting effective protection.

As the half-cell potential measurements are taken at a certain distance from the steel surface i.e. over the concrete surface and are thus influenced by the concrete between the steel bar and the surface at which porous plug of the CSE is placed. The presence of chloride ions, amount of moisture and the macro-cell corrosion rate, when measuring the half-cell potential at a particular point can influence the measurements. The half-cell potential values are also influenced by ohmic drop occurring in the cover concrete, cracking, carbonation, types of aggregate and the junction or the connection potentials. The half-cell potential measurements is a qualitative method, thus the electrochemical method used for quantification of corrosion in terms or corrosion rate was linear polarisation method and EIS.

4.7.2. *Polarisation Test (Stern-Geary Constant)*

Tafel plotting was carried out to obtain Stern-Geary constant (B) required for determining the corrosion current density. The values of B were found out using the Stern-Geary equation given below. The βa and βc values were found from Tafel plots as shown in Fig. 4.34.

97

$$B = \frac{\beta a * \beta c}{2.303(\beta a + \beta c)} \qquad \dots \dots \dots \dots \dots \dots \dots \dots \dots \dots (4.3)$$
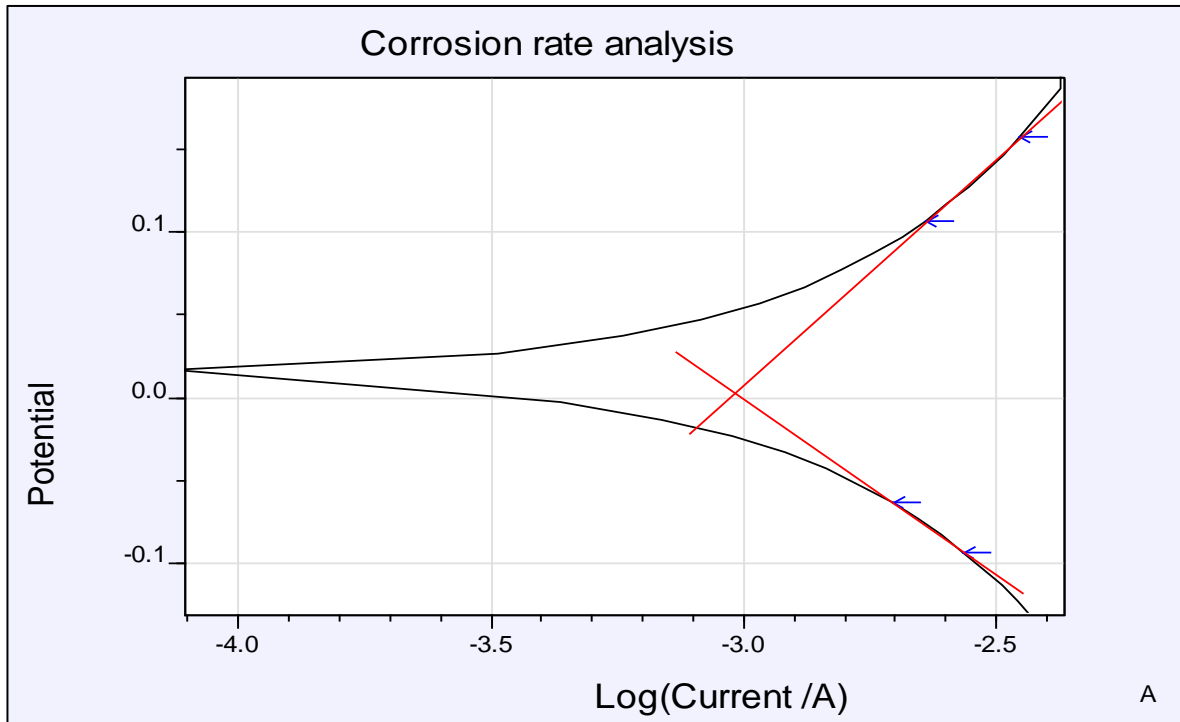
Figure 4.34. Determination of Tafel polarisation constants from polarisation plots

The calculated values of B by using Equation 4.3 by the help of polarisation constants obtained from the various Tafel plots are shown in Table 4.8.

Table 4.8. Stern-Geary constant for different conditions

Specimen	Time of Observation	βa (mV/dec)	βc (mV/dec)	$B = \dfrac{\beta a * \beta c}{2.303(\beta a + \beta c)}$	State of corrosion
CC1	Before accn.	210	202	44.70	Active
	After accn.	222	195	45.07	Active
	After 7 day of CP	185	162	37.50	Active
CC2	Before accn.	283	114	28.21	Active
	After accn.	154	116	31.22	Active
	After 7 day of CP	267	242	46.61	Active
CC3	Before accn.	389	88	31.16	Active
	After accn.	55	69	13.28	Active
	After 7 day of CP	155	94	25.41	Active
CC4	Before accn.	212	164	40.15	Active
	After accn.	88	74	17.45	Active
	After 7 day of CP	152	99	26.03	Active
CC5	Before accn.	286	105	33.35	Active
	After accn.	118	113	25.06	Active
	After 7 day of CP	137	105	25.81	Active
CC6	Before accn.	213	107	30.92	Active
	After accn.	167	167	36.25	Active
	After 7 day of CP	145	118	28.24	Active
CC7	Before accn.	196	103	29.31	Active
	After accn.	116	87	21.58	Active
	After 7 day of CP	157	113	28.53	Active
CC8	Before accn.	109	84	20.59	Active
	After accn.	127	101	24.42	Active
	After 7 day of CP	131	107	25.57	Active
CC9	Before accn.	158	104	27.23	Active
	After accn.	201	162	38.95	Active
	After 7 day of CP	125	129	27.56	Active

The calculated values of B are in the range of 26 to 55 mV for all the conditions in having active state of corrosion. The values of B is dependent on the state or the rate of anodic and cathodic reactions occurring on the portion of the steel bar surface under investigation and thus changes with time. So, it was proposed by Stern and Geary that rather than calculating corrosion current density depending on the actual B, a value of 26 mV should be used for actively corroding surfaces and 52 mV for the surfaces in passive conditions (Concrete society TR 60).

4.7.3. LPR measurements

The measurement of the corrosion current density and corrosion potential is carried out by using LPR techniques. The obtained E_{corr} and I_{corr} values for the different specimens are plotted in Fig. 4.35 and Fig. 4.36, respectively.
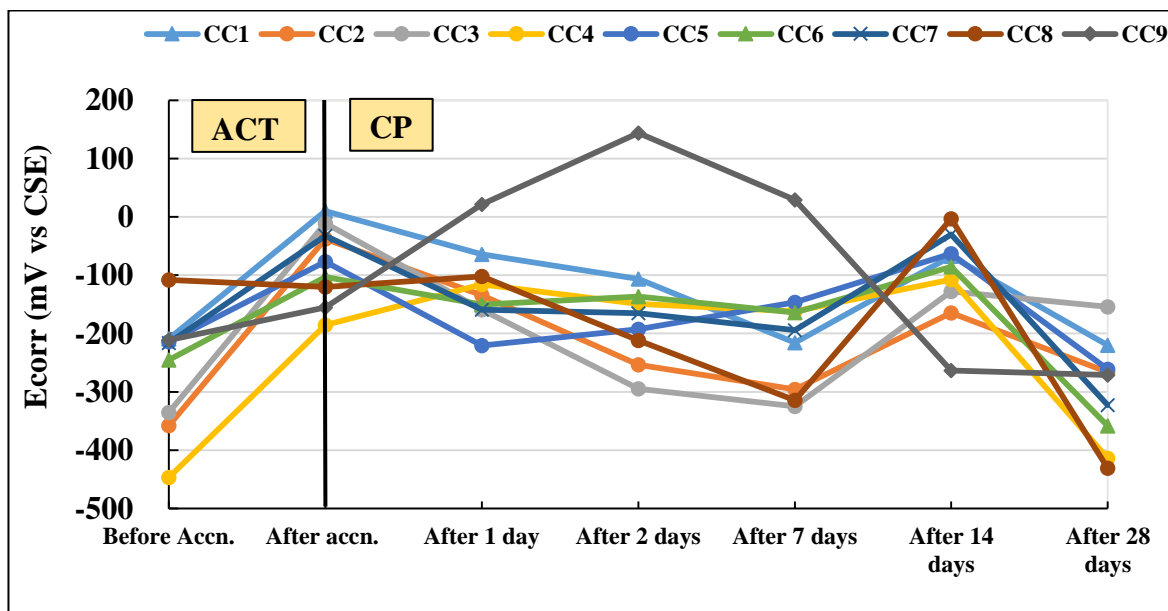
Figure 4.35 Effect of protection current on E_{corr} of steel

It can be observed from the plot that the corrosion potential of the steel surface embedded into the concrete is reducing with the time of protection. The initial increase in the potential was due to increase in the severity of the corrosion occurrence. It means that the corrosion of the steel surface is accelerated and the corrosion rate should have increased by application of impressed current in the opposite direction of protection current. As soon as the ICCP is switched on i.e. protection current starts flowing, the anodic reactions occurring on the surface of the steel rebar are suppressed and the corrosion potential tends to decrease.

The change in corrosion current density and corrosion rate obtained using the formula given in NACE-SP0308-2008 are shown in Fig. 4.36 and Fig. 4.37, respectively.
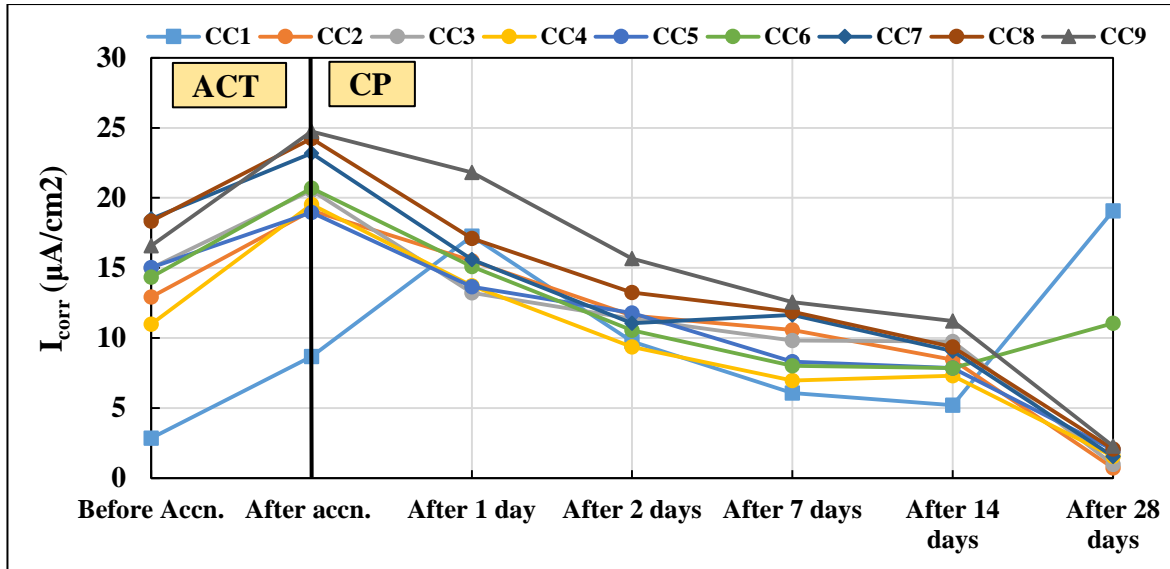
Figure 4.36 Effect of protection current on corrosion current density of steel bar

It can be observed that the corrosion current density tends to decrease with time when the protection current is switched on.
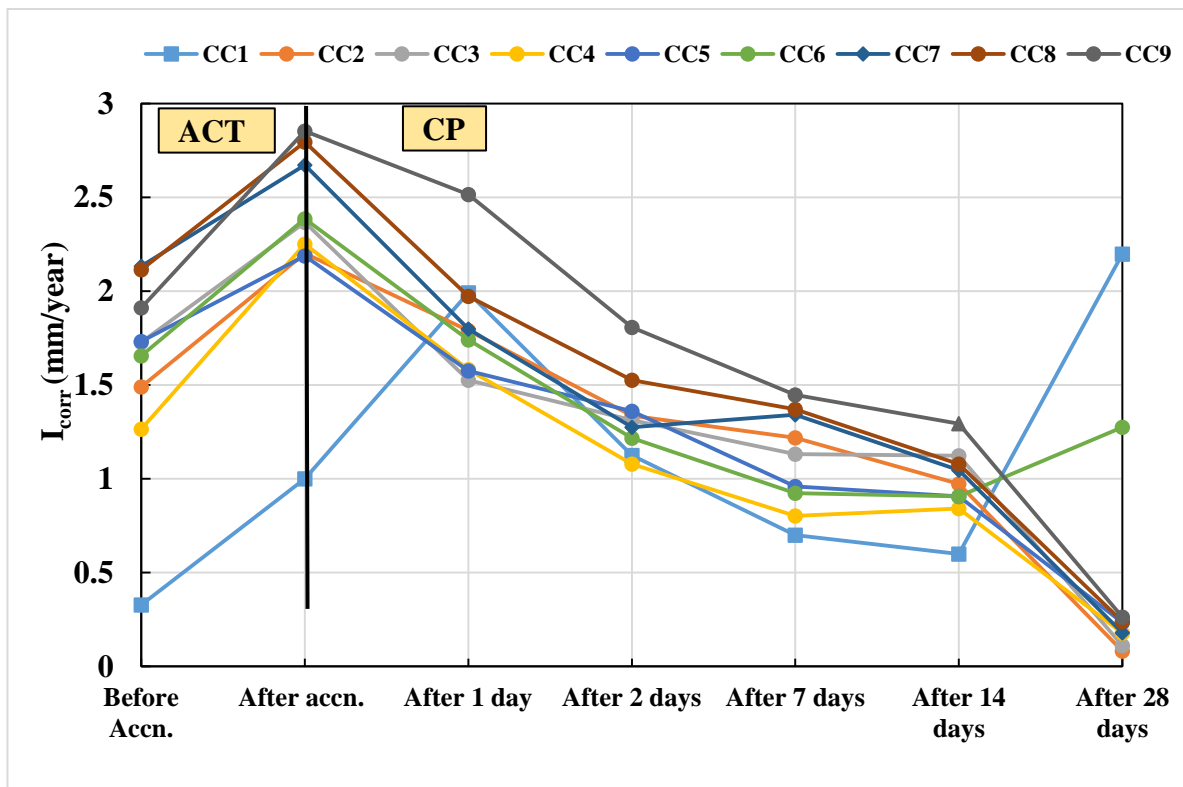
Figure 4.37 Change in corrosion rate with time after application of ICCP

Similar to the corrosion current density, the corrosion rate i.e. the rate at which steel bar dissolves (or the diameter of steel bar reduces) into the pore solution of the surrounding concrete. In this case, as the depolarization is very small due to high corrosion rates, the

accuracy of the LPR measurements increases which assumes a constant anodic and cathodic Tafel slopes.

4.7.4. *Electrochemical Impedance Spectroscopy*

Corrosion of steel bars embedded in concrete was also monitored using AC impedance technique. EIS is advantageous as it does not disturb the operation of the system but can also give additional information on the mechanisms by which surface protection is occurring. It can provide additional information like dielectric properties of concrete, diffusion coefficient, and the characteristics of the passivation of steel.

A typical impedance spectrum for different specimens is shown in Fig. 4.38.
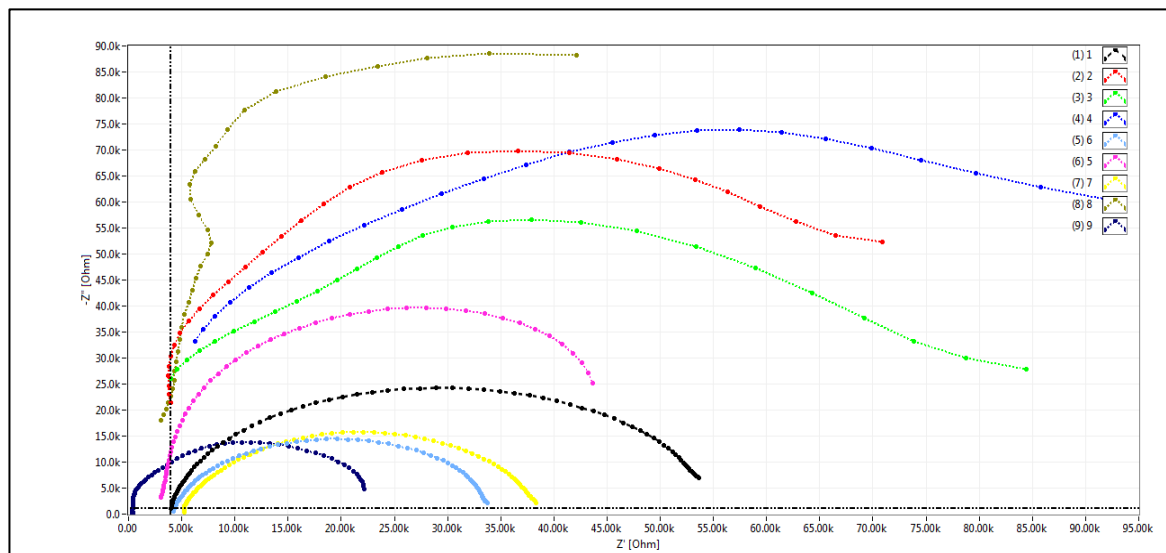
Figure 4.38 Comparison of Impedance Spectra for different samples after 14 days of ICCP

To understand the mechanism of processes occurring during the corrosion protection of the steel rebars, the impedance spectra were analysed using ZMAN software to obtain model parameters. The obtained model parameters after detailed analysis are listed in Table 4.9 – Table 4.18.

Table 4.9 Model parameters of slab with anodic layer of CC1

Time	R_o (Ω-cm^2)	R_b (Ω-cm^2)	$R = R_o + R_b$ (Ω-cm^2)	Q_b (F)	R_{ct} (Ω-cm^2)	Q_{dl} (F)
Before acceleration	1584.91	33024.02	34608.93	9.96E-09	2867.11	5.47E+03
After acceleration	7883.36	40005.73	47894.09	1.01E-08	297.30	4.07E-08
After 7 days of ICCP	5536.73	78532.2	84068.93	1.15E-09	346.26	4.87E-07
After 14 days of ICCP	3516.79	50040.25	53557.04	2.76E-09	511.13	1.59E-10
After 28 days of ICCP	8704.82	65979.98	74684.80	5.53E-10	3073.31	2.80E-09

Table 4.10 Model parameters of slab with anodic layer of CC2

| Time	R_o (Ω-cm^2)	R_b (Ω-cm^2)	$R = R_o + R_b$ (Ω-cm^2)	Q_b (F)	R_{ct} (Ω-cm^2)	Q_{dl} (F)
Before acceleration	1090.749	27179.32	28270.069	2.01E-08	273.61	8.27E-09
After acceleration	8533.44	28441.11	36974.55	1.88E-08	0.193546	7.34E-06
After 7 days of ICCP	4190.93	83502.30	87693.23	1.0E-08	1738.81	179.8114
After 14 days of ICCP	0.05956	99707.33	99707.38	5.27E-10	2218.38	6.65E-09
After 28 days of ICCP	14372.86	12836.93	27209.79	9.46E-10	4427.41	4.12E-07

Here, R_b is analogous of the resistivity of the concrete surrounding the steel bar and R_{ct} is analogous to the polarisation resistance of the steel or the charge transfer resistance of steel. For specimen with anodic layer CC1 and CC2, it can be observed that the R_{ct} decreased when the corrosion is accelerated and is increasing at a slower rate when ICCP is switched on. Q_{dl} represents the formation of the layer over the surface of the steel and as the capacitance is very small, the layer thickness is insufficient or the layer is essentially formed of porous corrosion products of corrosion which hasn't diffused from the surface of the steel. There is almost no change in the Q_{dl}, which implies the protection of the steel is occurring by the increase in the charge transfer resistance or slowing down of the corrosion reactions occurring at the surface of the steel bar.

Table 4.11 Model parameters of slab with anodic layer of CC3

Time	R_o (Ω-cm^2)	R_b (Ω-cm^2)	$R = R_o + R_b$ (Ω-cm^2)	Q_b (F)	R_{ct} (Ω-cm^2)	Q_{dl} (F)
Before acceleration	1051.13	158569.3	159620.43	5.57E-09	286.19	1.24E-09
After acceleration	3572.66	32674.76	36247.42	1.23E-09	900.06	4.49E-06
After 7 days of ICCP	5096.75	99431.35	104528.1	1.26E-09	4233.53	4.06E-04
After 14 days of ICCP	1.08E-08	87048.08	87048.08	1.29E-09	1585.47	4.13E-06
After 28 days of ICCP	6975.11	25988.51	32963.62	1.61E-06	10760.87	6.55E-09

Table 4.12 Model parameters of slab with anodic layer of CC4

Time	R_o (Ω-cm^2)	R_b (Ω-cm^2)	$R = R_o + R_b$ (Ω-cm^2)	Q_b (F)	R_{ct} (Ω-cm^2)	Q_{dl} (F)
Before acceleration	4083.99	63089.15	67173.14	2.37E-09	395.86	5.01E-09
After acceleration	4490.20	39886.9	44377.10	2.94E-09	35.25	9.03E-08
After 7 days of ICCP	4112.57	81513.91	85626.48	5.00E-10	658.46	1.59E-08
After 14 days of ICCP	4.92E-05	136994	136994.00	1.52E-09	2119.00	7.81E-03
After 28 days of ICCP	2846.67	78157.83	81004.50	3.20E-10	2350.10	1.55E-09

Table 4.13 Model parameters of slab with anodic layer of CC5

Time	R_o (Ω-cm^2)	R_b (Ω-cm^2)	$R = R_o + R_b$ (Ω-cm^2)	Q_b (F)	R_{ct} (Ω-cm^2)	Q_{dl} (F)
Before acceleration	5020.29	48914.17	53934.46	1.74E-09	7143.04	5.80E-06
After acceleration	4462.46	29968.02	34430.48	4.14E-09	1374.95	1.37E+02
After 7 days of ICCP	6285.548	185359.6	191645.14	7.57E-10	573.35	0.382669
After 14 days of ICCP	1975.836	76510.7	78486.54	7.59E-09	595.25	2.21E-06
After 28 days of ICCP	18271.36	169410.87	187682.23	1.18E-10	1171.58	1.08E-01

Table 4.14 Model parameters of slab with anodic layer of CC6

Time	Ro (Ω-cm^2)	Rb (Ω-cm^2)	R =Ro+Rb (Ω-cm^2)	Qb (F)	Rct (Ω-cm^2)	Qdl (F)
Before acceleration	4445.44	66856.70	71302.14	9.87E-10	869.73	1.98E-08
After acceleration	2897.63	53656.24	56553.87	2.44E-09	298.31	1.20E-04
After 7 days of ICCP	4056.01	145419.20	149475.21	1.79E-09	4526.92	1281.048
After 14 days of ICCP	4284.10	29864.47	34148.57	5.02E-09	3049.81	8.09E-07
After 28 days of ICCP	10586.43	108262.68	118849.11	5.13E-10	4175.84	2.22E-16

Table 4.15 Model parameters of slab with anodic layer of CC7

Time	Ro (Ω-cm^2)	Rb (Ω-cm^2)	R =Ro+Rb (Ω-cm2)	Qb (F)	Rct (Ω-cm^2)	Qdl (F)
Before acceleration	3528.45	43080.07	46608.52	3.80E-09	3301.37	3.10E-09
After acceleration	1839.03	31568.71	33407.74	2.53E-10	1445.18	7.70E-10
After 7 days of ICCP	8.11E-08	26638.14	26638.14	4.75E-09	1304.36	5.13E-06
After 14 days of ICCP	5248.08	33035.39	38283.47	5.50E-09	1347.87	2.23E-07
After 28 days of ICCP	8710.83	155284.32	163995.15	6.01E-09	5416.98	2.03E+05

Table 4.11 Model parameters of slab with anodic layer of CC8

Time	Ro (Ω-cm^2)	Rb (Ω-cm^2)	R = Ro+Rb (Ω-cm2)	Qb (F)	Rct (Ω-cm^2)	Qdl (F)
Before acceleration	5.83E-06	150926.60	150926.60	9.11E-08	808.0323	5.96E-08
After acceleration	4709.91	52708.23	57418.14	3.36E-09	86.3557	1.47E-04
After 7 days of ICCP	743.22	40979.02	41722.24	2.67E-09	518.829	1.55E-04
After 14 days of ICCP	2356.85	45784.54	48141.39	3.76E-09	715.845	7.85E-04
After 28 days of ICCP	3.21	200834.62	200837.83	6.35E-10	5735.02	9.48E-10

Table 4.16 Model parameters of slab with anodic layer of CC9

Time	Ro (Ω-cm²)	Rb (Ω-cm²)	R =Ro+Rb (Ω-cm2)	Qb (F)	Rct (Ω-cm²)	Qdl (F)
Before acceleration	3.53E-07	246576.60	246576.60	4.13E-09	1613.777	4.51E-09
After acceleration	5547.70	760574.10	766121.80	7.15E-10	335.2013	1.56E+06
After 7 days of ICCP	1.37E-05	159131.10	159131.10	1.10E-09	447.842	6.48E+07
After 14 days of ICCP	465.11	22039.36	22504.47	6.31E-09	714.628	3.14E-07
After 28 days of ICCP	0.00113	187848.59	187848.59	5.26E-08	2502.852	3.50E-09

From the model parameters, it can be concluded that the charge transfer resistance of the steel surface first decreases due to the acceleration of corrosion and then increases when the ICCP of the steel reinforcement starts. For all the specimens the protection current is same and thus the protection is occurring almost at the same rate in all the specimens. It can also be noted that the highest increase of R_{ct} is observed in the specimens CC6, CC8 and CC9 after application of 28 days of ICCP, this might be due to the application of uniform current density as a result of lower resistivity of the anodic layer along the length of the steel bar.

4.7.5. *Current Distribution in the Anodic Layer*

The uniformity of the current distribution was evaluated by taking half-cell potential measurements along the surface of the anodic layer by the means of CSE with reference to the primary anode connected to the rectifier.

The potential plot across the anodic layer for all the specimens are shown in the Fig. 4.39(1) - Fig. 4.39(9) for CC1 to CC9, respectively.
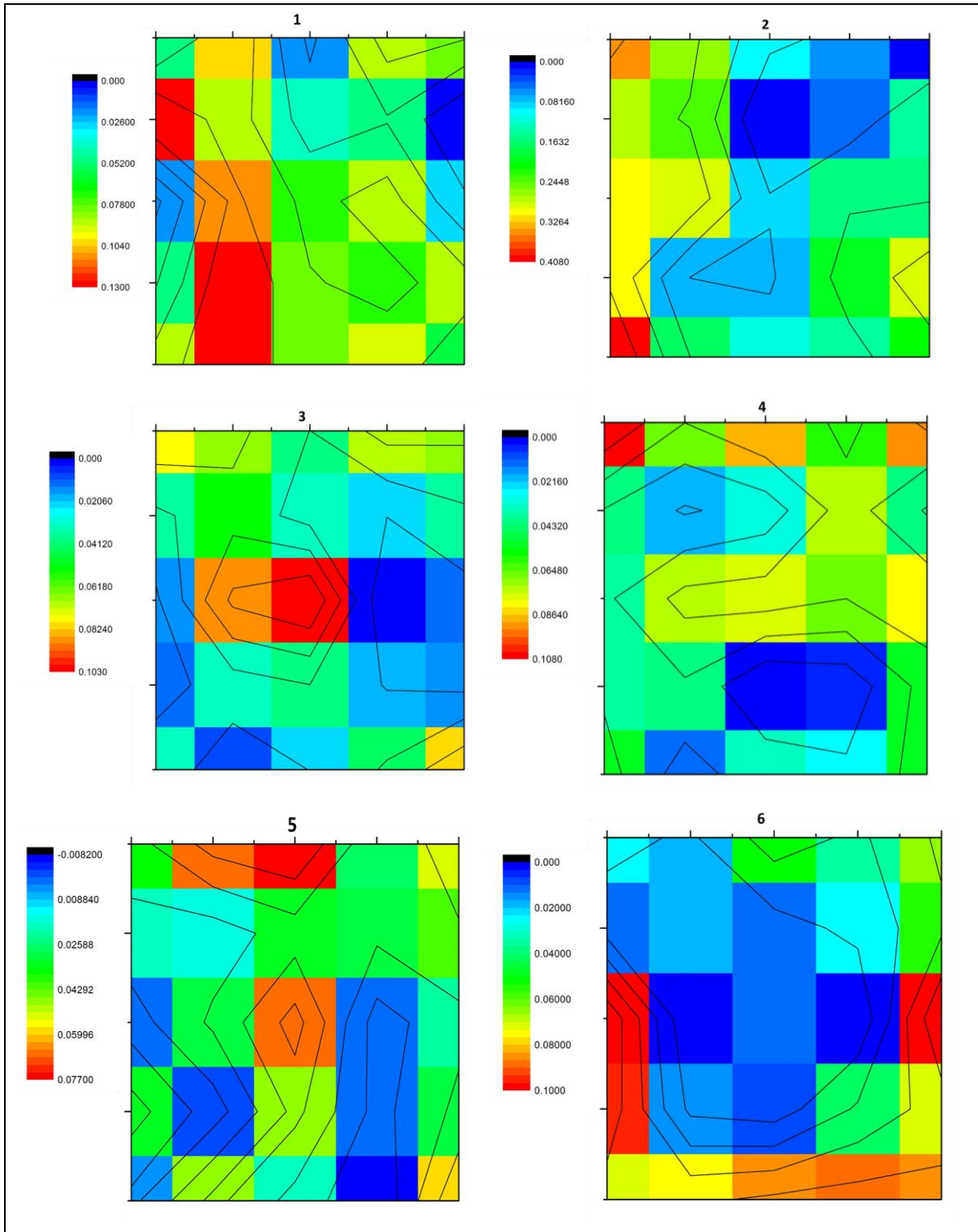
Figure. 4.39(a) Potential Plots of anodic layer on concrete slabs
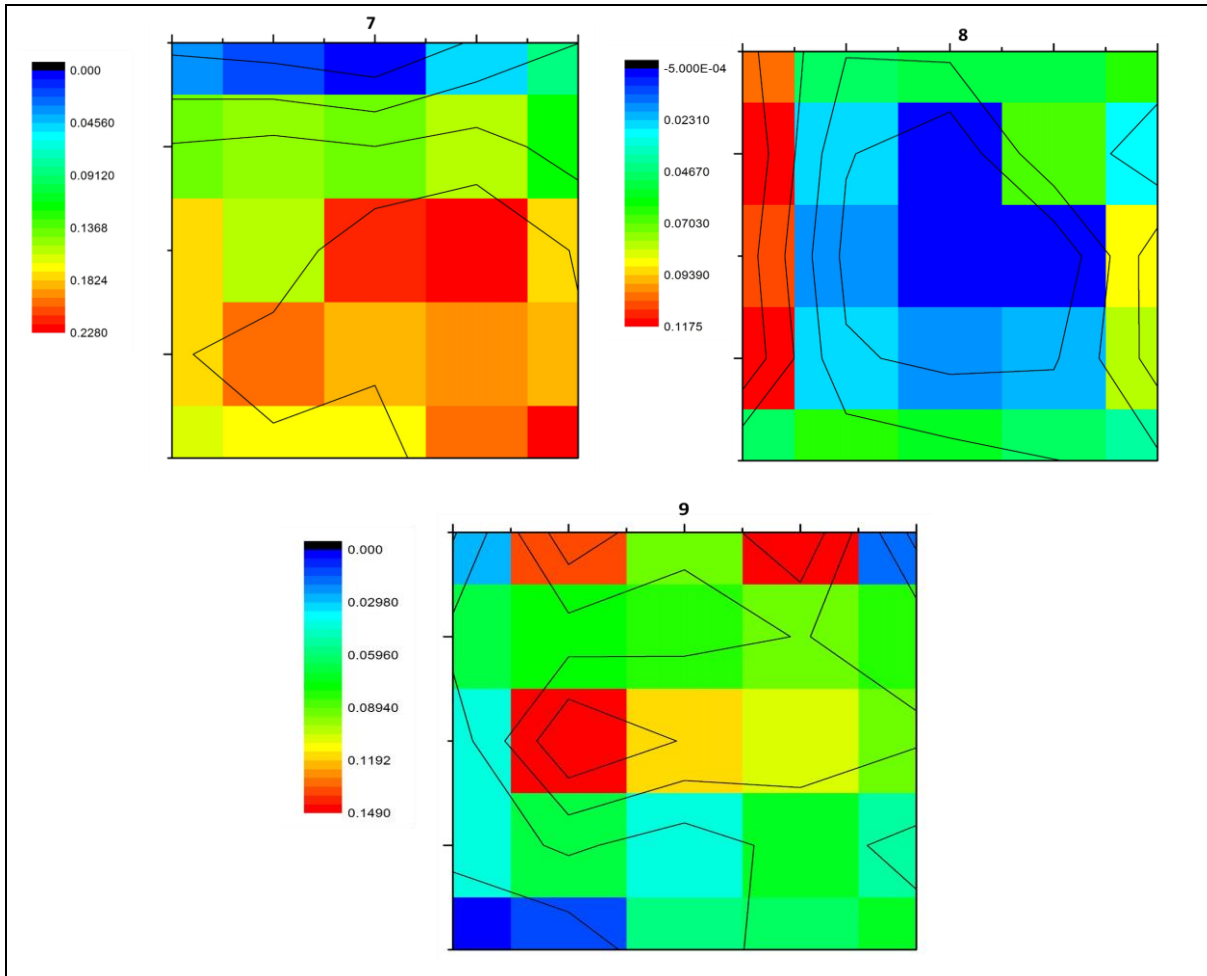
Figure 4.39(b) Potential Plots of anodic layer on concrete slabs

It can be observed that the maximum area covered by contours of same potential difference lies over the anodic surface layer of CC6 and CC8. The potential difference between the point of maximum and minimum voltage of the surface of CC6 and CC8 are 0.977 mV and 0.1171 mV, respectively. This is due to the fact that the resistance of these anodic layers were lowest of all and are very near to each other. Thus, it can be concluded that these anodic layers can very well fulfil the criteria of supplying current across the total surface area over which they are applied.

4.7.6. NACE criteria for ICCP

The monitoring of ICCP is also done on the basis of NACE SP0290-2007 and the effectiveness of the ICCP technique is found on the basis of 100 mV decay criteria. The protection is said to be effective when the 100 mV decay from the instant off potential has occurred. This can be checked by the potential decay plots with time. The decay plots after 7 days of CP and after 14 days of ICCP are shown in Fig. 4.40 and Fig. 4.41, respectively.
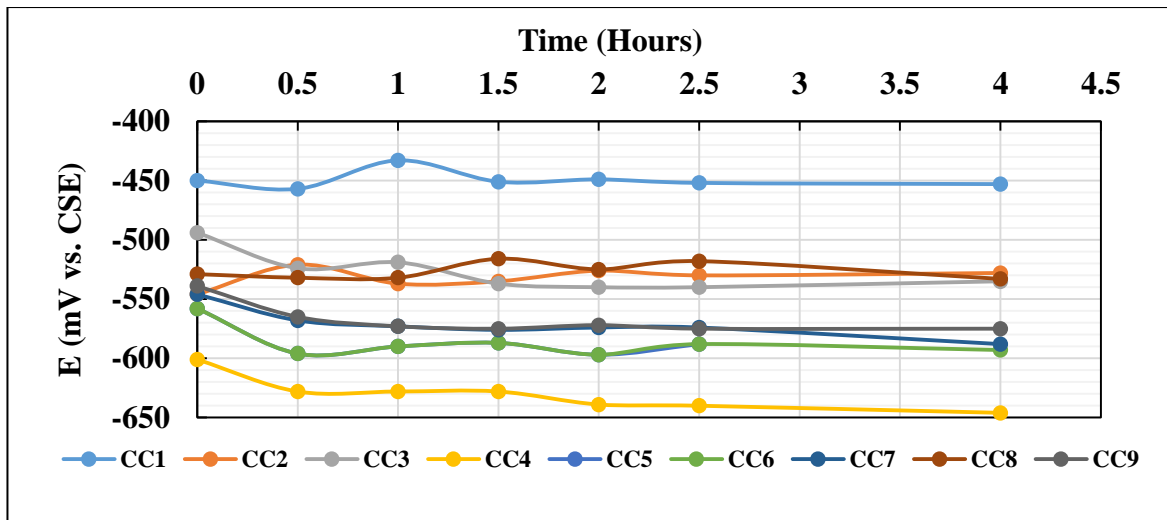
Figure 4.40 Depolarization curves after 7 days of ICCP with 10 mA/m^2

It can be observed from the depolarization plot that none of the specimens is having a 100 mV decay and thus are not in the protection zone according to NACE criteria which can also be said from the half-cell potential values and high corrosion rates found using LPR measurements.
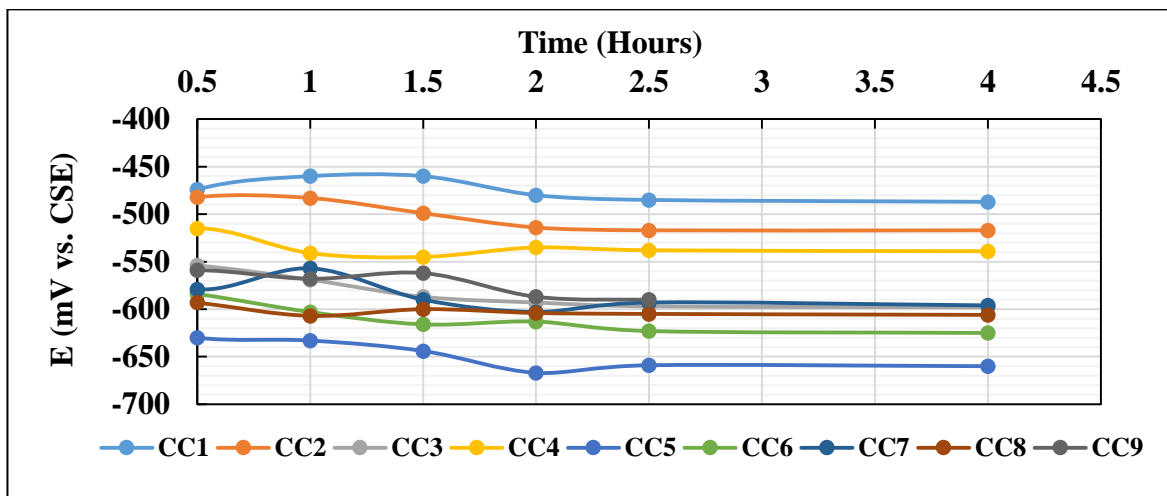
Figure 4.41 Depolarization curves after 7 days of CP with 20 mA/m^2

Similar to the depolarization curves of CP applied at 10 mA/m^2, the decay of 100 mV is not observed in any of the samples after 7 days and thus requires more time to be protected in accordance with the NACE criteria.
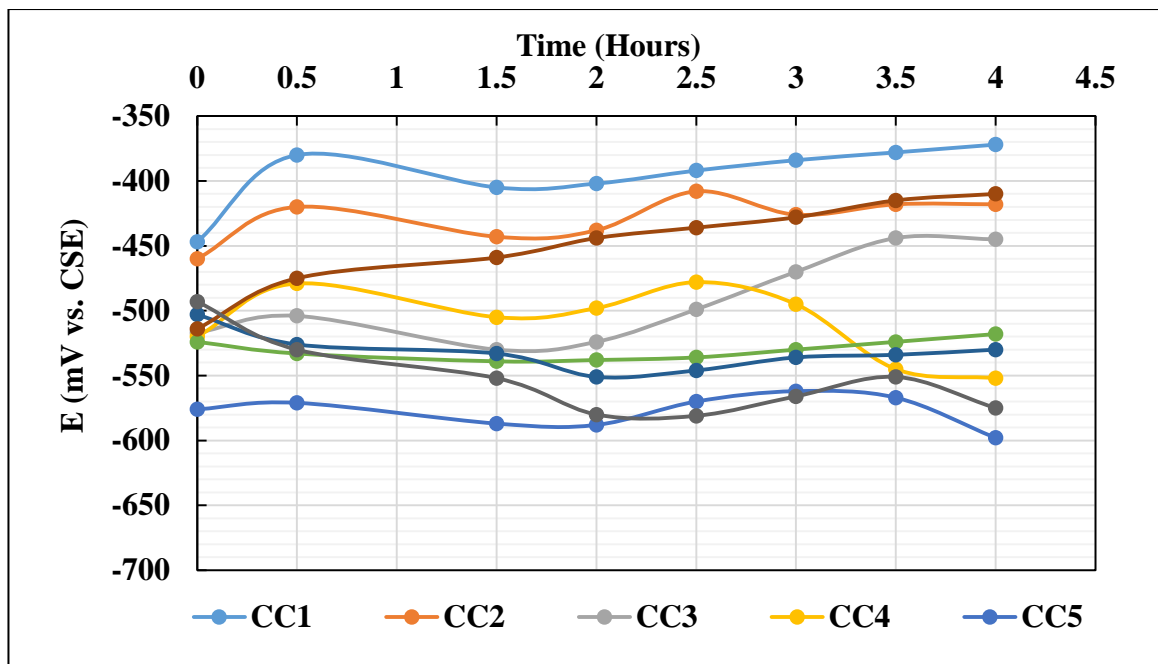
Figure 4.42 Depolarization curves after 28 days of CP with 20mA/m²

The depolarisation plots of According to NACE 100 mV criteria the specimen overlaid with CC8 has achieved a decay of 104 mV and can be said to be cathodically protected. Specimens with layer CC1 and CC3 have achieved a decay of 75 mV and 72 mV which means they need few more days for to fulfil protection criteria. All the other specimens showed increase in the negative potential meaning they either need a higher current density or greater time for protection as compared to other specimens.

4.7 Microstructural Study of Anodes

The microstructural study of the anodes were conducted to find out the homogeneity of the mix. The resistivity of the anodes depend on the proper dispersion of the fillers in the cement matrix. The micrographs are shown in the Fig. 4.43 and Fig. 4.44.
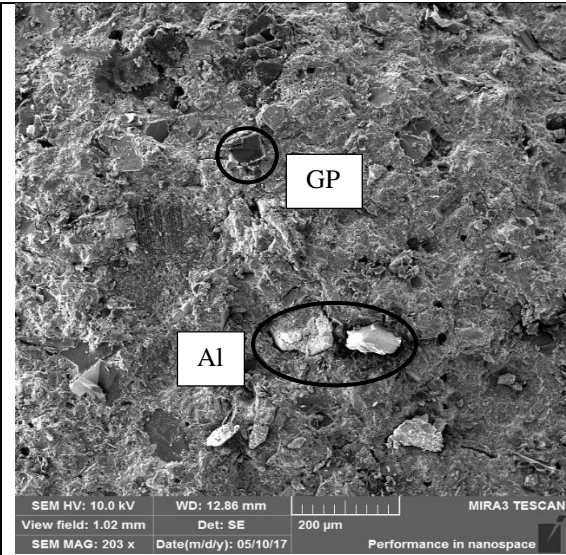
(CC1)
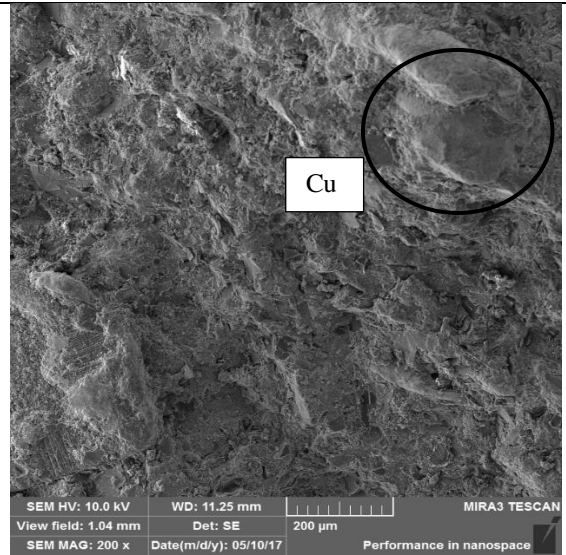
(CC3)

(CC3)

(CC4)

GP

(CC5)

(CC6)

111
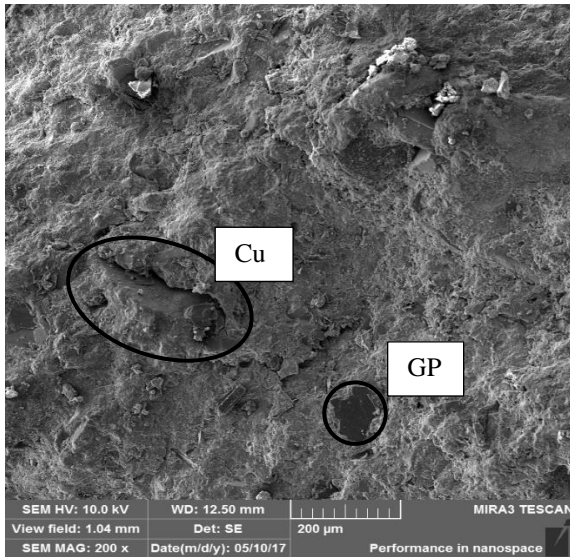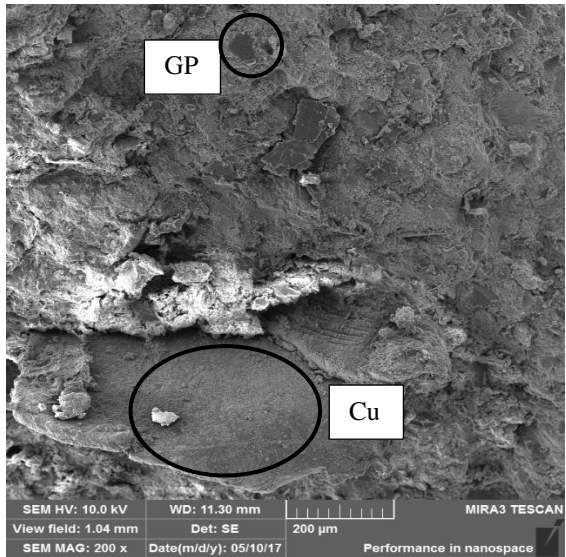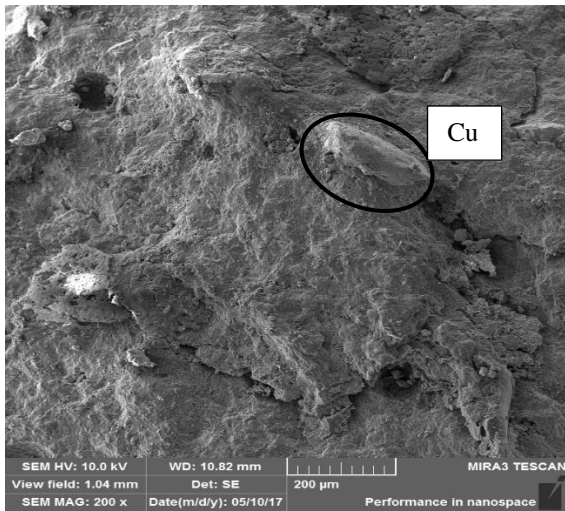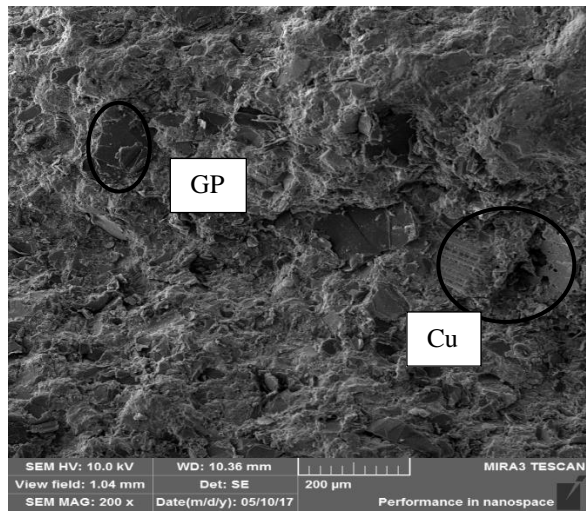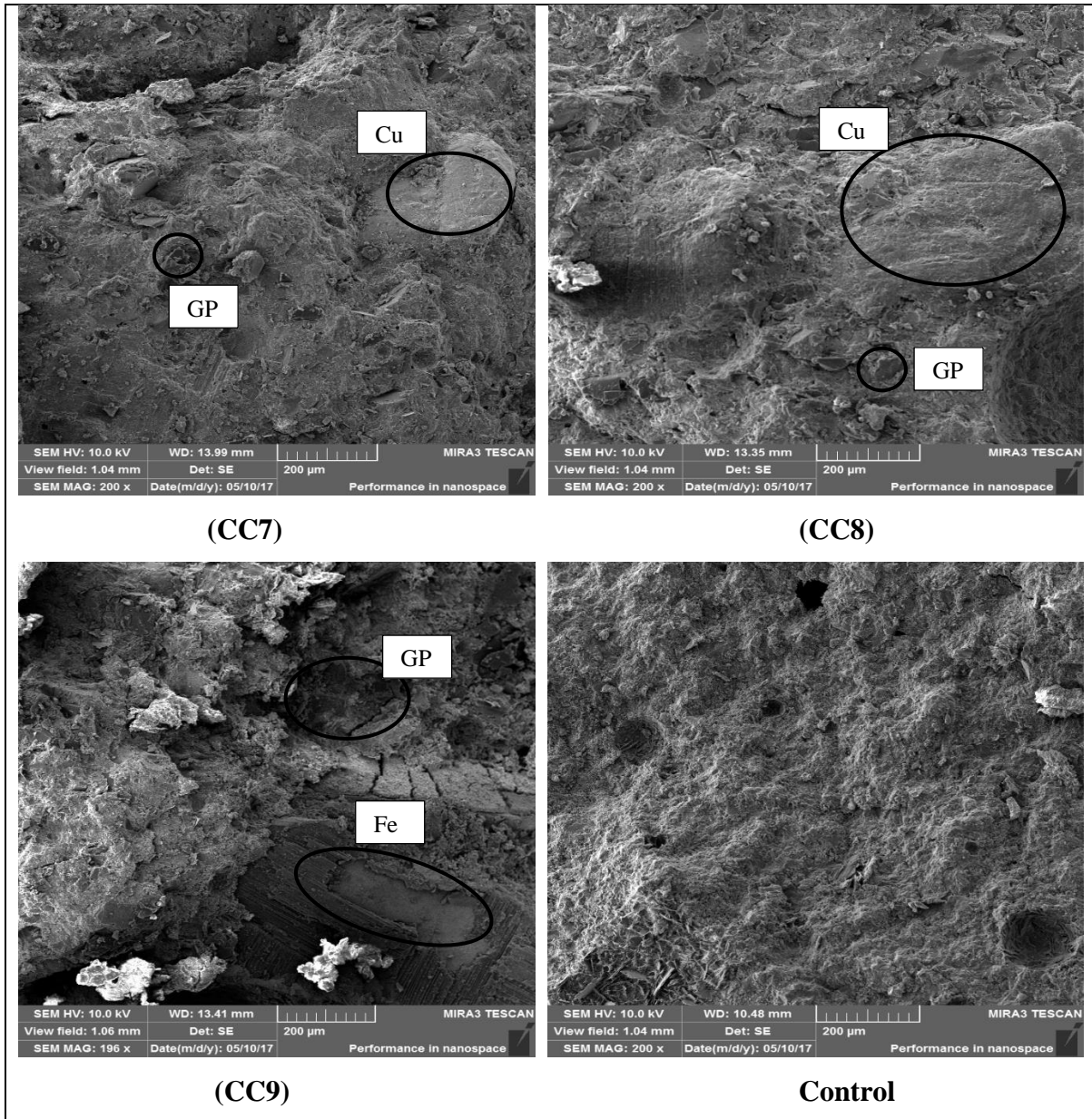
Figure 4.43 SEM micrographs of different composites at 200X magnification

It can be observed from the micrographs that particles of graphite powder (relatively darker) are homogeneously dispersed in the cement matrix. The metal can also be seen embedded into the cement composite and graphite particles are dispersed around the metal particles. The current thus is carried from the metal particles to the graphite particles through the hydrated cement composite. In the first image the metal particles (circled in the image) can be distinguished from the mix which are confirmed to be aluminium particles from the EDX analysis of the region. Similarly, in the other images the presence of other metal particles (Cu, Fe and Pb) embedded into the cement composite can be observed with products of hydration all over the particles.

One of the important components of the anode is the primary anode (Ti wire). To check the deterioration of the titanium wire after 14 days of AGT, anodic probe of CC7 was broken and the wire was taken out for SEM analysis. The images and micrographs are shown in the Fig. 4.40. The colour of the wire has changed from silver to light gold colour after supplying current for 14 days in the anodic composite as shown in the image above.

The colour of the wire has changed from silver to light gold colour after supplying current for 14 days in the anodic composite as shown in the image above.
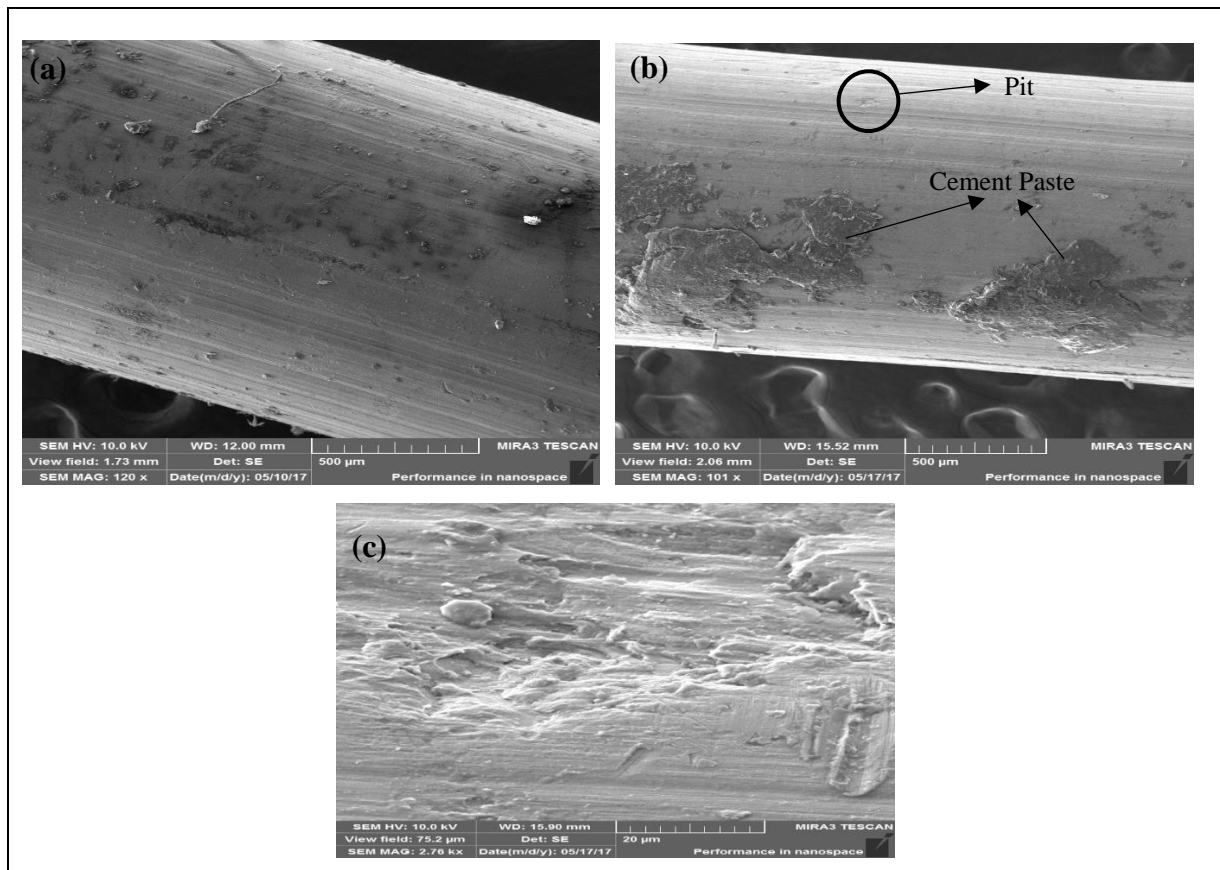
Figure 4.44 SEM micrographs of unused Ti wire (a), used Ti wire (b) and pit formed (c)

It was observed that the diameter of the unused wire was 1552.91 μm and that of the used wire after 14 days of current supply was 1478.93 μm. There is a reduction of 73.98 μm in the diameter of the Ti wire because of it dissolution and oxidation due to the anodic reactions. The corrosion of Ti wire is occurring uniformly but few pits can also be observed on the surface as shown in the Fig. 4.44(c).

CHAPTER 5

CONCLUSIONS AND RECOMMENDATIONS

5.1 Conclusions

The present study was aimed to explore the possibility of use of e-waste metallic powder as a conductive fillers in a cementitious mix to make conductive composite that can be used as secondary anode in the cathodic protection technique in reinforced concrete structures. The conductive cement composite developed by use of e-waste metallic powder and graphite powder has a slightly higher resistivity as compared to other cementitious overlays used. Keeping this in mind, the thickness of the anodic layer was decreased and it was found to be working well as a secondary anode. The prediction model for the compressive strength and DC resistivity of the conductive cement composite are established. The behaviour of anodic probes was investigated by using Tafel plots and accelerated galvanostatic test. After application of a 3 mm anodic layer, the effectiveness of the applied cathodic protection technique was evaluated by using HCP, LPR and EIS measurements. The concluding remarks of the study are as follows:

- Increase in the e-waste metallic powder content has a reducing effect on the compressive strength of the composite. The reduction of about 27% was observed due to addition of 37% e-waste metallic powder by mass in the cementitious mix.

- The compressive strength of the mix was found to be decreasing with increasing content of the graphite powder. The reduction in the compressive strength was about 82 % at a 40% addition of graphite powder by mass.

- The resistivity of the composite decreased by 28% at 25% (by volume) addition of e-waste metallic powder and by 44% by addition of 40% graphite powder by mass.

- The reduction of size of the metallic powder does not seem feasible due to high energy intensive process and increasing the content too much will increase the density of the composite that would in turn increase the dead load on the structure. So, both the fillers were used in combination.

- Cement composite with e-waste metallic powder content of 20% (by volume) and graphite powder of 30% (by weight) was found to be the optimum mix.

- The compressive strength and the resistivity of the optimised mix was found to be 27.4 MPa and 7.11 kΩ-cm, respectively, which meets the specified requirements.

- The anodic layer thickness was decided to be 3 mm to encase titanium wire with 1.5 mm diameter, and all filler particles i.e. under 2.36 mm. The resultant resistance of the anodic layer is only 2.37 kΩ which makes it a well suited secondary anode for ICCP.

- Electrical resistivity was measured by four probes using two techniques: AC and DC methods. There is a difference in the resistivity values obtained by two methods as a result of dielectric polarisation of the cement paste in the composite.

- The behaviour of the composite anodes (Ti wire + cement composite) changes with the duration and the amount of current passing through the anodes. The anodes showed a more stable behaviour in the presence of chloride ions. Thus, it can be stated that the cementitious anodes can behave well in the chloride contaminated environments.

- LPR and EIS measurements showed that the protection against corrosion is brought by increase in the charge transfer resistance of the steel bar.

- The potential difference along the anodic surface should be smaller in order to supply current uniformly which is examined by the optimised composite CC8.

- The developed conductive cement anode can serve well as a secondary anode in accordance to the standards.

5.2 Future scope of work

This study focused on the development of a conductive cement anode and its use as a secondary anode in the ICCP system. The performance of the cementitious anode was found to be satisfactory at laboratory level. The identified future areas where work needs to be done are:

- The chemical interactions between e-waste metallic powder and cement paste and the effect of addition of e-waste metallic powder on the hydration of cement needs to be studied.

- The bond behaviour and the contact resistivity of the anodic layer with the concrete substrate is to be evaluated.

- The use of same anode as a multifunctional anode for other electrochemical techniques like electrochemical chloride extraction and realkalisation in combination with cathodic prevention is to be evaluated.

- Further improvements in the ICCP anode systems can be brought out by numerical simulation of the corrosion control technique. Thus, numerical simulations for better current distribution and high efficiency can be conducted.

REFERENCES

ACI 318 (2014), "*Building Code Requirements for Structural Concrete.*" American Concrete Institute, Michigan, USA.

Adrian, S. (2014). "*One Global Definition of E-wast*e", Solving the e-waste problem (Step), United Nations University Annual Report.

Ahmad, S. (2003), "Reinforcement Corrosion in Concrete Structures, its Monitoring and Service Life Prediction - A Review". *Cement and Concrete Composites,* **25**(4-5), 459-471.

Al-Manaseer, A. A. and Dalal, T. R. (1997). "Concrete containing plastic aggregates." *Concrete International*, **19**(8), 47–52.

Amar Ujala (2016), "ई-कचरे से निपटने की समस्या |". In Amar Ujala. *Amar Ujala Press*, Dehradun. 2 August, 2016.

Anwar, M. S., Sujitha, B. and Vedalakshmi, R., (2014). "Light-weight cementitious conductive anode for impressed current cathodic protection of steel reinforced concrete application". *Construction & Building Materials*, **71**(November), 167–180.

Apostolopoulos, A. and Matikas, T. E. (2016)," Corrosion of bare and embedded in concrete steel bar - impact on mechanical behavior." *International Journal of Structural Integrity*, **7**(2), 240-259.

Apostolopoulos, C. A., and Papadakis, V. G. (2008). "Consequences of steel corrosion on the ductility properties of reinforcement bar." *Construction and Building Materials,* **22**(12), 2316–2324.

ASTM C 876 (2009), "*Standard Test Method for Corrosion Potentials of Uncoated Reinforcing Steel in Concrete*". ASTM International, Pennsylvania, USA.

ASTM C511 (2013), "*Standard Specification for Mixing Rooms, Moist Cabinets, Moist Rooms, and Water Storage Tanks Used in the Testing of Hydraulic Cements and Concretes*". ASTM International, Pennsylvania, USA.

ASTM G 57 (2012), "*Standard Test Method for Field Measurement of Soil Resistivity using Wenner Four Electrode Method".* ASTM International, Pennsylvania, USA.

AULIVE (2016). "Patent Inspiration (computer software). New South Wales, Australia. [Available at: https://app.patentinspiration.com].

Batayneh, M., Marie, I., and Asi, I. (2007). "Use of selected waste materials in concrete mixes". *Waste Management*, **27** (12), 1870– 1876.

Baldé, C.P., Wang, F., Kuehr, R., Huisman, J. (2015), "The global e-waste monitor – 2014", *United Nations University, IAS – SCYCLE*, Bonn, Germany.

Bayasi, Z., Zeng, J. (1993). "Properties of polypropylene fiber reinforced concrete". *ACI Materials Journal*, **90**(6), 605–610.

Barnard, E. H. (1965) "Electrically conductive concrete." *U.S. Patent No. 3,166,518,* Washington DC, U.S. Patent and Trademark Office.

Bennett, J. E., and Schue, T. J. (1999). "Galvanic Cathodic protection of reinforced concrete bridge members using sacrificial anodes attached by conductive adhesives" (Report No. FHWA-RD-99-112). Washington D.C, USA. 43-45.

Bertolini, L. (2008). "Steel corrosion and service life of reinforced concrete structures." *Structure and Infrastructure Engineering*, **4**(2), 123–137.

Bertolini, L., Bolzoni, F., Pastore, T., and Pedeferri, P. (2004). "Effectiveness of a conductive cementitious mortar anode for cathodic protection of steel in concrete." *Cement and Concrete Research*, **34**(4), 681–694.

Bertolini, L., Bolzoni, F., and Pedeferri, P. (1998). "Cathodic protection and cathodic preventionin concrete: principles and applications." *Journal of Applied Electrochemistry*, **28**(12), 1321–1331

Bertolini, L., Gastaldi, M., Pedeferri, M., and Redaelli, E. (2002). "Prevention of steel corrosion in concrete exposed to seawater with submerged sacrificial anodes." *Corrosion Science*, **44**(7), 1497– 1513.

Bhargav T. S. (2014). "Corrosion corrodes 6% of India's GDP every year". *Auto Components India.* Available at: http://autocomponentsindia.com/corrosion-corrodes-6-of-indias-gdp-every-year/. [Accessed on: 3 october 2016].

Bhuiyan, S., Law, D. & Molyneux, T., (2014). "The impact of the interruption of impressed current cathodic protection on the steel / concrete interface". *Concrete Solutions*, Taylor and Francis. 153–159.

Burillo, G., Clough, R.L., Czvikovszky, T., Guven, O., Moel, A.L., Liu, W., Singh, A., Yang, J., Zaharescu, T., (2002). "Polymer recycling: potential application of radiation technology". *Radiation Physics and Chemistry*. **64**(1), 41–51.

Broomfield, J. P. (2007). "*Corrosion of Steel In Concrete: Understanding, Investigation and Repair"*. Taylor & Francis, London.

BS 12696 (2016). "*Cathodic Protection of Steel in Concrete.*" BSI British standards publication.

BS 206 Part 1 (2000). "*Concrete - Specification, performance, production and conformity*". BSI British standards publication.

BS 7361 Part 1 (1991). "*Cathodic protection of reinforcing steel in Atmospherically Exposed Structures.*" BSI British standards publication.

BS 8110 Part 1 (1997). "*Structural use of concrete- code of practice for design and construction*". BSI British standards publication.

Byrne, A., Holmes, N. and Norton, B. (2016). "State-of-the-art review of cathodic protection for reinforced concrete structures". *Magazine of Concrete Research*, **68**(January), 1–14.

Cairns, J., Plizzari, G.A., Du, Y., Law, D.W. and Frnazoni, C. (2005), "Mechanical properties of corrosion-damaged reinforcement", *ACI Materials Journal*, **102**(4). 256-264.

Carmona, J., Garcés, P. and Climent, M.A. (2015). "Efficiency of a conductive cement-based anodic system for the application of cathodic protection, cathodic prevention and electrochemical chloride extraction to control corrosion in reinforced concrete structures". *Corrosion Science*, **96**(July), 102–111.

Cao, J. and Chung, D. D. L. (2003a). "Colloidal graphite as an admixture in cement and as a coating on cement for electromagnetic interference sheilding". *Cement & Concrete Research.* **33**(11). 1737-1740.

Cao, J. and Chung, D. D. L. (2003b). "Coke powder as an admixture in cement for electromagnetic interference sheilding". **41**.2433-2436

Chess, P., Grønvold, F., and Karnov, C. E. (1998). "*Protection of Steel in Concrete".* E & FN SPON, London, UK.

Choi, Y.W., Moon, D.J., Chumg, J.S., Cho, S.K., (2005). "Effects of waste PET bottles aggregate on the properties of concrete." *Cement and Concrete Research*. **35**(4), 776–781.

Choi, Y.W., Moon, D. J., Kim, Y. J. and Lachemi, M., (2009). "Characteristics of mortar and concrete containing fine aggregate manufactured from recycled waste polyethylene terephthalate bottles". *Construction and Building Materials*, **23**(8), 2829–2835.

Chu, H. and Chen, J., (2016). "The experimental study on the correlation of resistivity and damage for conductive concrete". *Cement and Concrete Composites*, **67**(March), 12–19.

Chung, D. D. L., (2004). Electrically conductive cement-based materials.pdf. *Advances in Cement Research*, **4**(16), 167–176.

Christodoulou, C., Glass, G., Webb, J., Austin, S. and Goodier, C. (2010) Assessing the long term benefits of impressed current cathodic protection. *Corrosion Science*. **52**(8): 2671–2679.

Concrete Society Technical Report 60 (2004). "*Electrochemical tests for reinforcement corrosion".* The Concrete Society, Surrey, UK.

Cui, J. and Forssberg, E., (2003). "Mechanical recycling of waste electric and electronic equipment: A review". *Journal of Hazardous Materials*, **99**(3), 243–263.

Darowicki, K., Orlikowski, J., Cebulski, S., and Krakowiak, S. (2003). "Conducting coatings as anodes in cathodic protection." *Progress in Organic Coatings*, **46**(3), 191–196.

Dodbiba, G., Takahashi, K., Sadaki, J. and Fujita T. (2008). "The recycling of plastic wastes from discarded TV sets: comparing energy recovery with mechanical recycling in the context of life cycle assessment". *Journal of Cleaner Production*. **16**(2008). 458-470.

Du, Y.G., Clark, L.A. and Chan, A.H.C. (2005), "Effect of corrosion on ductility of reinforcing bars". *Magazine of Concrete Research*, **57**(7), 407-419.

Durstewitz, C. B., López, F. B., Jaquez, R. N., Fajardo, G., Almeraya, F., Maldonado-Bandala, E., and Castorena, J. H. (2012). "Cement Based Anode in the Electrochemical Realkalisation of Carbonated Concrete." *International Journal of Electrochemical Science*, **7**(4), 3178–3190.

El Maaddawy, T. A. & Soudki, K. A., (2003). "Effectiveness of Impressed Current Technique to Simulate Corrosion of Steel Reinforcement in Concrete". *Journal of Materials in Civil Engineering*, **15**(1), 41–47.

Eldho, C.A. (2014) "*An Investigation of Cement Based Anodes for Cathodic Protection of RC Structures*", Master Thesis, AcSIR, CSIR-CBRI, Roorkee. 22-25.

Freeman, A. and William H. (1976). "Electrically conducting concrete." U.S. Patent No. 3,962,142. 8 Jun. 1976.

Gente, V., Marca F. L., Lucci F., Massacci, P. and Pani E. (2004). "Cryo-comminution of plastic waste". *Waste Management*. **24** (2004). 63–672.

Gupta, R., Puppala, H. and Rajesh N. (2015). "Application of Recycled Coarse Aggregates and E-Waste for Pavements with Low Traffic". *IOSR Journal of Mechanical and Civil Engineering*, **12**(2), 64-70.

Glass, G.K, Roberts, A. C., and Davison N. (2008). "Hybrid Corrosion Protection of Chloride-Contaminated Concrete". *Construction Materials*. **161**(November). 163–172.

Hassanein, A. M., Glass, G. K., and Buenfeld, N. R. (2002). "Protection current distribution in reinforced concrete cathodic protection systems". *Cement and Concrete Composites* **24**(1): 159–167.

Hays, G. F. (2010). "*The cost of corrosion*". World Corrosion Organization. Available at: http://events.nace.org/euro/corrodia/Fall_2010/wco.asp. [Accessed : 21 November 2016].

IS 383 (2016), "Specifications for coarsse and fine aggregates from natural source for concrete.", Bureau of Indian Standards, New Delhi, India.

IS 456 (2000), "*Plain and Reinforced Concrete.*", Bureau of Indian Standards, New Delhi, India.

IS: 516 (1959). "*Methods of tests for strength of concrete*". Bureau of Indian Standards New Delhi, India.

IS: 2386 (1963). "*Test methods for aggregates for concrete*". Bureau of Indian Standards, New Delhi, India.

IS: 4031 (2013)."*Methods of physical tests for hydraulic cement*". Bureau of Indian Standards, New Delhi, India.

IS 8112 (2013)."*Ordianry Portland Cement, 43 Grade-Specifications*". Bureau of Indian Standards, New Delhi, India.

IS 10262 (2009)."*Concrete mix proportioning Guidelines*". Bureau of Indian Standards, New Delhi, India.

Jahan, K. and Begum, A., (2013). "Electronic Waste (E-Waste) Management in India : A Review". *IOSR Journal Of Humanities And Social Science.* **10**(4), 46–57.

Javaherdashti, R. (2000). "How corrosion affects industry and life." *Anti-Corrosion Methods and Materials*, **47**(1), 30-34.

Jing, X., and Wu, Y. (2009). "Current distribution in reinforced concrete cathodic protection system with conductive mortar overlay anode". *Construction and Building Materials*, **23**(6), 2220–2226.

Jing, X., and Wu, Y. (2010). "Conductive mortar as anode material for cathodic protection of steel in concrete". *Journal of Wuhan University of Technology.* **25**(5), 883-888.

Jing, X., and Wu, Y. (2011). "Electrochemical studies on the performance of conductive overlay material in cathodic protection of reinforced concrete." *Construction and Building Materials*, **25**(5), 2655–2662.

Joseph K. (2007), "*Electronic Waste Management in India–Issues and Strategies*". Proceedings Sardinia, Eleventh International Waste Management and Landfill Symposium. S. Margherita di Pula, Cagliari, Italy; 1 - 5 October, 2007.

Karade S.R. (2016) "Performance of Cementitious Anodes for Cathodic Protection of RC Structures". *Cathodic Protection Summit*, New Delhi, 27-28 May 2016.

Karade S.R. & Goyal A (2016) "Corrosion of Steel in Seawater Mixed Concrete & Control Measures", *NACE NIGIS CORCON 2016,* New Delhi, Sept. 18-21, 2016. Paper No. 21.

Kean, R. L. and Davies, K. G. (1981). "Cathodic Protection, Guide Prepared by British Department Trade and Industry", Vol. 2–4. *National Physical Laboratory,* Teddington, UK.

Kumar, K. S. and Baskar K. (2014). "Development of Ecofriendly Concrete Incorporating Recycled High-Impact Polystyrene from Hazardous Electronic Waste". *Journal of Hazardous, Toxic, and Radioactive Waste.19 (3).*

Lakshmi, R. & Nagan, S., (2010). "Studies on Concrete containing E-plastic waste". *International Journal of Environmental Sciences*, 1(3), pp.270–281.

Lee, H.S. and Cho, Y.S. (2009), "Evaluation of the mechanical properties of steel reinforcement embedded in concrete specimen as a function of the degree of reinforcement corrosion", *International Journal of Fracture*, **157**(1), 81-88.

Liang T., Ping C., Was L., Bing S. S., Coldness F., Yi W., Jinhui L., Guo W., Yachun H., Yusheng Fu, Jian W. (2014). "*Method for preparing radiation-resistant concrete from lead-containing CRT (cathode ray tube) glass.*" Chinese Patent No.- CN 104177024 A. 15 Aug., 2014.

Lopez, W. (1993), "Influence of the degree of pore saturation on the resistivity of concrete and the corrosion rate of steel reinforcement". *Cement and Concrete Research. **23**(2). 368-376.*

Mantia, F. P. L. and Gardette, J. L. (2002). "Improvement of the mechanical properties of photo-oxidized films after recycling". *Polymer Degradation and Stability*. **75** (1), 1–7.

Marzouk, O.Y., Dheilly, R.M., and Queneudec, M., (2007). "Valorization of post-consumer waste plastic in cementitious concrete composites". *Waste Management.* 27, 310–318.

NACE SP 0290 (2007), "*Standard Practice: Impressed Current Cathodic Protection of Reinforcing Steel in Atmospherically exposed Concrete Structures*", NACE International, Houston, TX.

Nikolakakos, S. (1999). "Cathodic protection system design for steel pilings of a wharf structure". *ASTM Special Technical Publication*, No. STP1370, 52-70.

Neville, A., (1995). "Chloride attack of reinforced concrete: an overview". *Materials and Structures*, **28**(2), 63–70.

Neville, A. M. (2013) "Properties of Concrete". Indian edition: Dorling Kinderley India Pvt. Ltd. New Delhi, India.

Orlikowski, J., Cebulski, S. and Darowicki, K. (2004). "Electrochemical investigations of conductive coatings applied as anodes in cathodic protection of reinforced concrete". *Cement and Concrete Composites* **26**(6): 721–728.

Panneerselvam N,. & Gopalakrishna, G. V. T. (2016). "Recycle of E-Waste in Concrete", *International Journal of Science and Research* **5**(4), 1590-1593.

Parthiban, G.T., Ravi R., Saraswathy, V., Palaniswamy N., and Sivan V., (2008). "Cathodic protection of steel in concrete using magnesium alloy anode", *Corrosion Science*, **50**(21), 3329-3335.

Patil, S.A. and Sharma, N.M., (2015). "Electronic Waste - A Literature Review". *International Journal of Science and Research*. **4**(4), 2013–2015.

Park, Y. J. and Fray, D. J. (2009). "Recovery of high purity precious metals from printed circuit boards", *Journal of Hazardous Material*. 164(2-3), 1152-1158.

Pedeferri, P., (1996). "Cathodic protection and cathodic prevention". *Construction and Building Materials*, **10**(5), 391–402.

Pérez, A., Climent, M.A. and Garcés, P., (2010). "Electrochemical extraction of chlorides from reinforced concrete using a conductive cement paste as the anode". *Corrosion Science*, **52**(5), 1576–1581.

Polder, R. B., Andrade, C., Elsener, B., Vennesland, O., Gulikers, J.,Weidert, R and Raupach M. (2000). "Test methods for on site measurement of resistivity of concrete", RILEM TC 154-EMC (2000), *Materials and Structures*. **23**(10), 603-611.

Polder, R. B., Peelen, W. H., Lollini, F., Redaelli, E., and Bertolini, L. (2009). "Numerical design for cathodic protection systems for concrete." *Materials and Corrosion*, **60**(2), 130–136.

Polder, R. B., Peelen, W. H., Stoop, B. T. J., and Neeft, E. A. C. (2011). "Early stage beneficial effects of cathodic protection in concrete structures." *Materials and Corrosion*, **62**(2), 105–110.

Polder, R.B., and Peelen, W.H. (2014). "Experience and recent innovations in cathodic protection of steel in concrete.", In: *Concrete Solutions*. CRC Press, Croydon, UK. 209–213.

Poulakis, J. G. and Papaspyrides, C. D., (1997). "Recycling of polypropylene by the dissolution/ repreciptation technique: I. A model study". *Resources, Conservation and Recycling*. **20**(1), 31–41.

Pourbaix, M. (1974). "*Atlas of Electrochemical Equilibria in Aqueous Solutions"*, Trans. JA Franklin (Houston, TX: NACE International, 1974), 256.

Press Trust of India (2016). "India loses up to $100 billion annually to corrosion: Hind Zinc CEO Sunil Duggal." *The Economic Times*. Available at: http://economictimes.indiatimes.com/industry/indl-goods/svs/metals-mining/india-loses-up-to-100-billion-annually-to-corrosion-hind-zinc-ceo-sunil-duggal/articleshow/54878379.cms. [Accessed on: 2 November 2016].

Puckett, J, and Smith, T.,(2002). *"Exporting harm: the high-tech trashing of Asia"*. The Basel Action Network. Seattle, Silicon Valley Toxics Coalition.

Pye, G. B., Robert E. M., Mark, R. A., James, J. B. and Peter, J. T. (2003) "*Conductive concrete composition*." U.S. Patent No. 6,503,318. 7 Jan. 2003.

Rajya Sabha Secretariat, Rajya Research Unit (2011), "*E-WASTE IN INDIA*", Rajya Sabha, New Delhi.

Ramme, B. W., Noegel, J. J., Setchell, R. H. and Bischke, R. F. (2002). "*Electrically conductive concrete and controlled low-strength materials.*" U.S. Patent No. 6,461,424. 8 Oct. 2002.

Rawat, A., and Karade, S. R. (2017). "ई-कचरा : समस्या एवं निदान |" *निर्माणिका*, CSIR-CBRI **(2016-2017),** 26-29.

Reza, F., Yamamuro, J.A., Batson, G.B.(2004). "Electrical resistance change in compact tension specimens of carbon fiber cement composites", *Cement and Concrete Composites* **26**(7).873-881.

Roberge P. R. (2000), "*Handbook of Corrosion Engineering.*" The McGraw-Hill Companies, New York, USA.S

Sergi, G. (2011). "Ten-year results of galvanic sacrificial anodes in steel reinforced concrete." *Materials and Corrosion*, **62**(2), 98–104.

Shetty, M.S. (2005). "Concrete Technology: Theory and Practice". *S. Chand & Company Ltd*, India.

Sodhi M. S. and Reimer B. (2001), "Models for recycling electronics end-of-life products". *OR Spektrum*. **23**(1). 97–115.

Sohanghpurwala A. A. (2009) "*Cathodic Protection for Life Extension of Existing Reinforced Concrete Bridge Elements*". National Cooperative Highway Research Program (NCHRP) Synthesis 398. Washington D. C.

Soroushian, P., Plasencia, J. and Ravanbakhsh, S. (2003). "Assessment of Reinforcing Effects of Recycled Plastic and Paper in Concrete." *ACI Materials Journal* ,**100**(3) , 203–207.

Stratfull, R. F. (1974). "Experimental cathodic protection of a bridge deck." *Transportation Research Record*, (500), 1-15.

The Economic Times, Report on CORCON - 2010, Chennai, (28, September, 2010).

Tuan, C., and Yehia, S. (2004). "Evaluation of electrically conductive concrete containing carbon products for deicing." *ACI Materials Journal*, **101**(4), 287–293.

Virmani, Y.P. and Clemena, G.G. (1998). "Corrosion Protection-Concrete Bridges". Report No. FHWA-RD-98-088, *Federal Highway Administration*, Washington D.C.

Wang R. and Tengfei Z. (2011)."*Method for preparing environment-friendly concrete with waste circuit board nonmetal powder*". Chinese Patent No. CN 102503294 A. 8 Oct. 2011.

Wang, Z., Zhang, B. and Guan D. (2016). "Take responsibility for electronic-waste disposal". *Nature News*. Nature Publishing Group. 536(7614). Available on: https://www.nature.com/news/take-responsibility-for-electronic-waste-disposal-1.20345. [Accessed on: 5 August, 2016].

Wen S. and Chung D.D.L. (2000), "Enhancing the Seebeck Effect in Carbon Fiber Reinforced Cement by Using Intercalated Carbon Fibers", *Cement and Concrete Research* **30**(8). 1295-1298.

Wen, S. and Chung, D. D. L. (2001), "Electrical polarisation in carbon reinforced cement". *Cement and Concrete Research.* **31**(2001). 141-147.

Westhof, L. B. J., Frans, L. J. D. P., and George G. T. (1993). "*Modified cementitious composition.*" U.S. Patent No. 5,254,228. 19 Oct. 1993.

Whiting, D. A., Nagi, M. A., and Broomfield, J. P. (1996). "Laboratory Evaluation of Sacrificial Anode Materials for Cathodic Protection of Reinforced Concrete Bridges." *Corrosion*, **52**(6), 472– 479.

Widmer, R., Oswald-Krapf, H., Khetriwalb D. S., Schnellmannc M., Boni H. (2005). "Global perspectives on e-waste". *Environmental Impact Assessment Review*, **25**(5), 436–458.

Wilson, K., Jawed, M. and Ngala, V. (2013). "The selection and use of cathodic protection systems for the repair of reinforced concrete structures". *Construction and Building Materials*. **39**(February):19–25.

Wu, S., Mo, L., Shui, Z., and Chen, Z. (2005). "Investigation of the conductivity of asphalt concrete containing conductive fillers." *Carbon*, **43**(7), 1358–1363.

Xie, P., Gu, P., Fu, Y. and Beaudoin, J. J. (1995) "C*onductive cement-based compositions.*" U.S. Patent No. 5,447,564. 5 Sep. 1995.

Yehia, S. and Host, J. (2010). "Conductive Concrete for Cathodic Protection of Bridge Decks." *ACI Materials Journal,* **107**(6), 578–586.

Yuchun Z., Jiadong W., Xia X., and Yandong L. (2014). "*Method for preparing concrete kerbstones and paving bricks from nonmetal powder of waste circuit boards*". Chinese Patent No. CN 104030628 A. 25 June, 2014.